



Theses and Dissertations

2006-08-19

Analysis of the Sediment Transport Capabilities of FESWMS FST2DH

Mark K. Ipson
Brigham Young University - Provo

Follow this and additional works at: <https://scholarsarchive.byu.edu/etd>



Part of the [Civil and Environmental Engineering Commons](#)

BYU ScholarsArchive Citation

Ipson, Mark K., "Analysis of the Sediment Transport Capabilities of FESWMS FST2DH" (2006). *Theses and Dissertations*. 769.

<https://scholarsarchive.byu.edu/etd/769>

This Thesis is brought to you for free and open access by BYU ScholarsArchive. It has been accepted for inclusion in Theses and Dissertations by an authorized administrator of BYU ScholarsArchive. For more information, please contact scholarsarchive@byu.edu, ellen_amatangelo@byu.edu.

ANALYSIS OF THE SEDIMENT TRANSPORT
CAPABILITIES OF FESWMS FST2DH

by

Mark K. Ipson

A thesis submitted to the faculty of

Brigham Young University

in partial fulfillment of the requirements for the degree of

Master of Science

Department of Civil and Environmental Engineering

Brigham Young University

December 2006

BRIGHAM YOUNG UNIVERSITY

GRADUATE COMMITTEE APPROVAL

of a thesis submitted by

Mark K. Ipson

This thesis has been read by each member of the following graduate committee and by majority vote has been found to be satisfactory.

Date

Alan K. Zundel, Chair

Date

E. James Nelson

Date

Rollin H. Hotchkiss

BRIGHAM YOUNG UNIVERSITY

As chair of the candidate's graduate committee, I have read the thesis of Mark K. Ipson in its final form and have found that (1) its format, citations, and bibliographical style are consistent and acceptable and fulfill university and department style requirements; (2) its illustrative materials including figures, tables, and charts are in place; and (3) the final manuscript is satisfactory to the graduate committee and is ready for submission to the university library.

Date

Alan K. Zundel
Chair, Graduate Committee

Accepted for the Department

E. James Nelson
Graduate Coordinator

Accepted for the College

Alan R. Parkinson
Dean, Ira A. Fulton College of Engineering
and Technology

ABSTRACT

ANALYSIS OF THE SEDIMENT TRANSPORT CAPABILITIES OF FESWMS FST2DH

Mark K. Ipson

Department of Civil and Environmental Engineering

Master of Science

Many numeric models simulate the transport of sediment within rivers and streams. Engineers use such models to monitor the overall condition of a river or stream and to analyze the impact that the aggradation and degradation of sediment has on the stability of bridge piers and other features within a stretch of a river or stream. A model developed by the Federal Highway Administration, FST2DH, was recently modified to include the simulation of sediment movement within a channel. The tools for modeling sediment movement with FST2DH remain unproven.

This thesis examines the sediment capabilities of FST2DH. It evaluates the sediment results for reasonableness and compares the results to those obtained from a sediment transport model developed by the Army Corps of Engineers, SED2D WES. Resulting concentrations from another program created by the Army Corps of Engineers, SAMwin, provide additional data comparison for FST2DH sediment solutions. Several

test cases for laboratory flumes give additional insight into the model's functionality. Finally, this thesis suggests further enhancements for the sediment capabilities of the FST2DH model and provides direction for future research of the sediment transport capabilities of FST2DH.

Results show that FST2DH appropriately models sediment movement in channels with clear-water and equilibrium transport rate inflow conditions. Transport formulas found to be functional include the Engelund—Hansen, Yang sand and gravel, and Meyer-Peter—Mueller equations. FST2DH has difficulty modeling channels with user-specified inflow concentrations or transport rates, models with very small particles, models containing hydraulic jumps, and models with small elements. The test cases that successfully run to completion provide appropriate patterns of scour and deposition. Other trends in the results further verify the functionality of many of the sediment transport options in FST2DH.

ACKNOWLEDGMENTS

I appreciate Dr. Alan Zundel for his guidance and help throughout each phase of research and writing. Thanks to the other members of my committee, Dr. Nelson and Dr. Hotchkiss, for the instruction that they gave me as I worked on the research and this report. I thank the Federal Highway Administration for funding the study of the sediment transport capabilities of FST2DH. I also appreciate Janice Sorenson for her help in reviewing the formatting of this thesis, answering my many questions, and helping me along the path to graduation.

I appreciate the care that the professors in the Civil and Environmental Engineering Department here at BYU showed for me throughout my college education. They have passed a great enthusiasm for Civil Engineering on to me. Finally, I am especially grateful for the support, encouragement, and patience of my wife, Andrea, and other family members as I worked on this research.

TABLE OF CONTENTS

LIST OF TABLES	xi
LIST OF FIGURES	xiii
1 Introduction.....	1
1.1 Background.....	2
1.1.1 Coupling of Hydrodynamic and Sediment Runs	3
1.1.2 Sediment Transport Equations	5
1.1.3 Inflow Sediment Specification.....	7
1.1.4 Bed Shear Stress Equations	8
1.1.5 Particle Size Classes	8
1.1.6 Model Output	9
1.2 Research Objectives.....	9
2 Data Processing	11
2.1 Variation of Inflow Sediment Parameters and Transport Equations	13
2.2 Straight Flume with Varying Midsection Slopes.....	16
2.3 Flumes with Contractions	18
2.4 SED2D WES Flumes.....	21
2.5 SAMwin Flumes	23
2.6 Laboratory Models.....	25
2.7 Deposition in a Reservoir	26
3 Presentation of Results: Qualitative Analysis	29

3.1	Variation of Sediment Inflow and Transport Formulas.....	29
3.1.1	Sediment Volumetric Flow Rate at the Inflow Boundary.....	30
3.1.2	Sediment Transport Capacity Formula	35
3.2	Varying Midsection Slopes.....	38
3.2.1	Steep Midsection Slope.....	39
3.2.2	Moderate Midsection Slope	40
3.2.3	Shallow Midsection Slope	46
3.3	Flumes with Contractions	54
3.3.1	Gradual Contraction.....	54
3.3.2	Long Abrupt Contraction.....	61
3.3.3	Short Abrupt Contraction.....	65
4	Presentation of Results: Quantitative Analysis.....	73
4.1	SED2D WES.....	73
4.1.1	Moderate Midsection Slope	74
4.1.2	Gradual Contraction.....	76
4.2	SAMwin.....	79
4.3	Laboratory Models.....	83
4.3.1	Scour Patterns and Depths Around a Pier.....	85
4.3.2	Narrow Contraction Flume with Varying Entrance and Exit Angles	86
4.3.3	Scour at a Basin’s Entrance	86
4.3.4	Narrow Flume with Downstream Fining	88
4.3.5	Wide Flume with Downstream Fining.....	88
4.4	Deposition in a Reservoir	91
5	Conclusions.....	101
5.1	Conclusions.....	101

5.1.1	Test Case Results and Observations	101
5.1.2	Changes to the SMS Interface.....	107
5.1.3	Suggested Improvements for FST2DH.....	108
5.2	Future Work.....	108
	References.....	111
	Appendix A. FST2DH Sediment Transport Tutorial	115
	Introduction.....	115
	Opening the Mesh.....	116
	Assigning Boundary Conditions.....	117
	Material Properties.....	117
	Model Control.....	118
	Renumbering the Mesh.....	118
	Obtaining the Steady-State Hydrodynamic Solution.....	118
	Creating a Sediment Simulation	119
	Setting the Sediment Parameters in Model Control.....	120
	Specifying Equilibrium Transport Rate Inflow	123
	Running FST2DH for the 0.5 mm Grain Size Case	124
	Viewing the Results for the 0.5 mm Grain Size Case	125
	Creating a Second Sediment Simulation for a Grain Size of 2.0 mm	125
	Setting the Sediment Parameters in Model Control.....	126
	Running FST2DH for the 2.0 mm Grain Size Case	126
	Comparing the Results from the 0.5 mm and 2.0 mm Cases.....	127
	Conclusion	128

LIST OF TABLES

Table 1-1: Summary of the Applications of Various Formulas.....	6
Table 2-1: Parameters for the Straight Flume Used in Testing the Various Sediment Inflow Specifications and Sediment Transport Equations.....	14
Table 2-2: Parameters for the Upstream and Downstream Segments of the Flumes with Varying Midsection Slopes.....	16
Table 2-3: Slopes for the Middle Segments of the Flumes with Varying Midsection Slopes.....	17
Table 2-4: Parameters for the Flume with a Gradual Contraction.....	19
Table 2-5: Parameters for a Flume with a Short Abrupt Contraction.....	21
Table 2-6: Parameters for the SAMwin Flume.....	24
Table 2-7: Flowrates, Velocities, and Water Depths for the SAMwin Test Cases.....	25
Table 2-8: Parameters for the Flume Showing Deposition at the Entrance to a Reservoir.....	27
Table 2-9: Element Properties for the Test Cases for a Long Flume Emptying into a Reservoir.....	28
Table 3-1: Completion of Runs with Varying Transport Equations.....	35
Table 3-2: Scour Predicted by Various Equations for a 48 Hour Simulation.....	38
Table 3-3: Locations and Magnitudes of the Points of Maximum Scour and Deposition for the Gradual Contracion Test Cases.....	61
Table 3-4: Locations and Magnitudes of the Points of Maximum Scour and Deposition for the Long Abrupt Contracion Test Cases.....	65
Table 3-5: Locations and Magnitudes of the Points of Maximum Scour and Deposition for the Short Abrupt Contracion Test Cases.....	71
Table 5-1: Summary of Results for the Variation of Sediment Inflow Types.....	102

Table 5-2: Summary of Test Cases that Ran to Completion and Test Cases that Failed with the Variation of Sediment Transport Equations103

Table 5-3: Identification of the Midsection Sloped and Contraction Test Cases that Ran to Completion and Test Cases that Failed105

Table 5-4: Summary of the Laboratory Flumes Attempted in FST2DH107

LIST OF FIGURES

Figure 2-1: Profile of the Three Flumes with Varying Midsection Slope	18
Figure 2-2: Plan View of the Flume with a Gradual Contraction.....	19
Figure 2-3: Plan View of the Flume with a Long Abrupt Contraction.....	20
Figure 2-4: Plan View of the Flume with a Short Abrupt Contraction.....	21
Figure 2-5: Profile of Water Surface at the Downstream End of a Flume Emptying into a Reservoir	27
Figure 3-1: Variation of Bed Elevation along the Length of a Straight Flume	30
Figure 3-2: Initial and Final Bed Elevation Profiles for Clear-Water Inflow.....	31
Figure 3-3: Final Bed Elevations for Concentrations of 10 and 10,000 ppm (Essential Conditions).....	32
Figure 3-4: Final Bed Elevations for Sediment Transport Rates of 1 and 10 cms (Essential Conditions).....	33
Figure 3-5: Final Bed Elevations for an Equilibrium Transport Rate Inflow.....	34
Figure 3-6: Final Bed Elevations for the Sediment Transport Capacity Equation Test Cases	37
Figure 3-7: Steady-State Bed and Water Depth Profiles for a Flume with a Steep Midsection Slope	39
Figure 3-8: Initial Bed Elevation and Water Surface for a Flume with a Moderate Midsection Slope	40
Figure 3-9: Bed Elevations for the Clear-Water Moderate Midsection Slope Flume with a Uniform Particle Size of 0.2mm at 15 Minutes, 1 Hour, and 4 Hours.....	41
Figure 3-10: Bed Elevations for the Clear-Water Moderate Midsection Slope Flume with a Uniform Particle Size of 0.2mm at 6 Hours, 12 Hours, 24 Hours, and 48 Hours	42

Figure 3-11: Bed Elevations for Clear-Water and Equilibrium Transport Rate Inflows for a Moderate Midsection Slope Flume with a Uniform Grain Size of 0.2mm after 48 Hours	43
Figure 3-12: Bed Elevations for the Moderate Midsection Slope Test Case with a Uniform Grain Size of 0.2mm and an Inflow Equilibrium Transport Rate at 15 Minutes, 1 Hour, 2 Hours, 4 Hours, and 6 Hours	45
Figure 3-13: Bed Elevations after 48 Hours for a Moderate Midsection Slope Flume with an Inflow Equilibrium Transport Rate and Particle Sizes of 0.08mm, 0.2mm, 2.0mm, and 4.0mm	46
Figure 3-14: Initial Bed Elevation and Water Surface for the Flume with a Shallow Midsection Slope	47
Figure 3-15: Beginning Stages of the Bed Flattening over Time for the Clear-Water, Shallow Midsection Test Case with a Uniform Grain Size of 0.2mm.....	48
Figure 3-16: Advanced Stages of the Bed Flattening over Time for the Clear-Water, Shallow Midsection Test Case with a Uniform Grain Size of 0.2mm.....	49
Figure 3-17: Bed Elevations after 48 Hours for the Shallow Midsection Slope Test Cases with Clear-Water Inflow and Various Particle Sizes: 0.2mm, 2.0mm, and 4.0mm	50
Figure 3-18: Initial and Final Bed Elevations for a 48 Hour Simulation of the Shallow Midsection Slope Flume with an Equilibrium Transport Rate Applied to the Inflow Boundary and Particle Sizes of 0.08mm, 0.2mm, 2.0mm and 4.0mm	51
Figure 3-19: Change in Velocity Magnitude over 48 Hours for the Shallow Midsection Slope Flume with Clear-Water Inflow and a Particle Size of 0.2mm	53
Figure 3-20: Steady-State Solution for Water Depth in the Flume with a Gradual Contraction.....	55
Figure 3-21: Steady-State Solution for Velocity Magnitude for the Flume with a Gradual Contraction.....	55
Figure 3-22: Centerline Profile and Plan View of the Final Bed Elevations for a 48 Hour Simulation of the Clear-Water, 2.0mm Particle Size Test Case for a Flume with a Gradual Contraction	56
Figure 3-23: Centerline Profile and Plan View of the Final Bed Elevations for a 48 Hour Simulation of the Clear-Water, 4.0mm Particle Size Test Case for a Flume with a Gradual Contraction	57

Figure 3-24: Centerline Profile and Plan View of the Final Bed Elevations for a 48 Hour Simulation of the Gradual Contraction Test Case with an Equilibrium Transport Rate at the Inflow Boundary and a Bed Particle Size of 0.08mm	58
Figure 3-25: Centerline Profile and Plan View of the Final Bed Elevations for a 48 Hour Simulation of the Gradual Contraction Test Case with an Equilibrium Transport Rate at the Inflow Boundary and a Bed Particle Size of 0.2mm	58
Figure 3-26: Centerline Profile and Plan View of the Final Bed Elevations for a 48 Hour Simulation of the Gradual Contraction Test Case with an Equilibrium Transport Rate at the Inflow Boundary and a Bed Particle Size of 2.0mm	59
Figure 3-27: Centerline Profile and Plan View of the Final Bed Elevations for a 48-hour Simulation of the Gradual Contraction Test Case with an Equilibrium Transport Rate at the Inflow Boundary and a Bed Particle Size of 4.0mm	59
Figure 3-28: Oblique View of the Channel Bed after 6 Hours, 12 Hours, 24 Hours, and 48 Hours for the 2.0mm, Clear-Water Test Case for a Flume with a Gradual Contraction	60
Figure 3-29: Plan View of the Bed Elevations after 48 Hours for the Equilibrium Transport Rate, 0.2mm Grain Size Test Case for a Flume with a Long Abrupt Contraction	62
Figure 3-30: Centerline Profiles of Bed Elevation for a 48 Hour Simulation of a Flume with an Abrupt Long Contraction and an Equilibrium Transport Rate at the Inflow Boundary, with Particle Sizes of 0.08mm and 0.2mm	63
Figure 3-31: Centerline Profiles of Bed Elevation for a 48 Hour Simulation of a Flume with an Abrupt Long Contraction and an Equilibrium Transport Rate at the Inflow Boundary, with Particle Sizes of 2.0mm and 4.0m.....	63
Figure 3-32: Close-up Plan View of the Final Bed Elevations for a 48 Hour Simulation of a Flume with an Abrupt Long Contraction with an Equilibrium Transport Rate at the Inflow Boundary and Bed Particle Sizes of 0.08mm, 0.2mm, 2.0mm, and 4.0mm	64
Figure 3-33: Bed Elevations at 48 Hours for the Clear-Water, 0.2mm Test Case for the Flume with an Abrupt Short contraction, Showing Instability at the Inflow Boundary	66
Figure 3-34: Centerline Profile and Plan View of the Steady-State Solution for Water Depth in the Flume with a Short Abrupt Contraction	66

Figure 3-35: Centerline Profile and Plan View of the Steady-State Solution for Velocity Magnitude in the Flume with a Short Abrupt Contraction	67
Figure 3-36: Bed Elevations after 48 Hours for the Short Abrupt Contraction Flume with an Inflow Equilibrium Transport Rate and Particle Sizes of 0.08mm, 0.2mm, 2.0mm, and 4.0mm	68
Figure 3-37: Centerline Profiles of Bed Elevations at 48 Hours for the Test Cases of a Short Abrupt Contraction with an Equilibrium Transport Rate Inflow and Bed Particle Size of 0.08mm, 0.2mm, 2.0mm, and 4.0mm	69
Figure 3-38: Centerline Profiles of Velocity Magnitude for the Equilibrium Transport Rate, 0.08mm Test Case at 15 Minutes, 24 Hours, and 48 Hours.....	70
Figure 4-1: Bed Elevations from SED2D for the Clear-Water, 0.2mm Test Case for the Flume with a Moderate Midsection Slope after 2 Hours, 6 Hours , 12 Hours, and 24 Hours	75
Figure 4-2: Final Bed Profiles for SED2D and FST2DH for a 48 Hour Simulation of the Clear-Water, 0.2mm Test Case for the Flume with a Moderate Midsection Slope	76
Figure 4-3: Final Bed Elevations from FST2DH and SED2D for the 0.08mm Test Case for the Flume with a Gradual Contraction	77
Figure 4-4: Final Bed Elevations from SED2D for the Test Cases for the Flume with a Gradual Contraction with Particle Sizes of 0.08mm, 0.2mm, 2.0mm, and 4.0mm	78
Figure 4-5: Equilibrium Transport Concentrations Predicted by FST2DH and SAMwin for Varying Flowrates and Transport Equations for Test Cases with a 0.177mm Particle Size	81
Figure 4-6: Equilibrium Transport Concentrations Predicted by FST2DH and SAMwin for Varying Flowrates and Transport Equations for Test Cases with a 1.414mm Particle Size	81
Figure 4-7: Grid for Experiment 10 from Sheppard’s Experiments	85
Figure 4-8: Grid for Dey’s Experiment for the Flume with the Largest Contraction.....	86
Figure 4-9: Grid for Thuc’s Experiment.....	87
Figure 4-10: Bed Elevations for the Modified Toro-Escobar Test Case after 2 Hours, 6 Hours, 12 Hours, 24 Hours, and 32.5 Hours	90

Figure 4-11: Volumes of Sediment Deposited, Scoured, and Available for Deposition	91
Figure 4-12: Volumes of Sediment Deposited and Available for Deposition	92
Figure 4-13: Profiles for the Water Surface Elevation, Original Bed Elevations, and Bed Elevations after 30 Days.....	93
Figure 4-14: Change in Bed Profile over Time Due to Backwater.....	94
Figure 4-15: Volumes of Deposition and Material Available for Deposition for the Reservoir Test Case with Two Grain Sizes (0.5mm and 2.0mm)	95
Figure 4-16: Bed Profiles for the Reservoir Test Case with a Single Grain Size and the Test Case with Two Grain Sizes (0.5mm and 2.0mm)	95
Figure 4-17: Volumes of Erosion, Deposition, and Material Available for Deposition for Run A.....	97
Figure 4-18: Volumes of Erosion, Deposition, and Material Available for Deposition for Run B	97
Figure 4-19: Volumes of Erosion, Deposition, and Material Available for Deposition for Run C	98
Figure 4-20: Volumes of Erosion, Deposition, and Material Available for Deposition for Run D.....	98
Figure 4-21: Element Length and Time of Stability for the Long Flume Emptying into a Reservoir	99
Figure A-1: Screen Shot of the Initial Mesh.....	116
Figure A-2: FST2DH Sediment Parameters Dialog	121
Figure A-3: FST2DH Global Bed Control Dialog.....	123
Figure A-4: FESWMS Nodestring Boundary Conditions Dialog	124

1 Introduction

Engineers often use hydrodynamic numerical models in the design and analysis of channels, streams, and rivers. Many models simulate the flow of water in rivers and canals. Fewer simulate the movement of sediment through such bodies of water. The Federal Highway Administration recently added sediment transport capabilities to its Finite Element Surface Water Modeling Software (FESWMS) package, also referred to as the Depth-averaged Flow and Sediment Transport Model (FST2DH). Although the hydrodynamic portion of FST2DH has been used for many years and is well-tested, the new sediment capabilities of the software remain unproven.

This thesis examines FST2DH from a sediment transport perspective and studies the model's ability to accurately simulate the movement of sediment in a number of different ways. It first gives an overview of the various options available in FST2DH for modeling sediment transport. It then outlines the test cases developed for the analysis of the functionality of those options. Next, this thesis provides and interprets the results from test cases for a qualitative analysis of sediment transport in FST2DH. After the qualitative analysis, this thesis compares results from simple FST2DH sediment runs to those obtained with another sediment transport modeling software package developed by the U.S. Army Corps of Engineers, SED2D WES. Additional quantitative analysis gives a comparison between calculated concentrations from FST2DH results and those from

another simple numerical model, SAMwin. An outline of test cases attempted in the modeling of sediment transport results from previous laboratory flume studies in FST2DH provides insight into the model's current capabilities. This report concludes with suggestions for further development of the sediment transport capabilities of FST2DH and guidance for future research. Finally, the appendix contains a tutorial detailing the use of the FST2DH sediment capabilities within the Surface-water Modeling System (SMS) software package. SMS is commonly used as the pre- and post-processor for FST2DH.

1.1 Background

Over the years, numerous models to simulate sediment transport in rivers and streams and assist engineers in analyses of these processes have evolved. Some of these include SAM (later modified and renamed SAMwin) (Thomas 2002), HEC-6 (USACE 1991), GSTARS (Yang 2005), BRI-STARS (Molinas 2000), and SED2D WES (USACE 2004). As there is a great need to identify the applicability of such models, many studies have been completed to analyze the capabilities and accuracy of 1D, 2D, and 3D sediment transport models (Cancino 1999, Duc 2004, Shams 2002, Wu 2004, Zeng 2003).

Recently, a well-known hydraulic model, FST2DH, was modified to include the simulation of sediment movement within a channel. Because the sediment capabilities of FST2DH are relatively new, the tools for modeling sediment movement remain unproven. The next few sections of this report provide an overview of FST2DH, its key components, and the equations and methods that will be used for the research.

The Depth-averaged Flow and Sediment Transport Model (FST2DH) is a two-dimensional finite element numerical model that simulates water movement and the transport of non-cohesive sediment in rivers and estuaries (Froehlich 2003). It was developed by the Federal Highway Administration as part of their Finite Element Surface-water Modeling System (FESWMS) for the specific purpose of modeling the complexities of flow near the highway river crossings. FST2DH can solve for either steady-state or dynamic conditions and supports meshes consisting of six-node triangles, eight-node quadrilaterals, and nine-node quadrilaterals (Froehlich 2003). FST2DH models only non-cohesive sediment such as sands and gravels. The User's Manual for FESWMS FST2DH provides additional information on the hydrodynamic modeling capabilities of FST2DH (Froehlich 2003).

1.1.1 Coupling of Hydrodynamic and Sediment Runs

Numerical models of sediment transport employ one of three methods for the interaction of changes in the hydraulics of a channel and changes in the channel cross-section that result from the aggradation or degradation of the stream bed. These include:

1. Uncoupled
2. Semi-coupled
3. Fully coupled

In the uncoupled method, the hydrodynamic and sediment transport equations are solved separately. The hydrodynamics are independent of the sediment transport. In this case, it is assumed that the change in one variable, such as the cross-section, is small enough to not have a significant effect on another variable, such as the flow (Kassem 1998).

The second method for linking flow and sediment transport in a model is the semi-coupled method. In a semi-coupled situation, the equations for flow and sediment transport are used iteratively to obtain a final solution (Kassem 1998). The solutions can be thought of as being separate but not independent. For instance, the hydrodynamics of the channel for a given timestep are first calculated and those solutions are then used as input for the sediment calculations for that same timestep. Once the sediment calculations are completed, the sediment results are then used to calculate new parameters such as cross-sectional area for the hydrodynamic run for the succeeding timestep. This iterative process continues until all the timesteps have been analyzed.

The final method, the fully coupled approach, links sediment and flow calculations. In this method, the hydrodynamic and sediment solutions are neither separate nor independent, as the flow and sediment calculations are solved simultaneously in a given time step.

While a fair amount of conversation about which method is best to use exists, it has generally been found that the semi-coupled and fully coupled approaches provide results that best agree with measured field data (Kassem 1998). An uncoupled sediment model may not be completely invalid, however, if the change in bed elevation is not significant enough to have a large impact on the hydrodynamics of the channel. Thus, uncoupled sediment models may provide the user with the option to specify a percentage of the water depth that the bed change cannot exceed for any given node in a mesh (USACE 2004).

FST2DH has the functionality to automatically generate sediment solutions using either the uncoupled or the semi-coupled method (Froehlich 2003). It does not, however, support the fully coupled option.

1.1.2 Sediment Transport Equations

Traditional literature classifies the movement of sediment within a river or stream into three main categories: bed load, suspended load, and wash load. Bed load includes material moving (rolling or sliding) along the bed. Some of the formulas that predict bed-load transport include the DuBoys Formula (1879), the Shields Formula (1936), the Meyer-Peter—Mueller Formula (1948), the Einstein Bed-Load Function (1942, 1950), the Einstein—Brown Formula (1950), and the Parker et al. Formula (1982) (Chang 1992). Suspended load consists of the sediment that is transported downstream while suspended in the water column above the bed. Wash load includes the “finest portion of sediment, generally silt and clay, that is washed through the channel, with an insignificant amount of it being found in the bed” (Chang 1992).

Bed-material or Total load formulas take into account the suspended load and the bed load. They do not include the wash load. Some of the more well-known bed-material load formulas include the Colby Relations (1964), the Engelund-Hansen Formula (1967), the Ackers-White Formula (1973), and Yang’s Unit Stream Power Equation (1972) (Chang 1992).

Several studies have been completed to analyze the accuracy of individual sediment transport equations and several sources provide more detail on each of the formulas listed above as well as detail about many other sediment transport equations that have been developed (Chang 1992, Froehlich 2003, Nakato 1990, Richardson 2001,

Thomas 2002, Yang 1991). Table 1-1 provides a summary of several sediment transport equations and the material sizes for which they are most applicable (Froehlich 2003, Richardson 2001, Thomas 2002).

Table 1-1: Summary of the Applications of Various Formulas

<i>Formula</i>	<i>Range of Particle Sizes (mm)</i>	<i>Material Description</i>
Ackers-White (1973)	0.04 – 7.0	Sand, Fine Gravel
Ackers-White-Day (1983)	0.04 – 7.0	Sand, Fine Gravel
Brownlie (1981)	0.086 – 1.4	Medium to Course Sand
Colby (1964)	0.18 – 0.70	Medium Sand
Einstein (1950)	0.78 – 29.0	Course Sand, Gravel
Engelund-Hansen (1972)	Not Specified	Sand
Laursen (1958)	0.062 – 2.0	Sand, Fine Gravel
Meyer-Peter—Mueller (1948)	0.4 – 29	Sand, Gravel
Parker (1990)	18.0 – 28.0	Gravel
Schoklitsch (1937)	0.3 – 4.9	Sand, Gravel
Yang’s Sand and Gravel (1973, 1984)	0.15 – 7.0	Sand, Gravel

FST2DH provides users with eight different methods for calculating sediment transport in a model. These include the following (Froehlich 2003):

- Power Formula
- Engelund-Hansen Formula (1967)
- Ackers-White Formula (1973)
- Ackers-White-Day Formula (1983)
- Laursen Formula (1958)
- Yang’s Sand and Gravel Formula (1972, 1973, 1984)
- Meyer-Peter—Mueller Formula (1948)
- Garbrecht et al. Approach

The Garbrecht et al. approach listed above is actually a combination of three different formulas, and for that reason, was not included in Table 1-1. This approach uses Laursen's formula when the sediment diameter is smaller than 0.25mm, Yang's Sand and Gravel formula when the diameter is between 0.25mm and 8.0mm, and the Meyer-Peter—Mueller formula when the diameter is greater than 8.0mm (Froehlich 2003). The Power Formula was also not included in Table 1-1. It is a simple equation that relates the volumetric sediment transport rate to the flow rate in a channel using two coefficients that control that relation and can be applied to the transport of sand or gravel. The User's Manual for FESWMS FST2DH provides additional information on the power formula (Froehlich 2003).

1.1.3 Inflow Sediment Specification

The amount of sediment that enters the domain from upstream is an important aspect of a sediment transport analysis. Scour is more likely to occur when the water entering a domain is not carrying any sediment. This is often observed just downstream of a dam. The sediment falls to the bed as the water's velocity slows upon entering the reservoir. The water that passes through the dam thus contains very little sediment and often scours the riverbed just downstream of the dam. If, on the other hand, the water entering a domain is carrying the full sediment load possible, deposition will more likely occur (USACE 2004).

FST2DH allows the user to select between six different methods for assigning sediment inflow: no specification (clear-water), providing volumetric concentrations as essential or natural conditions, specifying volumetric transport rates for each size class and average discharge-weighted volumetric concentrations being specified as essential or

natural conditions, and finally, forcing FST2DH to calculate the transport rates required to obtain sediment equilibrium through the inflow portion of the channel (Froehlich 2003).

1.1.4 Bed Shear Stress Equations

Bed shear stress is the force per unit area that is exerted by a fluid flowing past the bed of a river or stream (Lagasse 2001). A particle will not move unless this force overcomes the resisting force that is keeping the particle in place (Chang 1992). The point at which the forces are equal is often referred to as the point of incipient motion. A model must account for the bed shear stress because that is how it is able to predict the amount of sediment that is transported downstream.

FST2DH provides users with two different formulas for the calculation of bed shear stress: the Manning's shear stress equation and the Chézy equation (Froehlich 2003). Manning's equation for bed shear stress will be used in the model run comparisons outlined in this report.

1.1.5 Particle Size Classes

The gradation of sediment that comprises the bed of a river or stream has a great influence on the bed form and the overall resistance to flow (Richardson 2001). These factors, in turn will affect the resulting sediment transport that occurs in a body of water. FST2DH provides users with the capability to specify up to eight separate particle sizes for the bed material (Froehlich 2003). In effect, this allows the user to more accurately represent the grain size distribution from the river being modeled than if only a single particle size was used.

1.1.6 Model Output

FST2DH writes a sediment data file while running a sediment simulation. This file contains the bed elevation, the time-derivative of bed elevation, and the thicknesses of the active, deposition, and original layers of the bed at each node for each timestep. In addition, it also contains five other values at each node for each timestep and particle size specified by the user. These include the discharge-weighted sediment concentration in volume of sediment per volume of water, the time-derivatives of the discharge-weighted sediment concentrations or the change in the volume of sediment per volume of water per second, and the fractions of each particle size class forming the active, deposition, and original bed layers (Froehlich 2003). The output sediment data file can be used as an input sediment data file for future runs of FST2DH. A separate text output file contains other general information about the sediment run for each timestep, including the sediment transport convergence parameters, the overall sediment concentrations and sediment flow rates for each node in the mesh, the concentrations of each particle size above each node, and the sediment transport rates in the x- and y-directions across each nodestring specified by the user.

1.2 Research Objectives

Before FST2DH can be used reliably for sediment transport simulation, it is critical that the sediment capabilities of the model first be evaluated. The overall purpose of this research is to examine the functionality of the FESWMS FST2DH sediment transport tools and to suggest further enhancements for this model. The following objectives will be met to obtain this purpose:

1. Evaluate the results from FST2DH sediment runs to ensure that they are logical and reasonable.
2. Compare and contrast the results from simple sediment runs in FST2DH and SED2D WES.
3. Compare the resulting equilibrium concentrations from FST2DH to concentrations calculated with several different transport formulas in SAMwin.
4. Analyze models of laboratory flumes created in FST2DH and compare sediment results from FST2DH to those from the laboratory data.
5. Provide additional insight and analysis of trends observed in FST2DH.
6. Provide direction for further development and research of the sediment transport capabilities of FST2DH.

Once these objectives are met, a clearer understanding of the applicability of FST2DH sediment transport modeling will be obtained. The model may then be used in more application work and further feedback can be given to model developers for future revision.

2 Data Processing

Two purposes motivated the research described in this report. The first was to determine the functionality of the various sediment transport options within FST2DH. These include modeling the erosion, transport, and deposition of sediment. The functionality of these options was determined before the fulfillment of the second purpose. The second purpose of the research was to verify the results produced by FST2DH through comparison of those results to observations from physical models and to results from other numerical models such as SAMwin and SED2D WES.

The research initiated the development of several test cases of hypothetical channels to identify the functionality of the individual sediment transport options within FST2DH. A systematic variation of input parameters for each of the sediment options identified the test cases that ran to completion. An analysis of the results from the successful runs identified trends of scour, deposition, and change in velocity. This analysis included an evaluation of whether or not the trends made sense intuitively and if they followed general observations from previous laboratory studies.

Three approaches assisted in the completion of the second objective. The first approach involved the comparison of sediment results from FST2DH to those obtained from a two-dimensional numerical sediment transport model developed by the Army Corps of Engineers, SED2D WES.

Another approach that the research utilized for completing the second objective involved the comparison of sediment concentrations calculated by FST2DH for equilibrium conditions to those output by a separate numerical model, SAMwin. SAMwin was developed by the Army Corps of Engineers, Engineer Research and Development Center (ERDC). It applies a variety of sediment transport functions at a single location in a stream or river to calculate a sediment discharge rating curve based on a specific hydraulic regime and the gradation of the bed. Output from SAMwin includes sediment transport capacity (in tons per day) and sediment concentration (in parts per million) of a river that is in general equilibrium (Thomas 2002). Because FST2DH reports concentrations as volume of sediment per unit volume of water-sediment mixture (Froehlich 2003) and SAMwin reports the concentrations as parts per million (Thomas 2002), the research required the conversion of the FST2DH concentrations to parts per million (ppm) using standard conversions (Richardson 2001) for the comparison.

The final approach that the research utilized to complete the third objective required the creation of models in FST2DH for the simulation of specific expected patterns of behavior and the creation of models to simulate previous laboratory sediment transport experiments outlined in journal articles. The results from each of these model runs provided valuable insight pertaining to the functionality and reliability of the sediment transport options in FST2DH.

The remaining sections of this chapter describe the different test cases created for FST2DH sediment transport analysis. Section 2.1 outlines the flume and associated parameters used for test cases examining the effects of the variation of sediment inflow

and sediment transport capacity equations. Section 2.2 details flumes with varied midsection slopes and Section 2.3 provides the parameters used to create flumes with different types of contractions. These flumes with varying slopes, widths, and input parameters all provided details about the current functionality of the sediment transport options in FST2DH. The next two sections outline the models used for analysis and comparison of FST2DH sediment results to those obtained from SED2D (Section 2.4) and from SAMwin (Section 2.5). The last two sections (Section 2.6 and Section 2.6) give details about the test cases created from physical flume data for FST2DH analysis and a test case built to examine the deposition of sediment that FST2DH predicts as water flows into a reservoir.

Chapter 3 presents the results from the test cases that ran to completion and details the trends observed in those results. Chapter 4 gives the results from runs produced by FST2DH and compares them to those obtained from SED2D WES and SAMwin. It also provides the results from model runs of the test cases built on physical flume data and examines the results from the test case representing the deposition that occurs upon a river's entrance into a reservoir. Finally, Chapter 5 contains the conclusions of the research and provides direction for future work.

2.1 Variation of Inflow Sediment Parameters and Transport Equations

The first set of tests identified the response of FST2DH to variations in the sediment being fed to the domain through the inflow boundary. The documentation for FST2DH includes six different methods for assigning a sediment volumetric flow rate to the inflow boundary:

- Type 0: No Specification (Clear-Water)
- Type 1: Discharge-Weighted Concentrations Assigned as Essential Conditions
- Type 2: Discharge-Weighted Concentrations Assigned as Natural Conditions
- Type 3: Transport Rates Assigned for each Size Class and Concentrations
Applied as Essential Conditions
- Type 4: Transport Rates Assigned for each Size Class and Concentrations
Applied as Natural Conditions
- Type 5: Equilibrium Transport Rates Are Calculated using Flow Parameters and
Are Applied to Inflow Boundary.

The test cases created for each of the inflow specifications consisted of a simple model of a straight flume. Because the test cases were not modeled after an actual flume, arbitrary values were selected for the flowrate, slope, width, and depth to obtain a velocity of approximately one meter per second. This velocity allowed for the movement of a good amount of sediment. Table 2-1 provides a summary of the parameters used in the test cases for various inflow sediment volumetric flowrates.

Table 2-1: Parameters for the Straight Flume Used in Testing the Various Sediment Inflow Specifications and Sediment Transport Equations

<i>Parameter</i>	<i>Value</i>
Flowrate (cms)	15.0
Velocity (m/s)	1.08
Channel Width (m)	30.0
Downstream Depth (m)	0.466
Cross-Sectional Area (m ²)	13.98
Manning's n	0.025
Channel Length (m)	300
Slope (m/m)	0.002
Timestep Length (hr)	0.25
Total Length of Run (hr)	48.0

The test cases for the variation of inflow sediment volumetric flowrate utilized the Engelund—Hansen transport formula because it applies well to the desired bed particle size of 0.2 mm—fine sand (Richardson 2001). Test cases for the sediment inflow concentration assignment (types 1 and 2) consisted of model runs for concentrations of 0, 10, 100, 1,000, and 10,000 parts per million (ppm). Likewise, the test cases for sediment inflow transport rates (types 3 and 4) consisted of runs for transport rates of 0, 1, 5, and 10 cubic meters per second (cms). The clear-water (type 0) and equilibrium transport rate (type 5) options do not allow for the specification of a concentration or transport rate. Therefore, a single test case represents each of these two options. The other parameters required for the model run held the default values recommended in the User's Manual for FESMWS FST2DH (Froehlich 2003).

Straight flume test cases with the same dimensions given above provided appropriate tests for the functionality of the sediment transport capacity equations available in FST2DH. These equations include the Power formula, the Engelund—Hansen formula, the Ackers—White formula, the Laursen formula, Yang's Sand and Gravel formula, the Meyer-Peter—Mueller formula, the Ackers—White—Day formula, and the Garbrecht et al. approach, which uses other formulas already mentioned here. The tests for each of the transport equations included a case for clear-water inflow and a case for an equilibrium transport rate applied to the inflow boundary. Because most of the sediment transport equations available in FST2DH apply to the transport of fine sand, a uniform grain size of 0.20 mm is modeled. The only exception is for the Meyer-Peter—Mueller formula test case, which modeled a slightly larger grain size of 1.0 mm.

2.2 Straight Flume with Varying Midsection Slopes

Three straight flumes with varying midsection slopes model the affect that various slopes along a channel have on the FST2DH sediment results. Each flume contains three segments of varying slope. The length of the flumes was chosen arbitrarily. The selected velocity of 0.5 m/sec in the upstream and downstream segments allowed for the largest amount of sediment movement to occur around the steeper, middle section of the flume. This velocity and arbitrarily-selected values for the width and depth of flow within the upstream and downstream sections resulted in a calculated flowrate of 12.5 cms. From this flowrate, the slope was found through Manning's equation to be 0.00016 m/m for the upstream and downstream segments. The slope of the middle segment varied from flume to flume, being very steep in one flume, moderate in the second flume, and quite shallow in the third. Table 2-2 gives the parameters for the upstream and downstream segments of all three flumes.

Table 2-2: Parameters for the Upstream and Downstream Segments of the Flumes with Varying Midsection Slopes

<i>Parameter</i>	<i>Upstream and Downstream Segments</i>
Flowrate (cms)	12.6
Width (m)	25.0
Downstream Depth (m)	1.0
Cross-Sectional Area (m ²)	25.0
Segment Length (m)	100.0
Manning's n	0.025
Timestep Length (hr)	0.25
Total Length of Run (hr)	48.0

Although done somewhat arbitrarily, an attempt was made to select slopes for each of the middle segments that provided a representation of various water depths and velocities through the middle of the channel. The results from the test case with the steep midsection slope given in Table 2-3 suggested that the other two test cases contain a much shallower midsection slope.

Table 2-3: Slopes for the Middle Segments of the Flumes with Varying Midsection Slopes

<i>Flume</i>	<i>Slope (m/m)</i>
Steep Midsection	0.0667
Moderate Midsection	0.0067
Shallow Midsection	0.0033

The test cases for the flumes with varying midsection slopes utilize the Engelund-Hansen transport formula because results from previous tests indicated that it was functional in FST2DH and because those results appeared reasonable, as will be described later in this report. The three cases tested both clear-water inflow and equilibrium transport rate inflow boundary conditions for beds with uniform particle sizes of 0.08mm, 0.2mm, 2.0mm, and 4.0mm.

Figure 2-1 includes a plot comparing the initial bed elevation profiles for each of the three flumes.

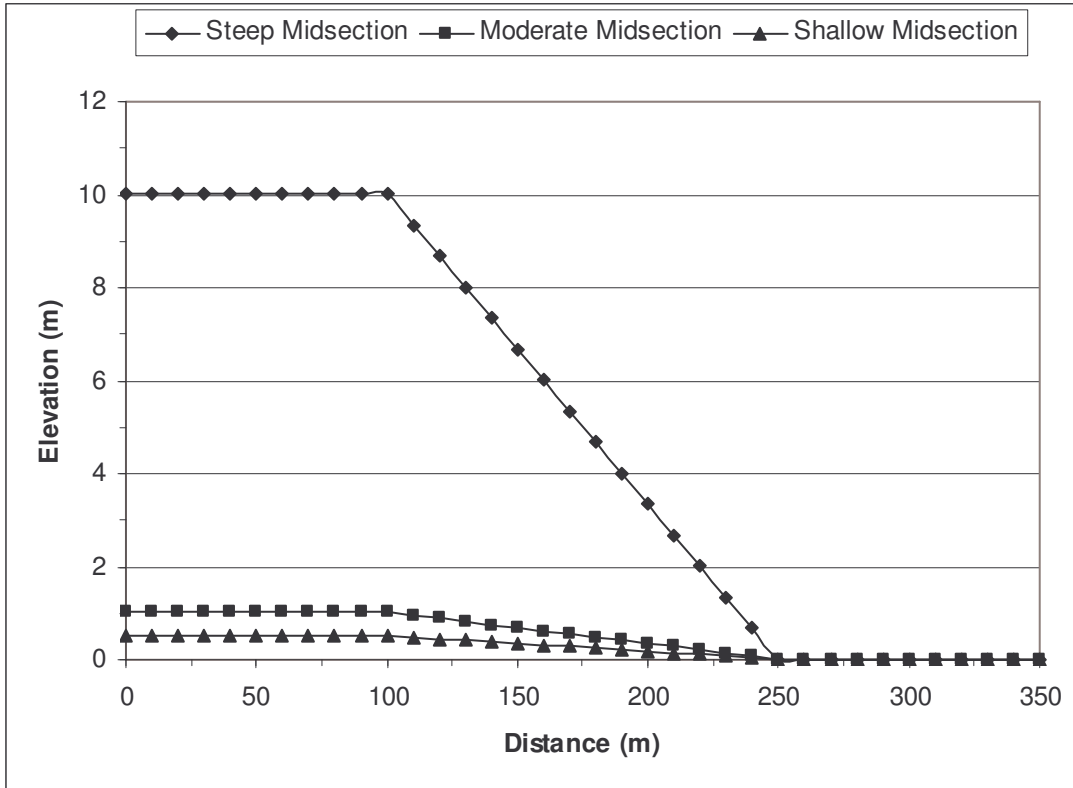


Figure 2-1: Profile of the Three Flumes with Varying Midsection Slope

2.3 Flumes with Contractions

The creation of three simple flumes with contractions allowed for further analysis of the sediment trends represented by FST2DH when the width of a channel changed in different ways. All three flumes with contractions had no slope. The first flume contained a gradual contraction. Its dimensions were chosen arbitrarily. It had a total length of 350 meters and upstream and downstream widths of 30 meters. The contraction started 130 meters downstream from the inflow boundary. The narrowest portion measured 30 meters in length and 10 meters in width, or 40 percent of the original width. The transitions to and from the contraction to the upstream and downstream widths of the

channel each measured 30 meters in length. The tests included cases for both the clear-water and equilibrium transport rate inflow specifications for each of four different particle sizes: 0.08 mm, 0.20 mm, 2.0 mm, and 4.0 mm. The parameters for the flume with a gradual contraction given in Table 2-4 were chosen arbitrarily, with an emphasis placed on obtaining an upstream velocity of 0.5 meters. This created an increased velocity through the contraction and provided informative sediment results in that area.

Table 2-4: Parameters for the Flume with a Gradual Contraction

<i>Parameter</i>	<i>Upstream and Downstream Segments</i>
Flowrate (cms)	12.5
Velocity (m/s)	0.50
Width (m)	25.0
Downstream Depth (m)	1.0
Cross-Sectional Area (m ²)	25.0
Manning's n	0.025
Slope (m/m)	0.000
Timestep Length (hr)	0.25
Total Length of Run (hr)	48.0

Figure 2-2 shows a plan view of the flume with a gradual contraction.

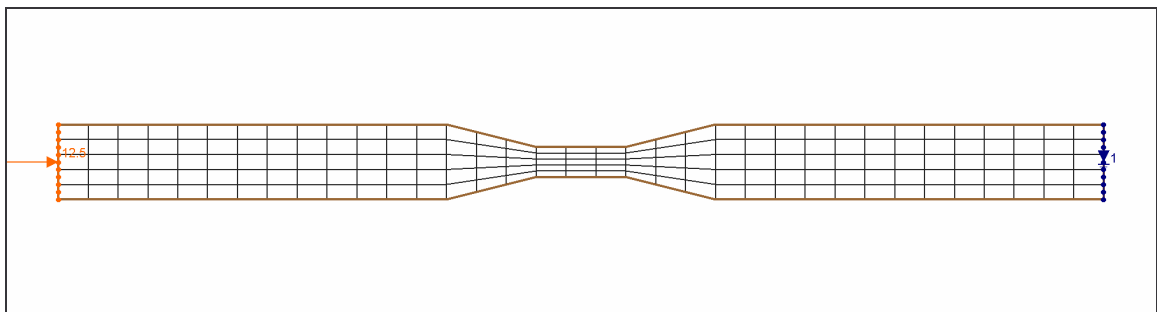


Figure 2-2: Plan View of the Flume with a Gradual Contraction

The second set of test cases for contractions modeled a flume with a long abrupt contraction. This flume followed the same general description as the one described above, except that the contraction began and ended abruptly. The parameters given above in Table 2-4 applied to this set of test cases in addition to those of the flume with a gradual contraction. Figure 2-3 provides a plan view of the flume with a long abrupt contraction.

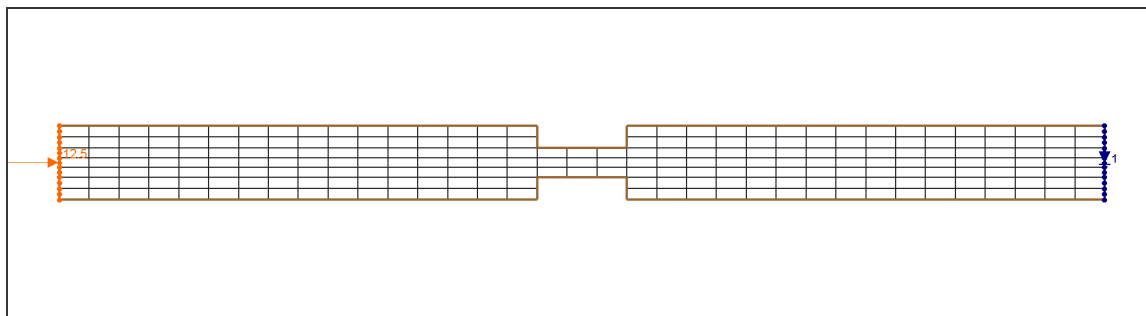


Figure 2-3: Plan View of the Flume with a Long Abrupt Contraction

The final set of test cases for a flume with a contraction modeled a channel that contained a short abrupt contraction, similar to that often observed at a narrow river opening under a highway bridge. The test case for the flume with an abrupt contraction represented a hypothetical channel. The flowrate, depth, widths for the main channel and the contraction, and other related parameters were again chosen arbitrarily with the intent of providing a reasonable velocity of 0.5 m/s both upstream and downstream of the contraction. Table 2-5 lists the main parameters applied to this test case and Figure 2-4 provides a plan view of the flume with a short, abrupt contraction.

Table 2-5: Parameters for a Flume with a Short Abrupt Contraction

<i>Parameter</i>	<i>Upstream Segment</i>	<i>Contraction</i>	<i>Downstream Segment</i>
Flowrate (cms)	12.5	---	12.5
Velocity (m/s)	0.50	0.50	0.50
Channel Width (m)	25.0	6.5	25.0
Downstream Depth (m)	---	---	0.75
Manning's n	0.025	0.025	0.025
Segment Length (m)	107.5	10.0	107.5
Slope (m/m)	0.000	0.000	0.000
Timestep Length (hr)	0.25	0.25	0.25
Total Length of Run (hr)	48.0	48.0	48.0

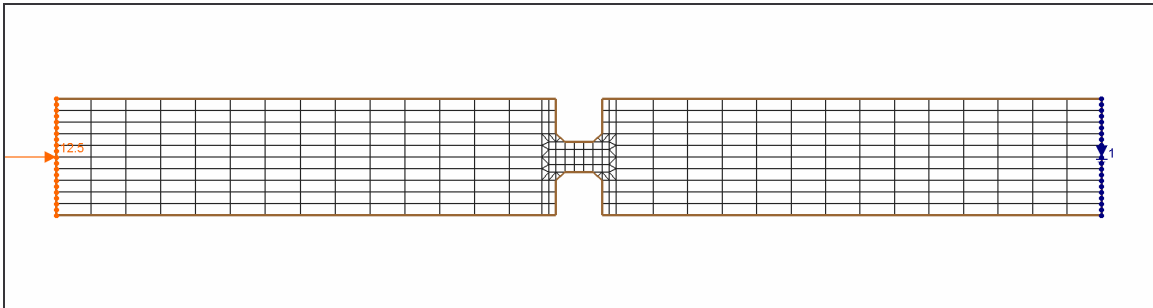


Figure 2-4: Plan View of the Flume with a Short Abrupt Contraction

2.4 SED2D WES Flumes

SED2D WES is the sediment transport program within the TABS-MD Numerical Modeling System, developed by the U.S. Army Corps of Engineers. It relies on the hydrodynamic output from a companion program, RMA2 for its sediment calculations, and therefore only supports the uncoupled option. Thus, if the user desires to obtain a semi-coupled solution, he or she must manually iterate between the RMA2 hydrodynamic and SED2D WES sediment models for each timestep to create the final solution.

SED2D WES computes the movement of cohesive (clay) or non-cohesive (sand and gravel) sediment and only supports a single grain size (USACE 2004). The output from SED2D WES includes one file containing the new bed geometry, a separate file containing the concentration of sediment and the total change in bed at each node, and a third file, the bed structure file, that contains information about the consolidation and age of each of the bed strata for cohesive materials or the thickness of the erodible bed layer for non-cohesive modeling (USACE 2004).

The research included two different test cases for comparison of results from FST2DH and SED2D WES. The first case consisted of the flume with a moderate midsection slope described earlier in this report (section 2.2). Because of the different input options supported by SED2D WES and FST2DH, the parameters entered for each of the two sediment simulations differed slightly. However, the input parameters for SED2D WES were chosen so as to best replicate the same conditions that existed in the FST2DH test case. Initially, test cases were to be developed for each of the four particle sizes used in the FST2DH clear water analysis. However, the results from the first test indicated that doing so would not be beneficial, so the first test case only consisted of a single run in SED2D WES, with a uniform particle size of 0.2 mm. The clear water condition was applied to the inflow boundary.

The second test case used in the comparison of sediment results from FST2DH and SED2D consisted of tests for the flume with a gradual contraction. As with the moderate midsection slope test case, the parameters for the flume with a gradual contraction were assigned in such a manner that the SED2D WES simulation most closely matched that described previously for the FST2DH gradual contraction test case.

The test cases for SED2D WES contained uniform particle sizes of 0.08 mm, 0.2 mm, 2.0 mm and 4.0 mm. While two of the FST2DH test cases for the gradual flume with clear water inflow failed to run to completion, the results from SED2D WES could still be compared with those from the FST2DH equilibrium transport rate cases. The comparison was appropriate because none of the tests for that flume showed scour or deposition upstream from the contraction. Therefore, the clear water and equilibrium transport rate results were identical, as will be explained in more detail in chapter 3. For now, it is sufficient to note that the comparison between the clear water and equilibrium transport rate test case results is appropriate for this flume.

While SED2D outputs values at each timestep for the change in bed at each node, it does not directly provide bed elevations. On the other hand, FST2DH outputs bed elevations at each node and not the change in bed. Therefore, comparisons of the final bed elevations for each model were established by creating a new dataset representing the sum of the initial bed elevation and the final change in bed for the SED2D WES test cases. Chapter 4 contains the resulting bed elevations from each of the models.

2.5 SAMwin Flumes

The next set of test cases consisted of straight flumes used for comparing sediment concentrations calculated by FST2DH for equilibrium conditions to those output by SAMwin. SAMwin applies a variety of sediment transport functions at a single location in a river to calculate a sediment discharge rating curve based on a specific hydraulic regime and the gradation of the bed. Output from SAMwin includes the sediment transport capacity (in tons per day) and sediment concentration (in parts per

million) for a river in general equilibrium (Thomas 2002). FST2DH reports concentrations as the volume of sediment per unit volume of the water-sediment mixture (Froehlich 2003) and SAMwin reports the concentrations as parts per million (Thomas 2002). Because of this difference, the equilibrium concentrations calculated by FST2DH were converted to parts per million (ppm) for comparison to SED2D WES output using standard conversions (Richardson 2001).

The research created simple, straight-flume test cases for comparison between the concentrations predicted by FST2DH and SAMwin. The parameters arbitrarily selected for these test cases allowed for the creation of a rectangular flume with a relatively moderate slope, providing velocities that fell in the desired range of 2.5 fps and 5.5 fps. Table 2-6 lists the main parameters used in these test cases.

Table 2-6: Parameters for the SAMwin Flume

<i>Parameter</i>	<i>Value</i>
Upstream Elevation (ft)	1.5
Downstream Elevation (ft)	0.0
Length (ft)	1,000.0
Slope (ft/ft)	0.0015
Width (ft)	70.0
Left Side Slope (Horiz to 1.0)	0.0001
Right Side Slope (Horiz to 1.0)	0.0001
Manning's n	0.025
Water Temperature (°F)	40.0
Specific Gravity	2.65
Kinematic Viscosity (ft ² /sec)	1.662*10 ⁵

For simplicity, most of the parameters held the default values set by SAMwin. The same values were assigned to the appropriate parameters during the setup of each FST2DH simulation. Each test case included a run for a uniform particle size of 0.177

mm and one for a uniform size of 1.414 mm. These sizes were chosen because SAMwin writes out information for these specific size classes and because they fell closest to the particle sizes used in previous FST2DH test cases.

The suite of tests was first run in SAMwin for the various flowrates given in Table 2-7. The flowrates were chosen arbitrarily. Test cases with similar parameters then ran in FST2DH. A comparison of the resulting equilibrium concentrations from each model followed.

Table 2-7: Flowrates, Velocities, and Water Depths for the SAMwin Test Cases

<i>Test Case</i>	<i>Flowrate (fps)</i>	<i>Velocity (ft/s)</i>	<i>Water Depth (ft)</i>
1	300	2.95	1.45
2	500	3.62	1.97
3	700	4.14	2.41
4	900	4.58	2.81
5	1100	4.96	3.17
6	1300	5.31	3.50

2.6 Laboratory Models

In addition to the test cases described above, the research included several model runs based on data given for previous sediment transport research completed with laboratory flumes. Most of the research completed in the laboratory consists of simulations of sediment movement in relatively small flumes as opposed to actual rivers. As will be explained in a later chapter, the small size of the modeled flumes presented some difficulties. These test cases included the following FST2DH models found in articles describing previous research:

- A flume showing the scour patterns and depths around a pier (Sheppard 2004)
- A flume with varying entrance and exit angles for a long contraction (Dey 2005)
- A basin illustrating the scour from clear water inflow (Duc 2004, Wu 2004)
- A narrow flume demonstrating downstream fining (Seal 1997)
- A wide flume demonstrating downstream fining (Toro-Escobar 2000)

The journal articles listed as references for each bullet in the list above provided the data for each their respective test cases. The different attempts to simulate the laboratory models in FST2DH illustrated the effect that the size of the domain had on the FST2DH simulation results. They also brought to light the need for the various options that should be functional in FST2DH sediment transport. While research led to many other laboratory sediment experiments, they required advanced modeling features that are not currently functional in FST2DH. Detailed information about each of the laboratory test cases given in this report may be found in their respective papers.

2.7 Deposition in a Reservoir

As part of a journal article, Hotchkiss et al. explained how aggradation occurs due to backwater when a dam is placed across a river (Hotchkiss 1991). As a river enters a reservoir, its depth and cross-sectional area increases and the velocity of the water quickly decreases. The slowing velocity causes some of the sediment within the river to deposit on the riverbed. Over time, this deposited material forms a delta. The final test case examined by the FST2DH research modeled this aggradation.

The test case for the flume entering the reservoir contained arbitrary parameters but still provided insight into how FST2DH models such a situation. The straight flume

created for this test was 150,000 meters long and 300 meters wide. It had a slope of 0.00075 m/m and an upstream normal depth of 1.44 meters. The first run with this flume contained a single particle size of 0.5mm for the bed and sediment inflow. A second run included two particle sizes—0.5mm and 2.0mm. Table 2-8 gives these and other important parameters used in the creation of the flume. Figure 2-5 shows the water surface and elevation profiles for the steady-state solution.

Table 2-8: Parameters for the Flume Showing Deposition at the Entrance to a Reservoir

<i>Parameter</i>	<i>Value</i>
Length (m)	150,000
Width (m)	300
Slope (m/m)	0.00075
Upstream Normal Depth (ft)	1.44
Depth at Outflow Boundary(m)	7.0
Manning's n	0.025
Flowrate (m ³ /sec)	604.0
Upstream Velocity (m/sec)	1.40
Downstream Velocity (m/sec)	0.29
Timestep Length (hours)	24.0
Total Length of Run (days)	180

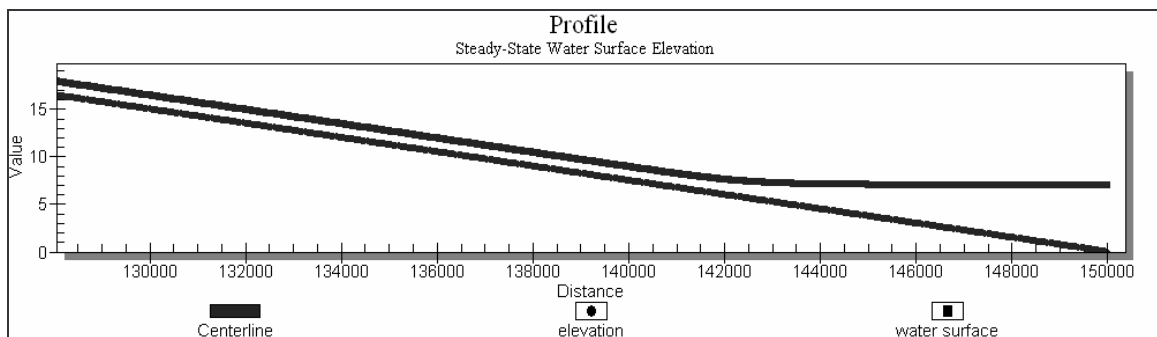


Figure 2-5: Profile of Water Surface at the Downstream End of a Flume Emptying into a Reservoir

Research also created a second set of test cases for the flume showing deposition in a reservoir. The purpose for these test cases was to discover how well FST2DH handles sediment transport in a long, shallow-sloped river, where a delta forms over a long period of time. The tests included four different element sizes in an attempt to create a stable solution over a long model run. The 200,000 meter long, 500 meter wide flume had a slope of 0.00025, which was about one-third the value of the slope used in the first reservoir deposition test case. The flume's upstream velocity was 1.0 m/sec and the upstream water depth was 2.0 meters. Table 2-9 shows the different element sizes tested.

Table 2-9: Element Properties for the Test Cases for a Long Flume Emptying into a Reservoir

<i>Test Case</i>	<i>Element Length (m)</i>	<i>Element Width (m)</i>	<i>Number of Elements Along Channel Length</i>
A	8,695.7	100	23
B	3,448.3	100	58
C	1,739.1	100	115
D	865.8	100	231

3 Presentation of Results: Qualitative Analysis

The purposes of this report include identifying the areas of functionality within the sediment transport portion of FST2DH and determining the accuracy of the model in representing the movement of sediment. The research accomplished this in the three ways described in the previous chapter. This chapter provides and interprets the sediment results from FST2DH for each of the test cases. The next chapter of this report gives a comparison of results from FST2DH to those from SAMwin and SED2D WES and also explains the sediment results from FST2DH models of real laboratory flumes and compares them to results obtained through previous research.

3.1 Variation of Sediment Inflow and Transport Formulas

The examination of the sediment transport functionality within FST2DH began with a look at the effects of the variation of the sediment volumetric flow rate that was specified for the inflow boundary. For these initial runs, the research focused on two factors which included:

1. Did the model run to completion? If not, when did the failure occur and what caused it?
2. Does the changing bed elevation for the successful runs seem reasonable and intuitive?

The research moved to a second set of runs that contained variation of the sediment transport capacity formula applied to the test cases. It was anticipated with these runs that the bed elevation would not vary from one side of the channel to the other because the test cases were rectangular flumes of uniform width and constant slope. As was expected, the variation of bed elevations occurred along the length of the channel for all test cases given in this section of the report. Figure 3-1 shows an example of the bed elevation variation along the length of the channel and the lack of variation from one side of the channel after two days. The time given in the upper left hand corner of this and all the remaining plan views gives the timestep that the contoured image represents, shown in days, hours, minutes, and seconds. For these test cases, a longitudinal profile of the bed elevations presents a clear representation of the simulation. The following sections present a series of longitudinal profiles for the various test runs.

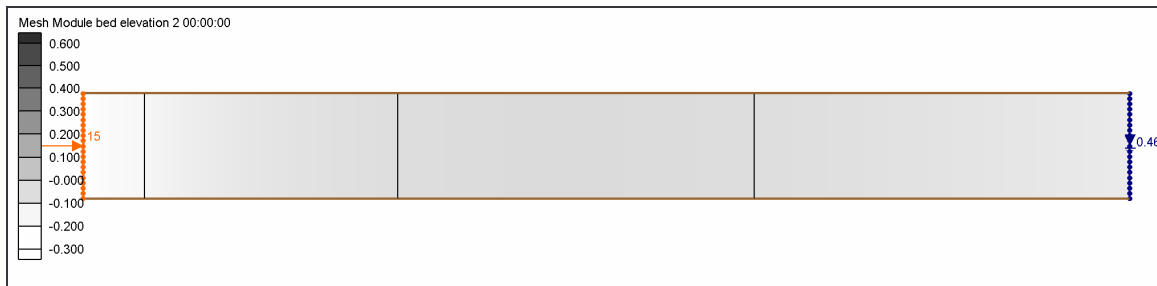


Figure 3-1: Variation of Bed Elevation along the Length of a Straight Flume

3.1.1 Sediment Volumetric Flow Rate at the Inflow Boundary

As was explained earlier, FST2DH provides the user with six different options for the specification of a sediment volumetric flow rate at the inflow boundary. All six

inflow specifications were tested with the same flume. The test cases with what the FST2DH documentation refers to as natural conditions both failed within the first hour of the simulation due to an access violation within the FST2DH program. This included type 2 (natural sediment concentration) and type 4 (natural transport rate). The test cases for the remaining sediment flow rate specifications all ran to completion. Their results follow.

The first profile comes from the test cases with clear water entering the domain (type 0). The plot (Figure 3-2) includes the initial bed elevation profile along with the final bed elevation profile after a 48-hour simulation.

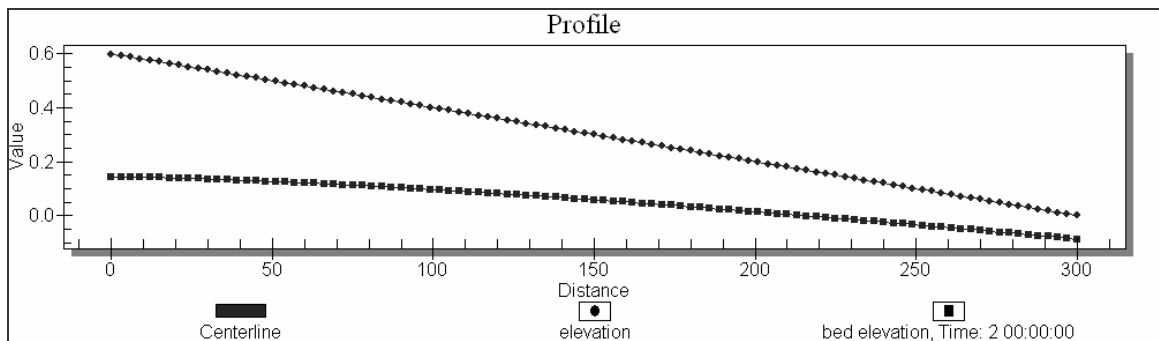


Figure 3-2: Initial and Final Bed Elevation Profiles for Clear-Water Inflow

When clear water enters the mesh, the clear-water should quickly pick up sediment near the inflow boundary, scouring the bed drastically. Further downstream, once the water is already carrying some sediment, less scour should occur. Figure 3-2 reflects this pattern.

The test cases for the sediment concentration being specified at the inflow boundary as essential conditions (type 1) all ran to completion. The FST2DH

documentation indicates that these concentrations are in parts per million (ppm). In the test cases presented in this section, the inflow concentration ranged from 0 ppm to 10,000 ppm. It would be expected that as the inflow concentration increases, the amount of sediment that is picked up by the incoming water would decrease. Extending this concept, at some point, deposition should begin. All of these cases generated identical results (Figure 3-3) indicating that this option is not currently functioning correctly in FST2DH and the results are not reliable. The fact that all of these cases generated more scour than the clear-water cases casts more suspicion on the model with this option.

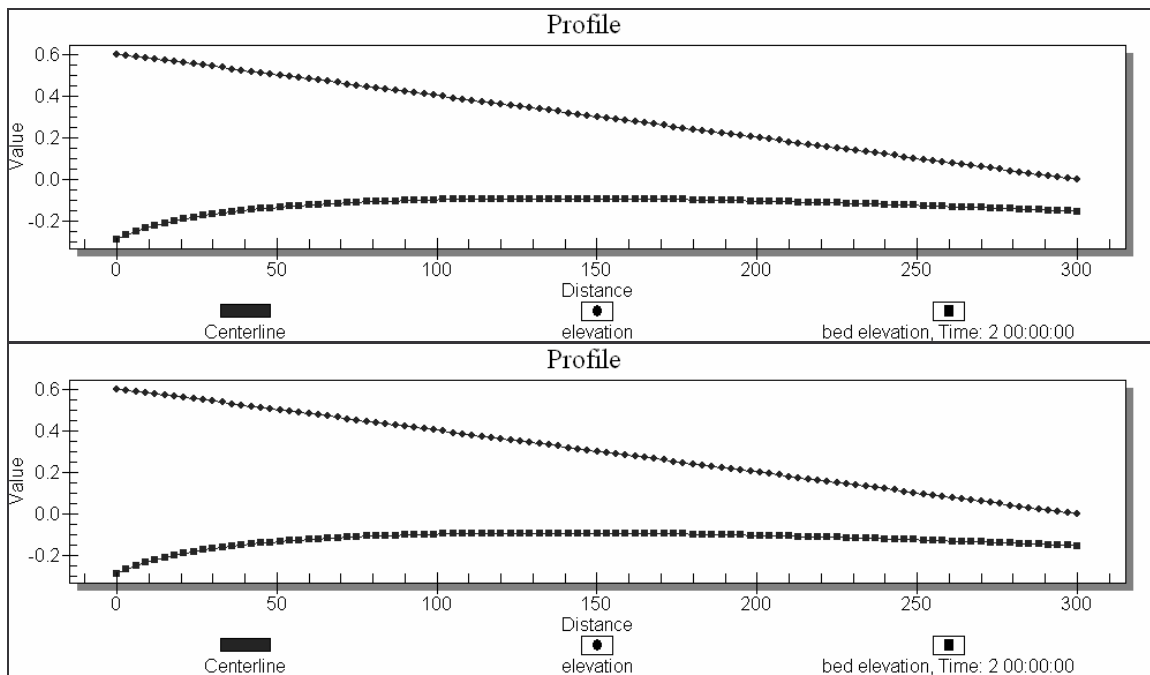


Figure 3-3: Final Bed Elevations for Concentrations of 10 and 10,000 ppm (Essential Conditions)

Another option included in FST2DH for inflow of sediment supports the specification of the sediment transport rate at the inflow boundary as essential conditions (type 3). As with type 1, this series included several tests with progressively larger

transport rates. The resulting bed profiles for each 48-hour simulation were again identical to each other, regardless of the actual transport rate being specified at the inflow boundary. This is shown in Figure 3-4. Furthermore, the resulting bed elevation profiles from these test cases were identical to the profiles shown in Figure 3-3 for the sediment concentration being specified as essential conditions (type 1). Thus, this research concluded that FST2DH does not appropriately handle variation in either sediment concentrations or flow rates assigned to the inflow boundary, and the results obtained with the use of either option are not reliable.

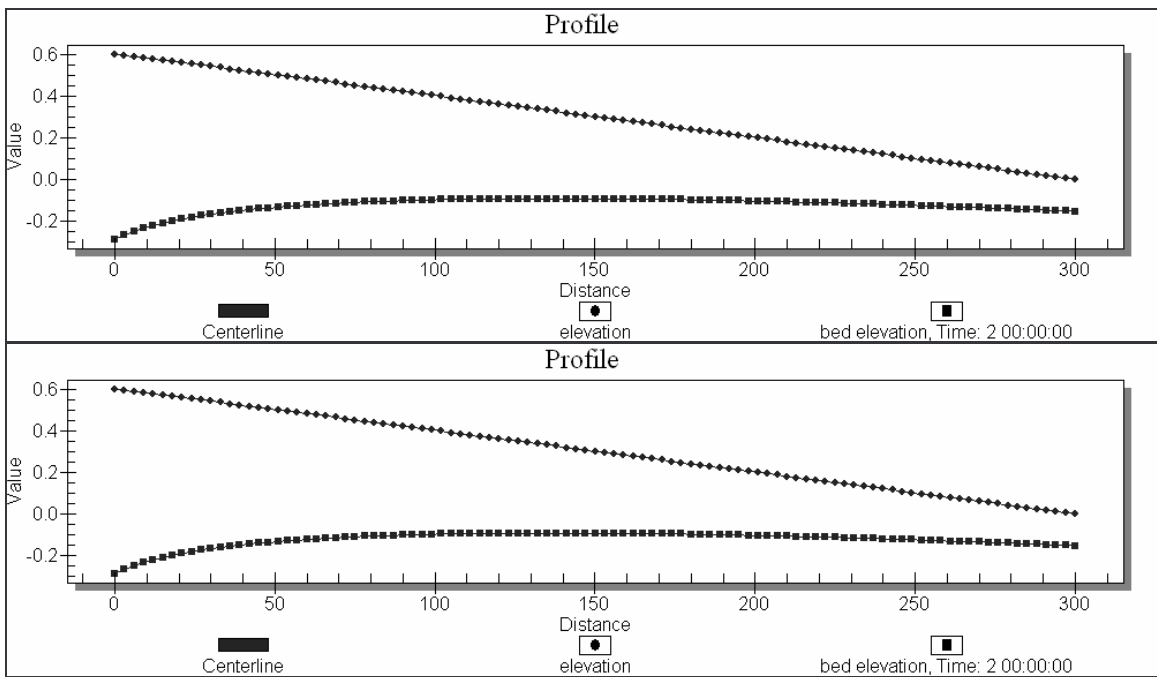


Figure 3-4: Final Bed Elevations for Sediment Transport Rates of 1 and 10 cms (Essential Conditions)

The final option included in FST2DH for inflow of sediment applies an equilibrium sediment transport rate to the inflow boundary (type 5). In this case,

FST2DH calculates the water's sediment carrying capacity for the conditions along the upstream boundary and applies that sediment load to the incoming water. Thus, neither scour nor deposition should take place at the inflow boundary. Furthermore, because the channel is of a uniform width and slope, the entire channel bed should not change in elevation over time. Figure 3-5 shows both the initial and final profile as the same, which seems to indicate that the simulation was appropriately modeled by FST2DH.

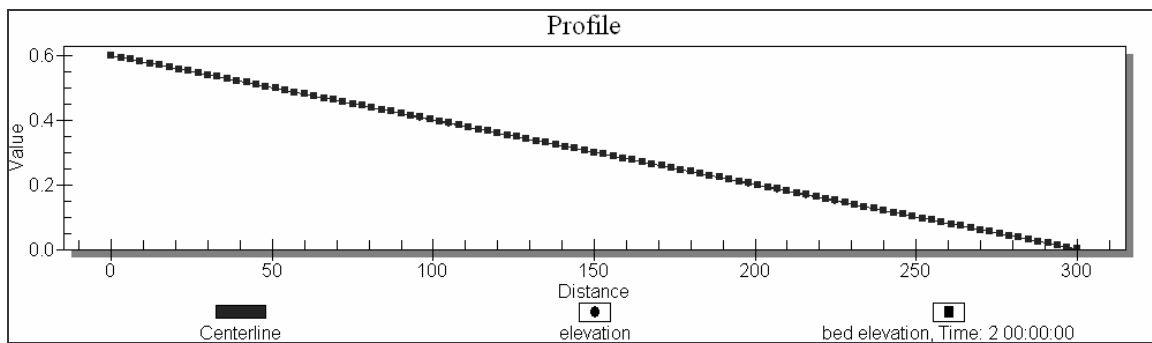


Figure 3-5: Final Bed Elevations for an Equilibrium Transport Rate Inflow

The test cases for the variation of sediment flow rate options showed that although several different methods for specifying clear water entering the domain exist, each method provides different solutions when the solutions should be identical. The test case with a concentration of 0 ppm specified as essential conditions (type 1) provided the same result as the test case with the specification of a sediment transport rate of 0.0 cms with concentrations being applied as essential conditions (type 3). The final bed elevation profiles from these two cases after a 48-hour run showed more scour than the profile obtained from the clear water (type 0) case. Individually, the results from each

test case seem reasonable. However, the difference in scour between the test cases raises questions about their reliability.

The results from the test cases for clear water entering the domain (type 0) and an equilibrium sediment transport rate being applied to the inflow boundary (type 5) best represented expected results and patterns. As such, the remaining test cases included tests for one or both of these sediment inflow rate methods.

3.1.2 Sediment Transport Capacity Formula

FST2DH provides the user with the choice of eight different equations for calculating the sediment transport capacity within a modeled stream. The next set of test cases included a run for each of the eight equations for both the clear-water inflow and equilibrium transport rate inflow conditions. An additional test case for each inflow condition was also created for a variation of the a and b parameters used in the Power equation. Table 3-1 shows that five of the nine test cases ran to completion.

Table 3-1: Completion of Runs with Varying Transport Equations

<i>Transport Equation Used</i>	<i>Run To Completion?</i>
Power (a=1.0, b=1.0)	No
Power (a=0.5, b=0.75)	No
Engelund-Hansen	Yes
Ackers-White	No
Laursen	Yes
Yang Sand and Gravel	Yes
Meyer-Peter—Mueller	Yes
Ackers—White—Day	Yes
Garbrecht et al. (Combination Approach)	No

The runs that failed most commonly provided the error message, “!ERROR - RowCount > MaxFrontWidth in xAssemble. Stopping...” The test cases that ran to completion all did so for both the clear-water and equilibrium transport rate inflow conditions. Furthermore, all the ones that failed did so for both inflow conditions. The successful models that were assigned an equilibrium transport rate inflow condition all maintained the same bed profile as that of the initial bed throughout the entire 48-hour simulation, regardless of sediment transport equation used. This provides evidence that the equilibrium inflow specification works appropriately with the currently-functional transport equations in that FST2DH is calculating the correct transport rate so as to keep scour and deposition from occurring.

The test cases with clear water entering the mesh all resulted in scouring of the bed. The amount of erosion varied with the transport equation being used. This makes sense, as the different equations each use different methods to calculate the transport capacity of the channel, which results in a different amount of sediment being carried away in each case. None of the test case results suggested that deposition had occurred. However, this is not surprising since the slope and cross section remain constant and clean, sediment-hungry water is entering the domain.

Figure 3-6 provides a comparison of the initial bed profile and final bed profiles after a 48-hour simulation using the Engelund—Hansen formula, the Laursen formula, the Yang Sand and Gravel formula, the Meyer-Peter—Mueller formula, and the Ackers—White—Day formula.

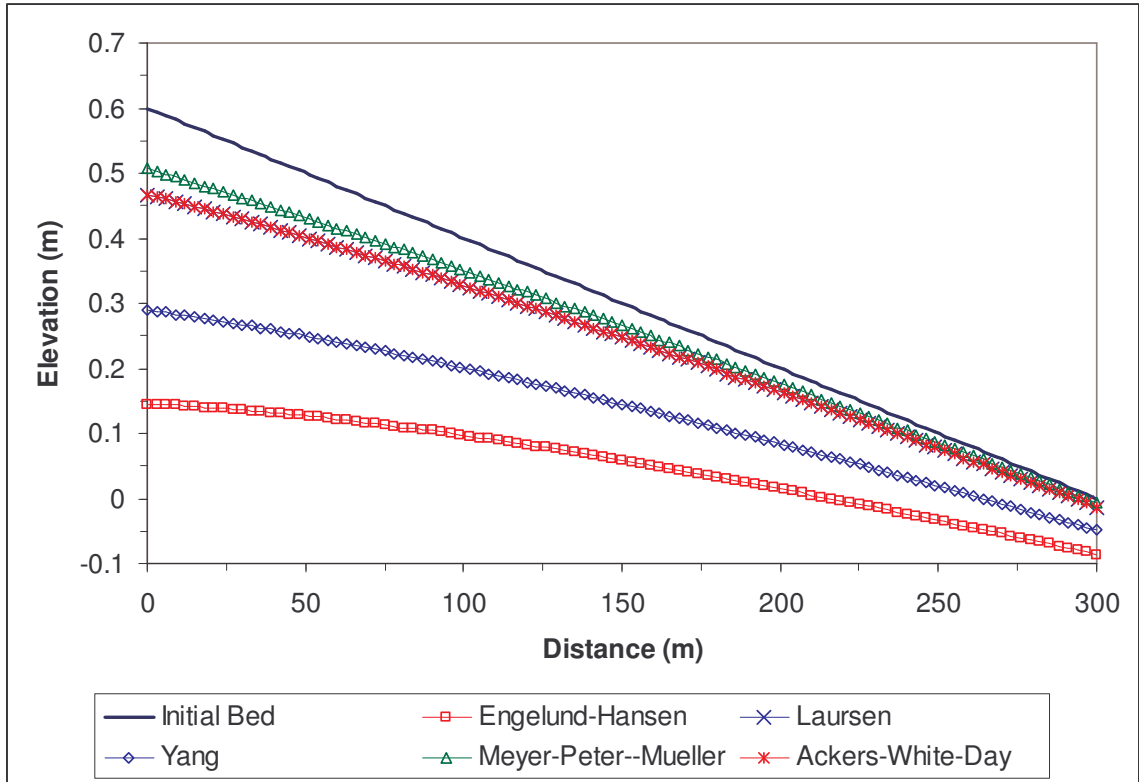


Figure 3-6: Final Bed Elevations for the Sediment Transport Capacity Equation Test Cases

The results from the FST2DH sediment runs with varying transport equations showed that the Meyer-Peter—Mueller equation predicted the least amount of scour over the 48-hour time period. This makes sense because the test case for the Meyer-Peter—Mueller formula contained a slightly larger bed particle size than the other tests (0.5 mm compared to 0.2mm) due to its applicability to a slightly larger minimum particle size (Thomas 2002). The Ackers—White—Day and Laursen formulas predicted nearly the same change in bed profile and also predicted the least amount of scour for the group of test cases that used the 0.2mm uniform grain size. Because the results from the two equations are nearly identical, it may be possible that one of them was incorrectly implemented, and the implementation should be investigated by the FST2DH developers.

The Engelund—Hansen predicted the most scour. Table 3-2 provides a comparison of the depths of scour predicted by the equations. Chapter 4 includes more discussion of the variation of results for different transport equations when comparing those from FST2DH to those from SAMwin.

Table 3-2: Scour Predicted by Various Equations for a 48 Hour Simulation

<i>Transport Equation</i>	<i>On Inflow Boundary (m)</i>	<i>Average in Channel (m)</i>
Meyer-Peter—Mueller	0.093	0.04
Ackers—White—Day	0.133	0.059
Laursen	0.133	0.059
Yang Sand and Gravel	0.310	0.163
Engelund—Hansen	0.455	0.251

3.2 Varying Midsection Slopes

The test cases described thus far have only shown scour and not deposition. However, due to the fact that only sediment inflow types 0 and 5 appear to be working, the results seem reasonable. The results from test cases with varying slopes along the longitudinal axis will now be discussed. For these cases, the middle segment of each of the test cases described in this section of the report had a steeper slope than its upstream and downstream counterparts. This condition leads to the expectation that erosion would occur on the upstream portion of the central slope due to increased transport capacity, and that deposition would occur on the downstream portion as the slope flattens again. This expected trend was tested with the flumes with varying midsection slopes. These test cases also provided further identification of the aspects of sediment transport options in FST2DH that are currently functional. The following three sections describe the results

from the three test cases with varying midsection slopes. The tests included three central slopes: 0.0667 m/m, 0.0067 m/m, and 0.0033 m/m. The results from the test case with the steepest slope will be given first, followed by those from the moderate slope test case, and then those from the case with the shallowest slope will be provided.

3.2.1 Steep Midsection Slope

The steady state hydrodynamic solution showed that the slope of the channel's middle segment was steep enough to create supercritical flow through that section, resulting in a hydraulic jump near the break in slope at the downstream end of the steeper section, as the water jumped back to subcritical flow downstream. This is illustrated in the profiles of the initial bed elevation and the water surface calculated by a steady-state hydrodynamic run of FST2DH and shown in Figure 3-7. All of the test cases for the steep midsection slope failed to run to completion once the sediment calculations were added. Thus, neither the variation of the type of sediment inflow specification (clear-water or equilibrium transport rate), nor the variation of sediment particle size seemed to

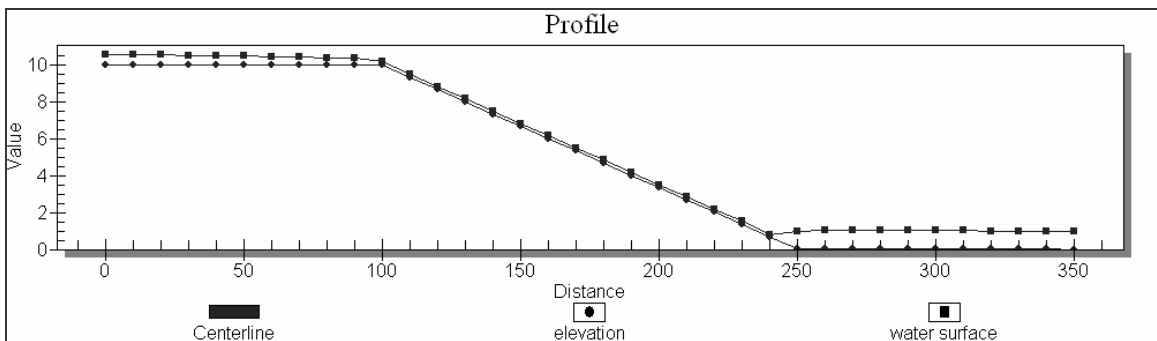


Figure 3-7: Steady-State Bed and Water Depth Profiles for a Flume with a Steep Midsection Slope

affect the outcome. The instability within the sediment model run may have been caused by the presence of the hydraulic jump and/or the shallow water depth (0.13 meters) just upstream of the jump.

3.2.2 Moderate Midsection Slope

The steady-state hydrodynamic solution for the test cases with a moderate midsection slope (0.0067 m/m) shows that the flow throughout the entire channel remained subcritical. Furthermore, the solution, shown in Figure 3-8, suggests that the backwater curve from the change in the bed extends upstream beyond the inflow boundary.

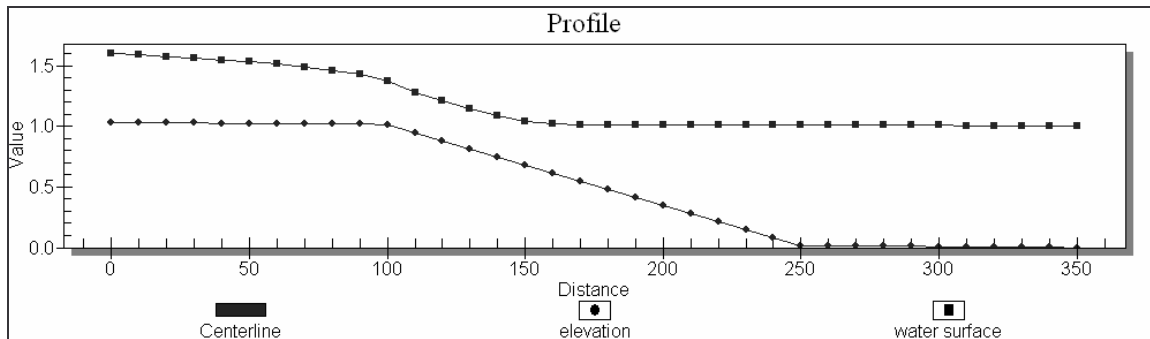


Figure 3-8: Initial Bed Elevation and Water Surface for a Flume with a Moderate Midsection Slope

The test cases for a moderate midsection slope showed that the simulation of sediment transport in FST2DH was much more stable for the equilibrium transport rate option for the inflow boundary than it was for the clear-water inflow case. While only one of the four test cases with clear water entering the mesh ran to completion (the case

for 0.2mm), all four of the test cases with the equilibrium transport rate option ran to completion.

The next two figures (Figure 3-9 and Figure 3-10) show the progression of the change in the bed profile throughout the 48-hour simulation for the test case with clear water and a uniform grain size of 0.2mm. Each plot includes the initial bed elevations for comparison.

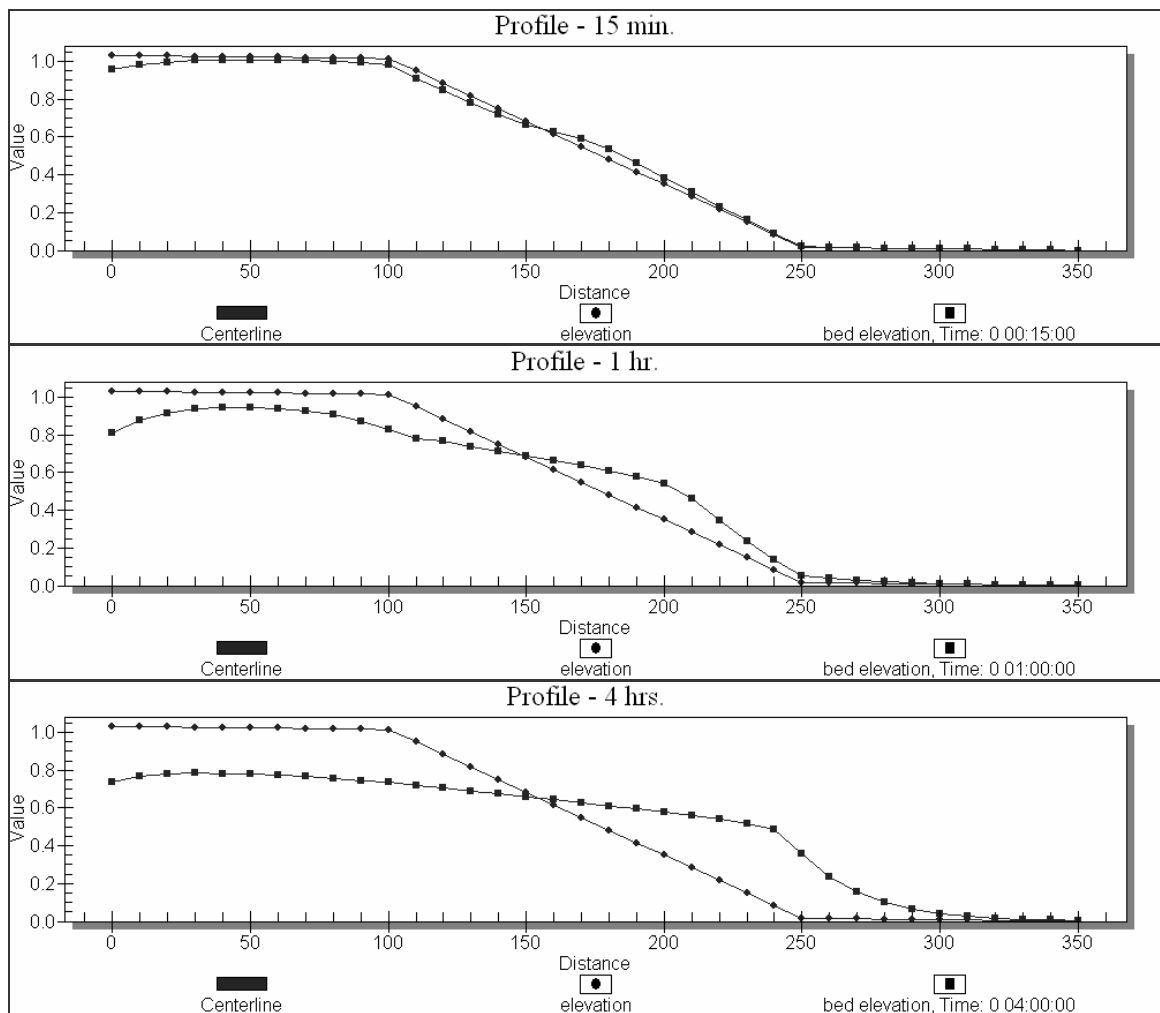


Figure 3-9: Bed Elevations for the Clear-Water Moderate Midsection Slope Flume with a Uniform Particle Size of 0.2mm at 15 Minutes, 1 Hour, and 4 Hours

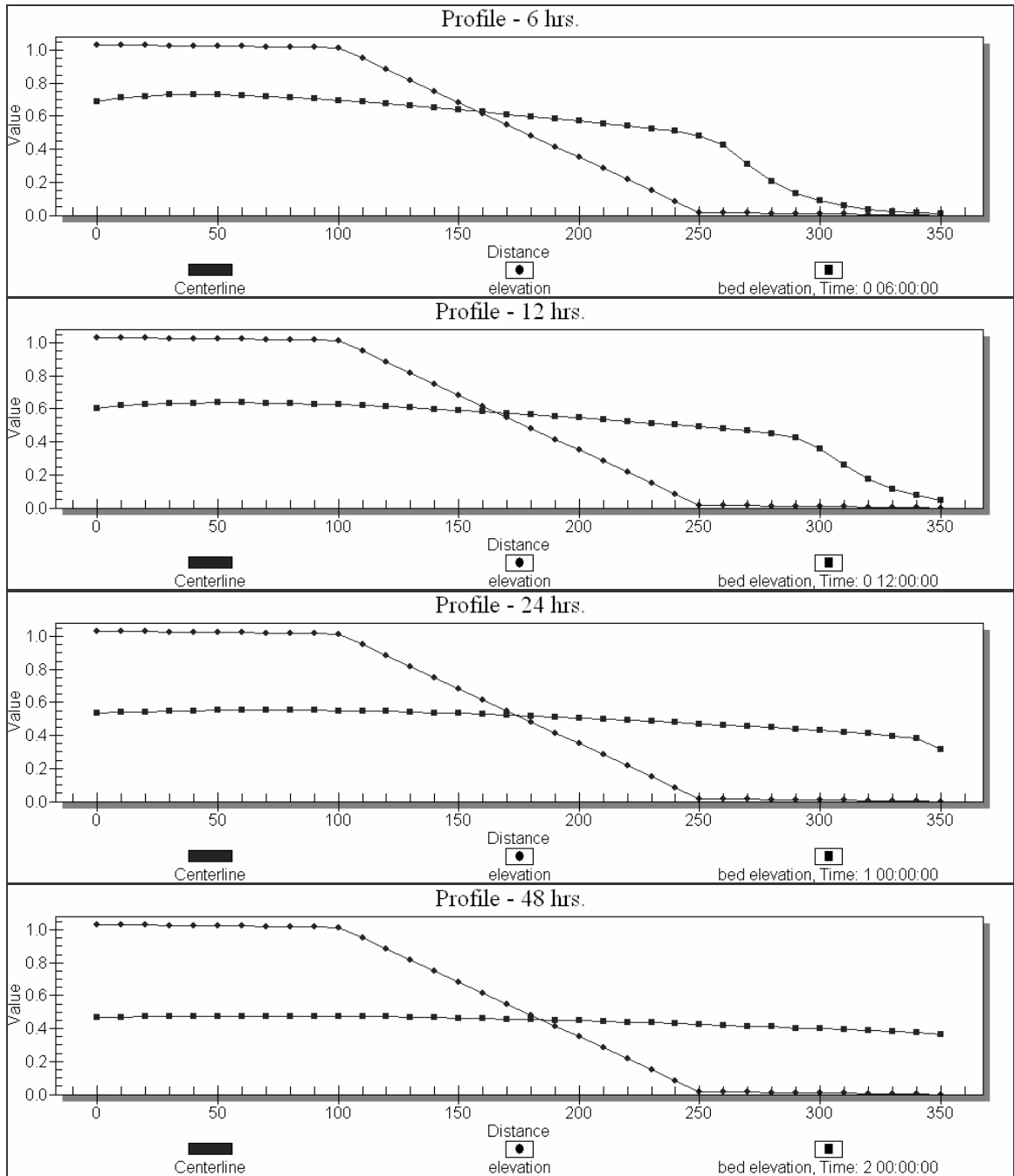


Figure 3-10: Bed Elevations for the Clear-Water Moderate Midsection Slope Flume with a Uniform Particle Size of 0.2mm at 6 Hours, 12 Hours, 24 Hours, and 48 Hours

The profiles in the figures show that, as would be expected, scouring began right at the upstream boundary, with the clear water picking up whatever sediment it can. The

plots also show that over time, the bed at the upstream end of the steeper midsection eroded away and that deposition of sediment occurred near the downstream end of the middle section. Eventually, the bed flattened out. Brush et al. observed similar patterns of change in the bed profile over time in laboratory experiments of a channel with a steepened midsection (Brush 1960). Thus, these trends follow very closely to the anticipated behavior. The simulation continued to follow anticipated behavior over time as it showed that equilibrium would never be reached because clear water continues to enter at the upstream end and the bed would just continue to scour away.

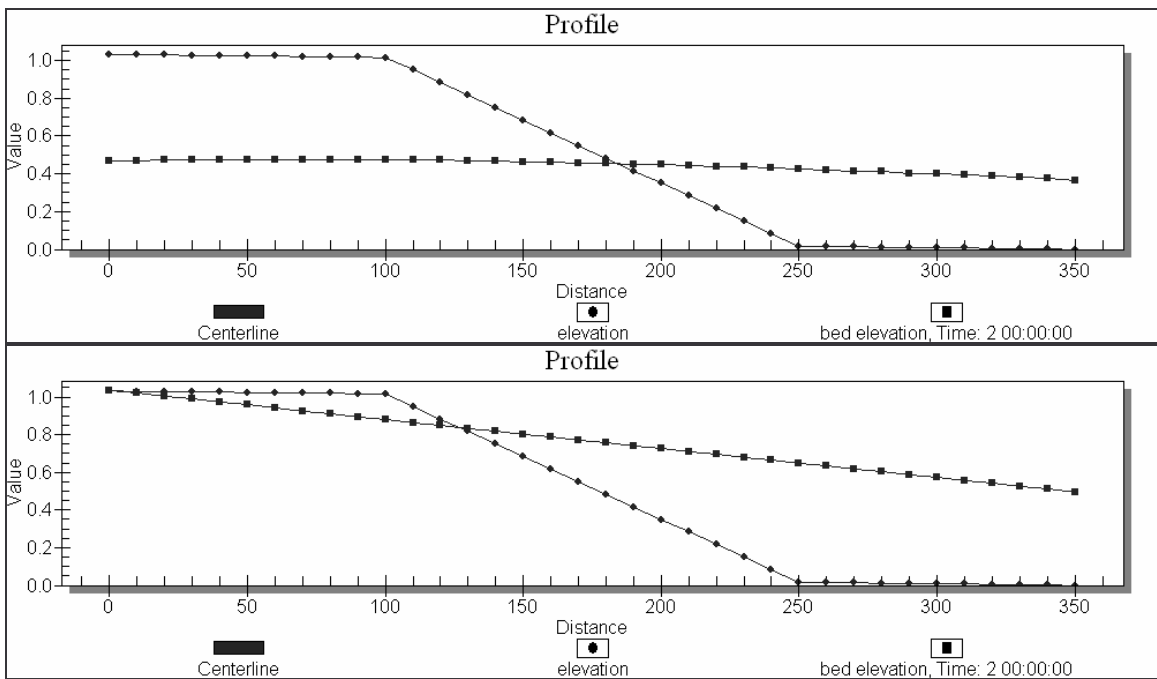


Figure 3-11: Bed Elevations for Clear-Water and Equilibrium Transport Rate Inflows for a Moderate Midsection Slope Flume with a Uniform Grain Size of 0.2mm after 48 Hours

All of the test cases with an equilibrium transport rate at the inflow boundary ran to completion. The resulting bed elevations for these runs appear appropriate, as the

profile of the final elevations of the bed show that the bed does not change over time at the upstream end of the channel. Figure 3-11 gives the final bed elevations for a 48-hour simulation of the moderate midsection slope flume with clear-water and equilibrium transport rate inflow boundaries and a uniform bed particle size of 0.2mm.

The test cases for the moderate midsection-sloped channels with an equilibrium transport rate assigned to the inflow boundary included those with uniform grain sizes of 0.08mm, 0.2mm, 2.0mm, and 4.0mm. In each of these test cases, the channel first started to scour at the upstream break in slope and deposition initially occurred at the lower end of the steeper midsection (Figure 3-12). By the 24-hour mark, the entire bed had a relatively uniform slope. Because FST2DH calculates the equilibrium transport rate at the inflow boundary, the results show much more material depositing in the channel than there is material that scours. The extra sediment coming into the mesh at the inflow boundary as the channel's slope increases deposits at the downstream end of the middle slope.

The test cases for the flumes with a moderate midsection slope also showed that as the grain size increased, the magnitude of scour and deposition within the channel decreased. Furthermore, research found that the zone of deposition fell further upstream as the size of the sediment particles increased. Figure 3-13 gives final bed elevation profiles that show these trends. The profiles show large fluctuations in the bed elevations at the lower end of the sloped section for particle sizes of 2.0 mm and 4.0 mm. These fluctuations most likely indicate the need for more a more refined grid. With more refinement, the fluctuations would most likely disappear.

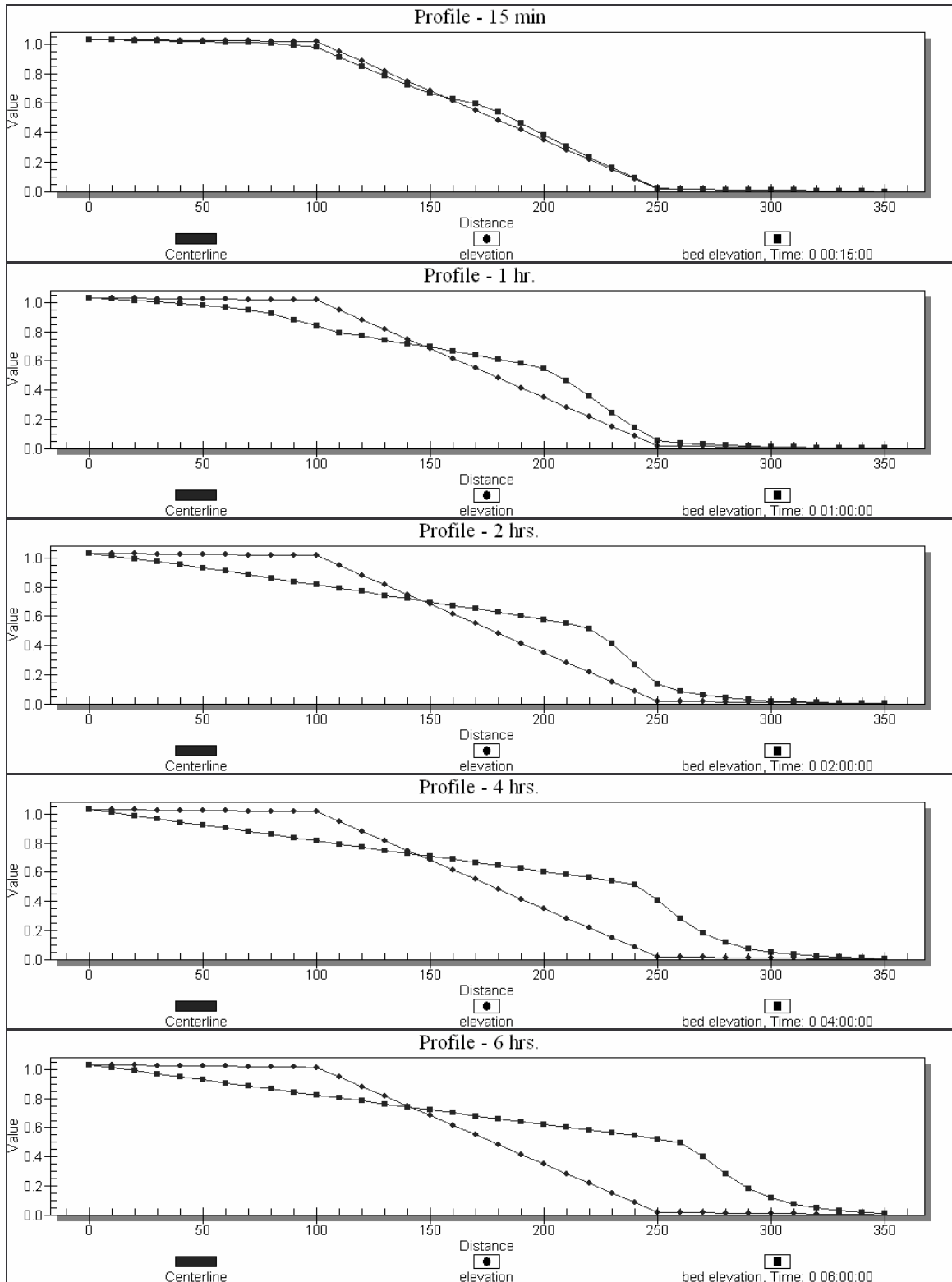


Figure 3-12: Bed Elevations for the Moderate Midsection Slope Test Case with a Uniform Grain Size of 0.2mm and an Inflow Equilibrium Transport Rate at 15 Minutes, 1 Hour, 2 Hours, 4 Hours, and 6 Hours

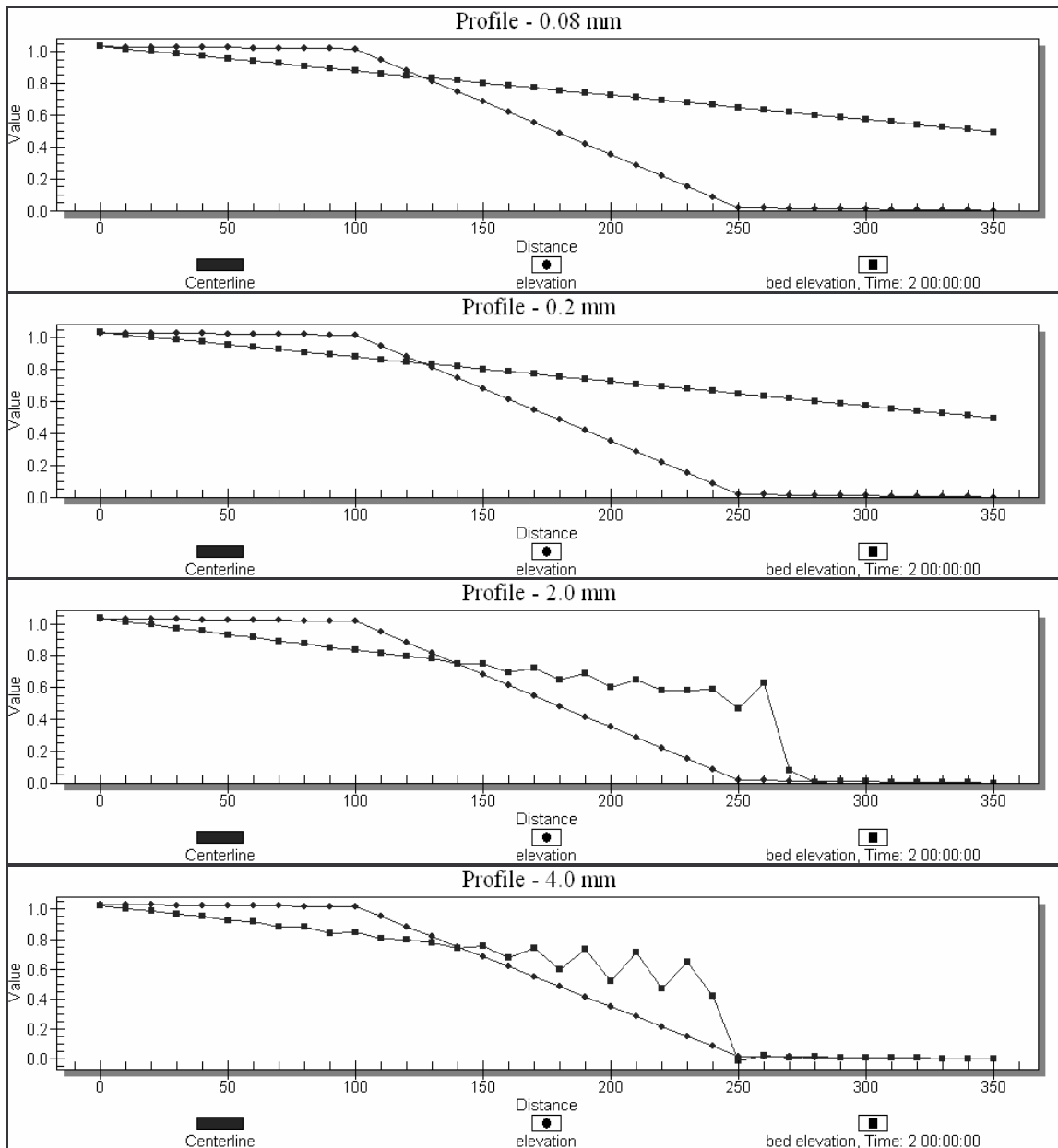


Figure 3-13: Bed Elevations after 48 Hours for a Moderate Midsection Slope Flume with an Inflow Equilibrium Transport Rate and Particle Sizes of 0.08mm, 0.2mm, 2.0mm, and 4.0mm

3.2.3 Shallow Midsection Slope

All but one of the test cases for the shallow midsection slope (0.0033 m/m) ran to completion. The clear-water, 0.08mm test case failed, giving the error, “!ERROR -

RowCount > MaxFrontWidth in xAssemble. Stopping...” during calculations for the first timestep. The remaining test cases that were successful provide seemingly reasonable results.

The steady-state solution for the flume with a shallow midsection slope showed that the change in slope had an effect on the water surface elevation along the longitudinal axis. The solution further suggested that a backwater curve extends upstream of the inflow boundary (Figure 3-14) and that if the quantity of scour at the inflow boundary of a model of a real flume needed to be identified, the inflow boundary should be pulled further upstream.

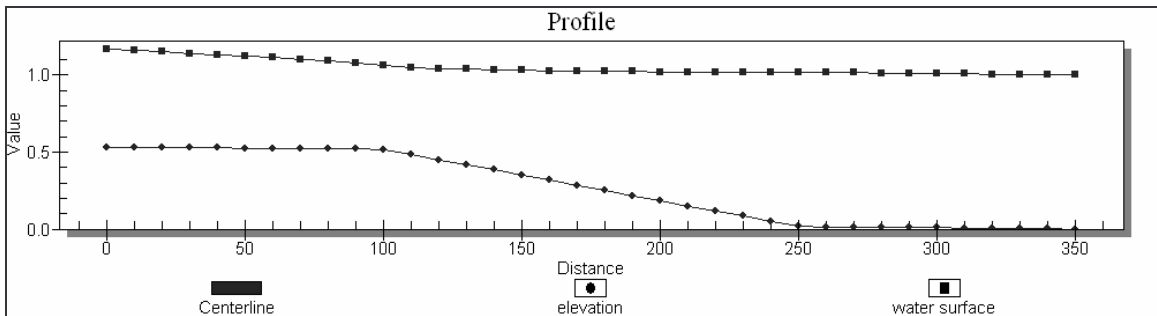


Figure 3-14: Initial Bed Elevation and Water Surface for the Flume with a Shallow Midsection Slope

The results from the shallow midsection slope test cases provided a pattern similar to that observed in the results from the moderate midsection slope test cases—that of the gradual flattening out of the bed over time. Similarly, the erosion in the shallow midsection test cases first occurred along the upstream segment of the channel and deposition first occurred almost immediately downstream. This result was expected because the maximum velocity occurred near the first break in slope and then the velocity quickly slowed down soon thereafter, allowing the sediment to be picked up by the water

briefly and then quickly deposited again. As was also seen with the moderate midsection test cases, the entire bed of the shallow midsection cases flattened out over the two-day simulation. Again, this same pattern was observed in laboratory experiments by Brush et al. (Brush 1960). The next two figures (Figure 3-15 and Figure 3-16) illustrate this change in bed for the clear-water, 0.2mm uniform grain size test case. Additional simulation time would show that the bed does eventually flatten out at the downstream end of the channel.

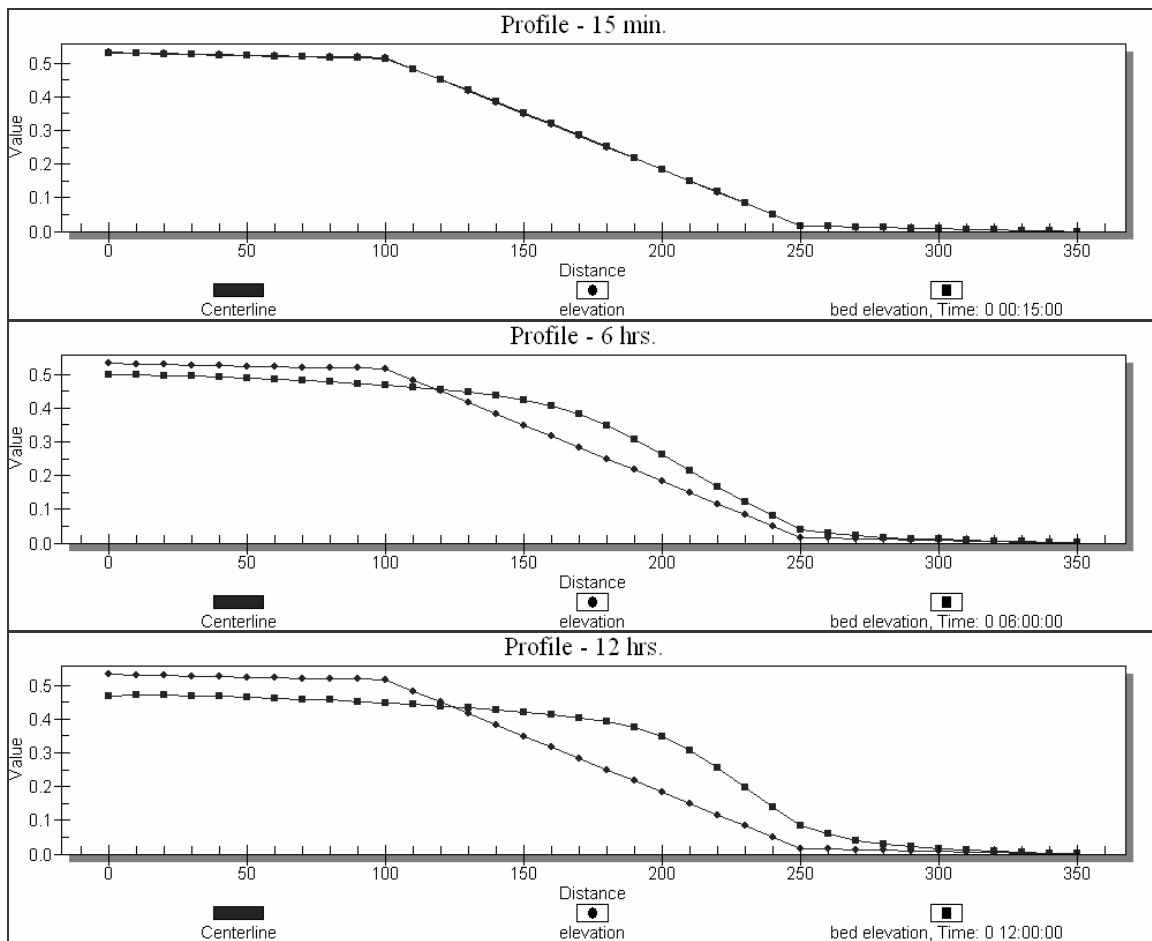


Figure 3-15: Beginning Stages of the Bed Flattening over Time for the Clear-Water, Shallow Midsection Test Case with a Uniform Grain Size of 0.2mm

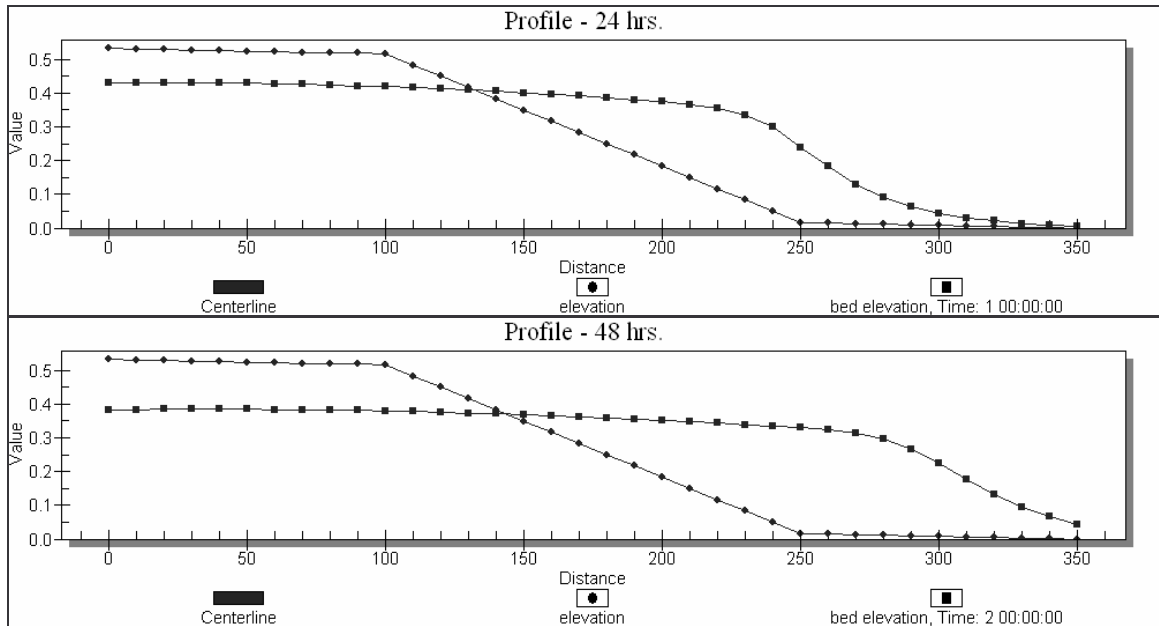


Figure 3-16: Advanced Stages of the Bed Flattening over Time for the Clear-Water, Shallow Midsection Test Case with a Uniform Grain Size of 0.2mm

The shallow midsection test cases also illustrate that as the particle size is increased while all other parameters are held constant, the erosion and deposition that occur within the flume decrease in magnitude. This trend matches anticipated patterns—the larger the sediment within a riverbed, the less likely it will be transported, and the smaller the amount of scour and deposition that will occur. In Figure 3-17, the final bed profiles from 48-hour simulations of a shallow midsection flume with a clear-water inflow show this trend. The plots in the figure were created using particles of increasing size: 0.2mm, 2.0mm, and 4.0mm. Because the test for the clear-water conditions with a bed particle size of 0.08mm failed to run to completion, the bed profile for that case was not output by FST2DH.

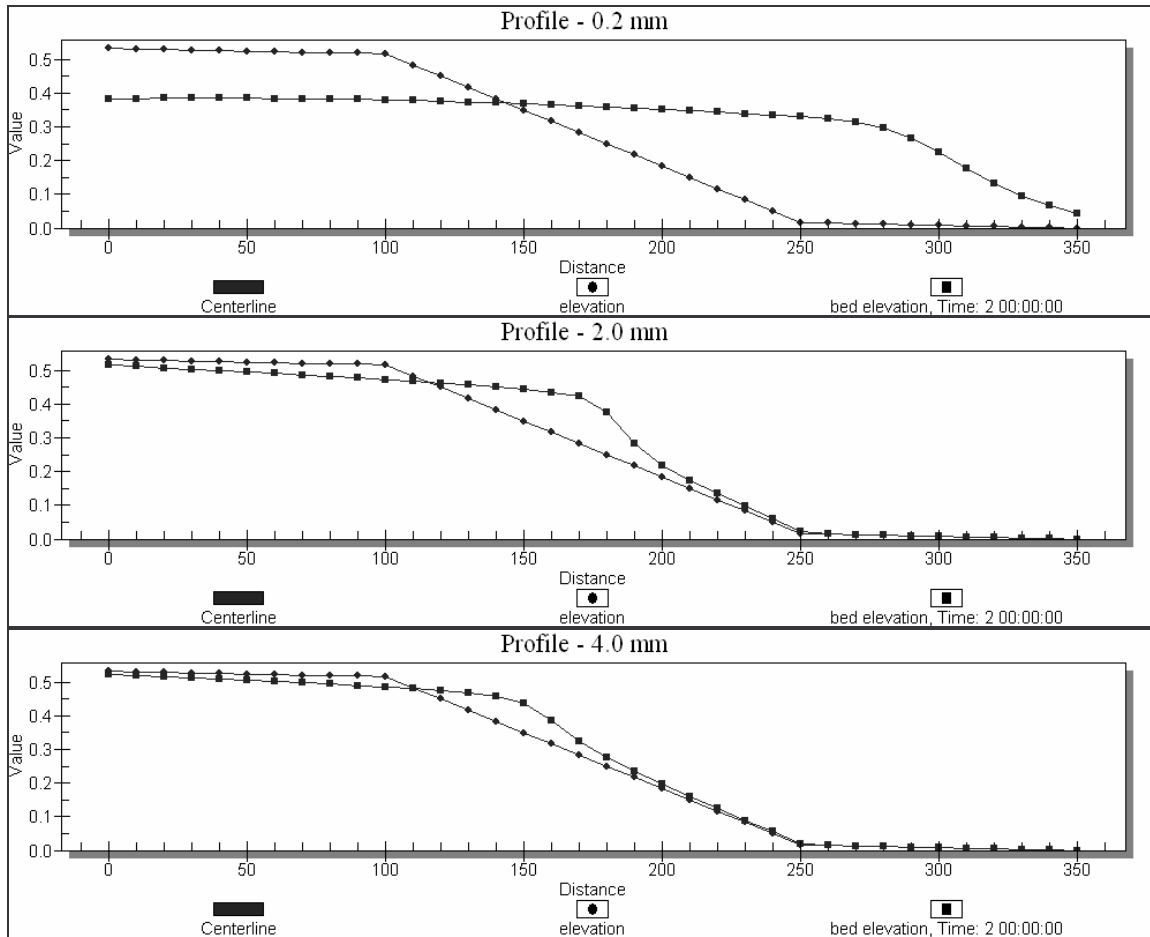


Figure 3-17: Bed Elevations after 48 Hours for the Shallow Midsection Slope Test Cases with Clear-Water Inflow and Various Particle Sizes: 0.2mm, 2.0mm, and 4.0mm

Figure 3-18 shows the final bed profiles from 48-hour simulations of a shallow midsection flume with an equilibrium transport rate assigned to the inflow boundary and particles of increasing size: 0.08mm, 0.2mm, 2.0mm, and 4.0mm. Of particular interest within this figure is how, unlike the clear-water cases, the test cases with an equilibrium inflow transport rate show that the inflow boundary's bed elevations remain the same, regardless of sediment size, as is expected. This reflects that FST2DH not only adjusts to the change in bed particle size, but that the sediment size is appropriately taken into account when FST2DH calculates the sediment transport rate at the inflow cross section

for equilibrium conditions. The figure also shows that more material deposits in the channel than is scoured from further upstream. The amount of sediment required to keep

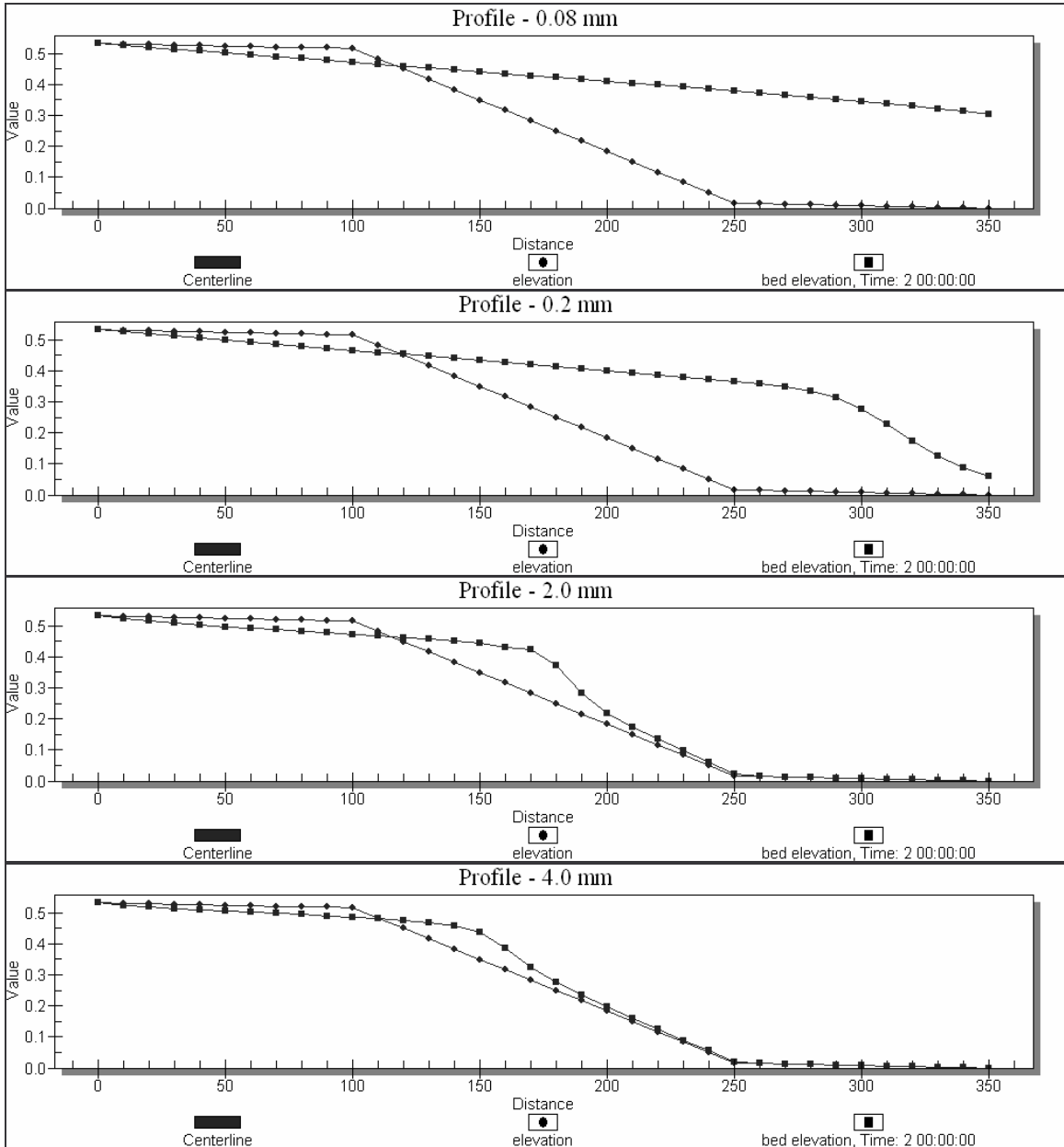


Figure 3-18: Initial and Final Bed Elevations for a 48 Hour Simulation of the Shallow Midsection Slope Flume with an Equilibrium Transport Rate Applied to the Inflow Boundary and Particle Sizes of 0.08mm, 0.2mm, 2.0mm and 4.0mm

equilibrium conditions at the upstream end of the channel increases as the slope in that region becomes steeper over time. Thus, FST2DH gradually increases the transport rate of sediment entering the mesh over the course of the simulation. Upon entering the mesh, the water holds a lot of sediment. When the sediment-laden water slows down in the downstream portion of the mesh, much of the sediment it was carrying deposits. This increases the downstream bed elevations very quickly over time, but does not provide for much scouring upstream.

Another observation made in the evaluation of the results from the shallow midsection slope test cases is that the change in the geometry with the movement of the bed has a great effect on the channel's hydrodynamic parameters over time. As the bed continues to flatten out with each new timestep, the range of velocities for each new timestep decreases. This result follows anticipated patterns, as flatter channels tend to result in a more even velocity distribution throughout the domain than do channels with varying slopes. Figure 3-19 shows the shift in the location of the maximum velocity. It also shows that the range of velocities observed for a given timestep slowly decreases through time. The profiles given in the figure are for the clear-water 0.2mm uniform bed grain size test case. At the beginning of the model run, the velocity profile showed somewhat of a sharp peak where the bed's slope increased dramatically. After the six-hour mark, the general shape of the profile remained the same but the magnitude and location of the peak velocity changed. Furthermore, the decrease of velocity that occurred in the downstream portion of the channel became more abrupt over time.

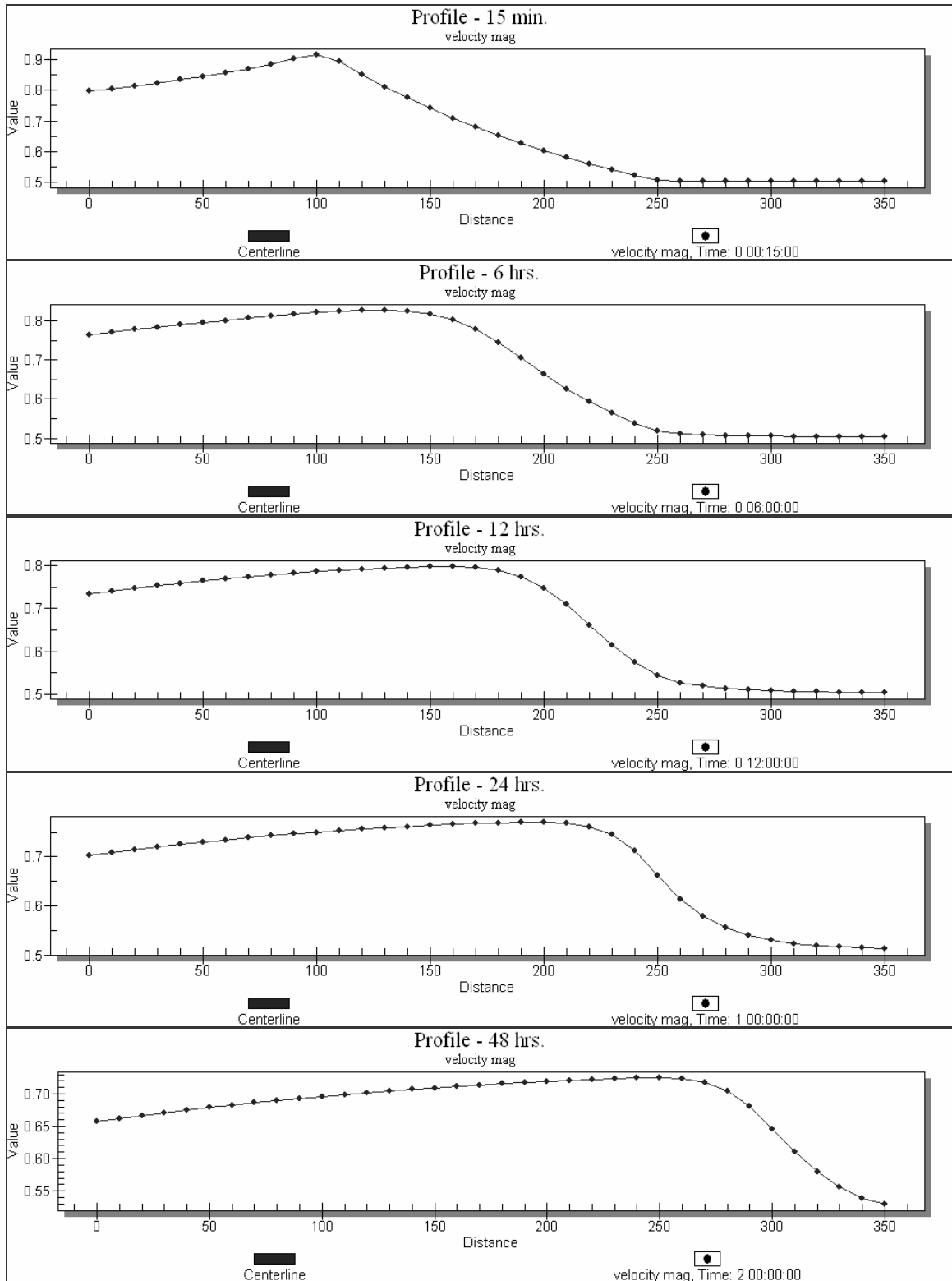


Figure 3-19: Change in Velocity Magnitude over 48 Hours for the Shallow Midsection Slope Flume with Clear-Water Inflow and a Particle Size of 0.2mm

3.3 Flumes with Contractions

This section contains the sediment results from the test cases for the three flumes with different midsection contractions. It provides and briefly explains the patterns observed in the final bed elevations for model runs of various types of contractions, inflow sediment specifications, and sediment particle sizes. The change in channel width through the contraction forces an uneven distribution of scour and deposition across a given cross-section. Because of this, the patterns of scour and deposition are best seen in plan view. The results provided in this section will thus show contoured bed elevations as well as centerline profiles of the bed elevations.

3.3.1 Gradual Contraction

The test cases for a flume with a gradual contraction show a changing location and magnitude of scour through the narrowest portion of the contraction. They also show how the scour and deposition are distributed within the channel as it begins to widen at the end of the contraction. The steady state hydrodynamic solution for the gradual contraction flume (Figure 3-20) shows the backing up of water upstream from the contraction with a centerline profile and spatial distribution of water depth.

The velocity dramatically increases through the contraction and then drops again to nearly the same magnitude as upstream of the contraction. Figure 3-21 shows the profile and spatial distribution of the initial velocity magnitude.

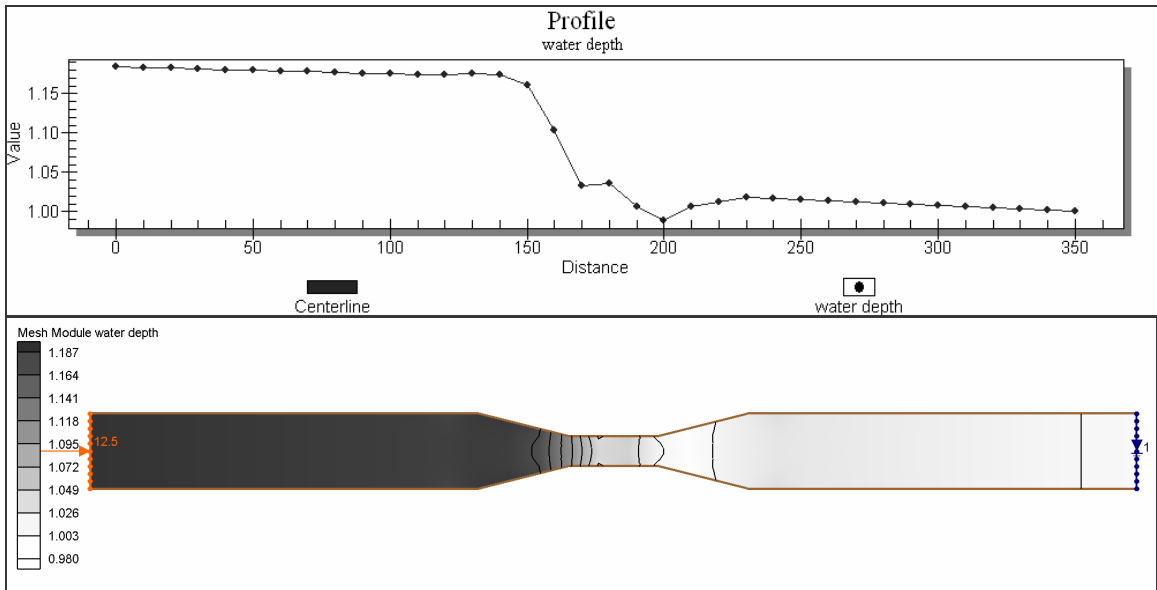


Figure 3-20: Steady-State Solution for Water Depth in the Flume with a Gradual Contraction

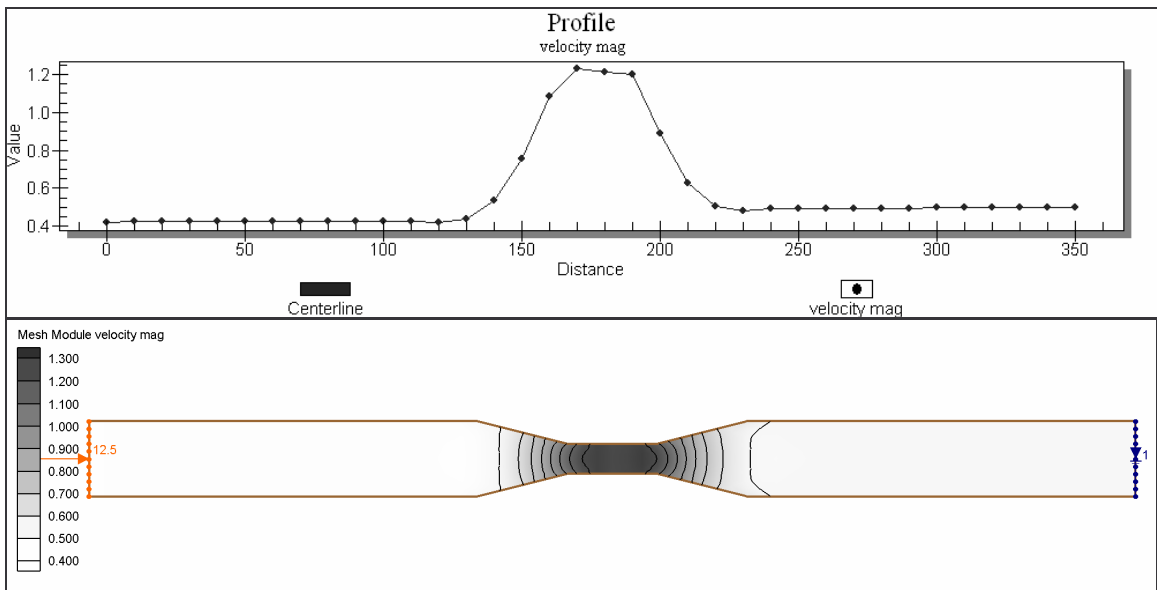


Figure 3-21: Steady-State Solution for Velocity Magnitude for the Flume with a Gradual Contraction

The research included gradual contraction test cases for both the clear-water and equilibrium sediment transport rate conditions with uniform particle sizes of 0.08, 0.2,

2.0, and 4.0 mm. All but two of these test cases ran to completion. The cases that failed included those with clear-water inflow and uniform bed particle sizes of 0.08 mm and 0.2 mm. All test cases that ran successfully produced results that appear reasonable when compared to expected scour and deposition patterns. In all tests, neither deposition nor erosion occurred at the inflow boundary, regardless of whether clear-water or an equilibrium transport rate was assigned. This probably indicates that the upstream velocity is slow enough that the larger particles (2.0 and 4.0 mm) can't be carried by the water.

The next two figures (Figure 3-22 and Figure 3-23) show the centerline profiles and spatial distributions of the final bed elevations after a 48-hour simulation for the clear-water, 2.0mm particle size (Figure 3-22) and 4.0mm particle size (Figure 3-23) test

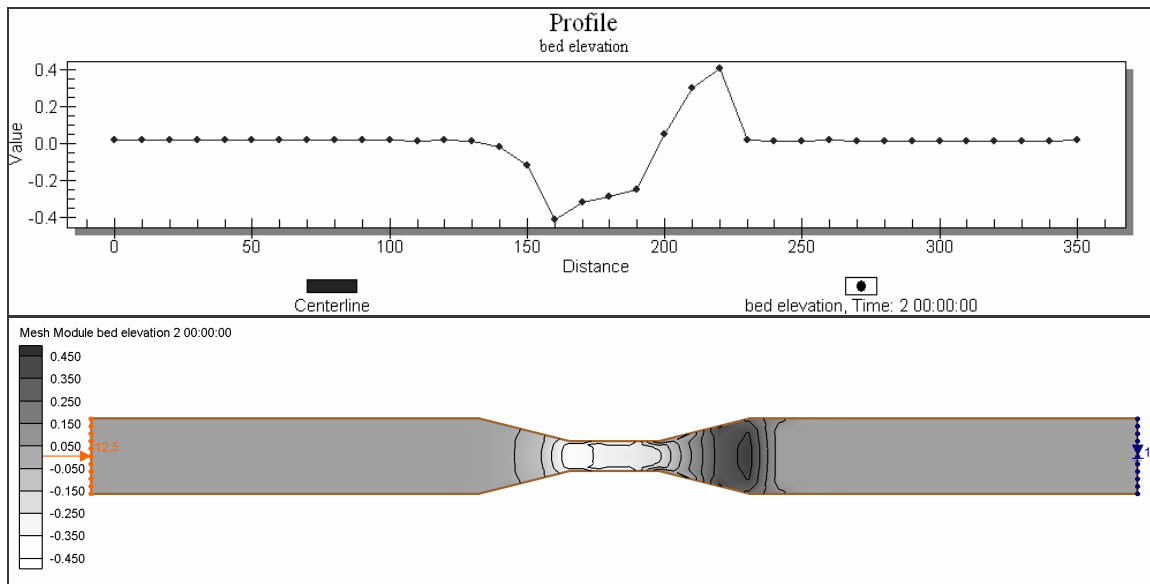


Figure 3-22: Centerline Profile and Plan View of the Final Bed Elevations for a 48 Hour Simulation of the Clear-Water, 2.0mm Particle Size Test Case for a Flume with a Gradual Contraction

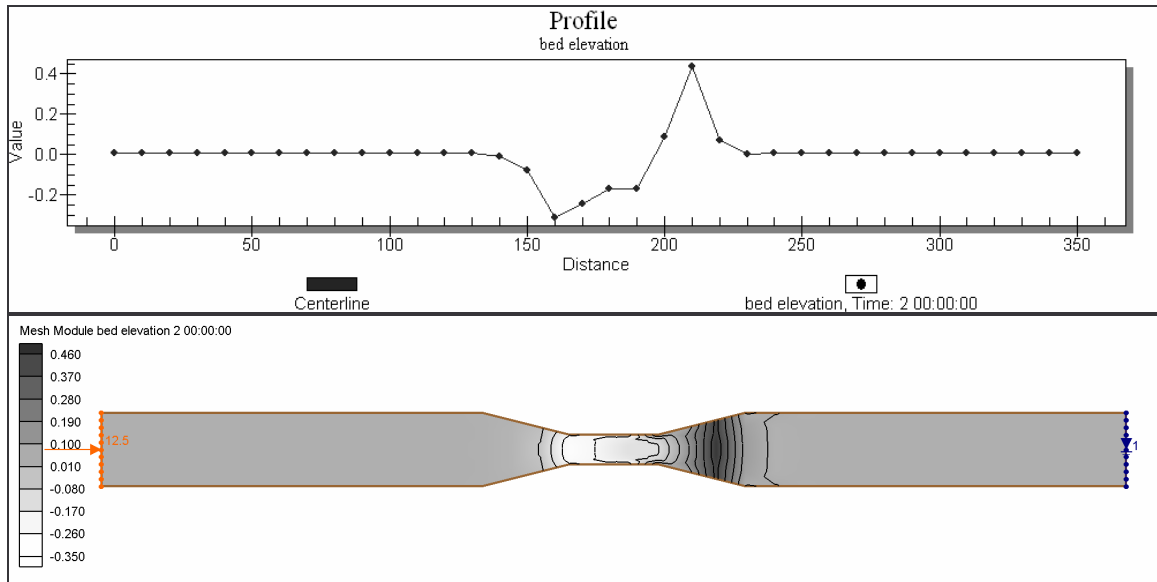


Figure 3-23: Centerline Profile and Plan View of the Final Bed Elevations for a 48 Hour Simulation of the Clear-Water, 4.0mm Particle Size Test Case for a Flume with a Gradual Contraction

cases. As shown in the figures, an increased bed particle size results in a decreased amount of scour within the contraction. The figures also show that as the sediment size increases, FST2DH predicts deposition further upstream, closer to the area of scour within the narrowest part of the contraction. These trends follow anticipated patterns.

The results of the test cases with an equilibrium transport rate applied to the inflow boundary show the same results as those with clear water flowing into the domain. Again, this is probably due to a low velocity at the inflow, resulting in little to no sediment movement until the water reaches the contraction and the velocity increases.

The next set of figures (Figure 3-24, Figure 3-25, Figure 3-26, and Figure 3-27) show centerline profiles and plan views of the final bed elevations for a 48-hour simulations of a flume with a gradual contraction and an equilibrium transport rate assigned to the inflow boundary with increasing particle sizes for the bed (0.08mm in Figure 3-24, 0.2mm in Figure 3-25, 2.0mm in Figure 3-26, and 4.0mm in Figure 3-27).

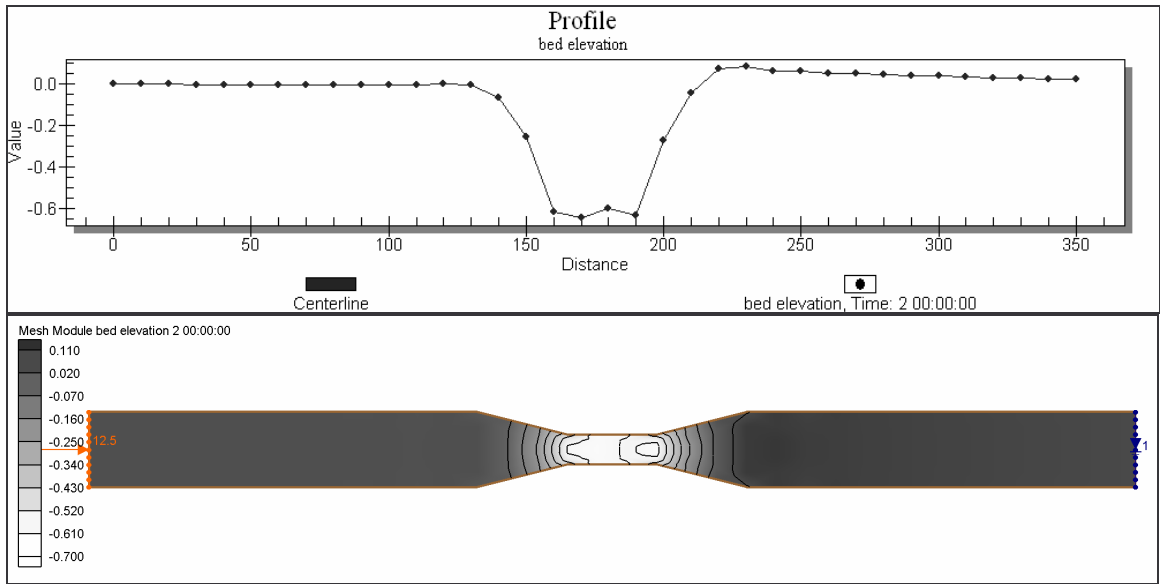


Figure 3-24: Centerline Profile and Plan View of the Final Bed Elevations for a 48 Hour Simulation of the Gradual Contraction Test Case with an Equilibrium Transport Rate at the Inflow Boundary and a Bed Particle Size of 0.08mm

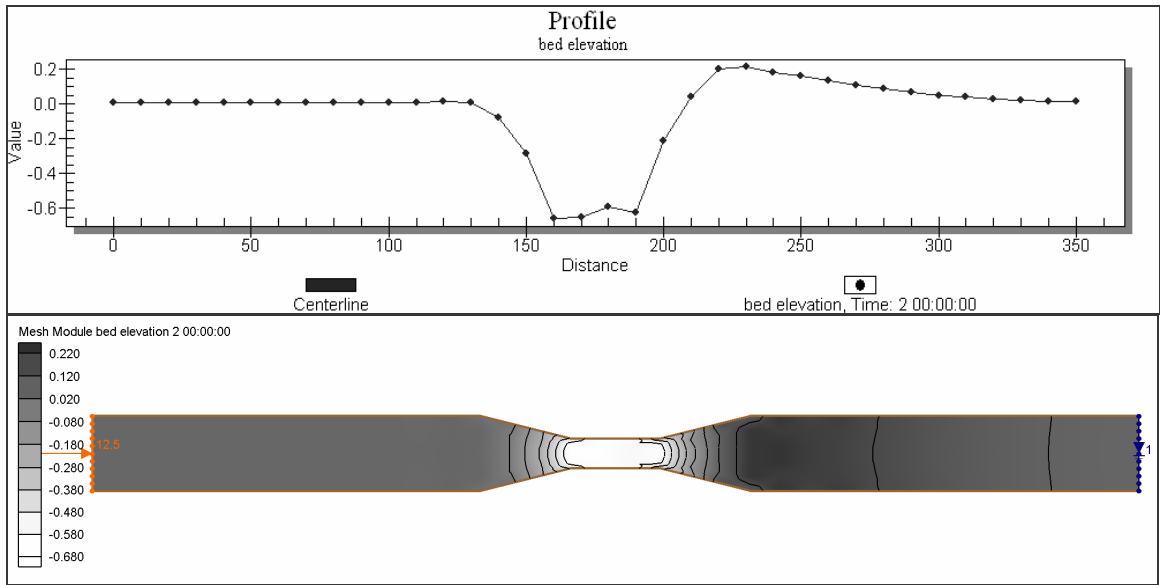


Figure 3-25: Centerline Profile and Plan View of the Final Bed Elevations for a 48 Hour Simulation of the Gradual Contraction Test Case with an Equilibrium Transport Rate at the Inflow Boundary and a Bed Particle Size of 0.2mm

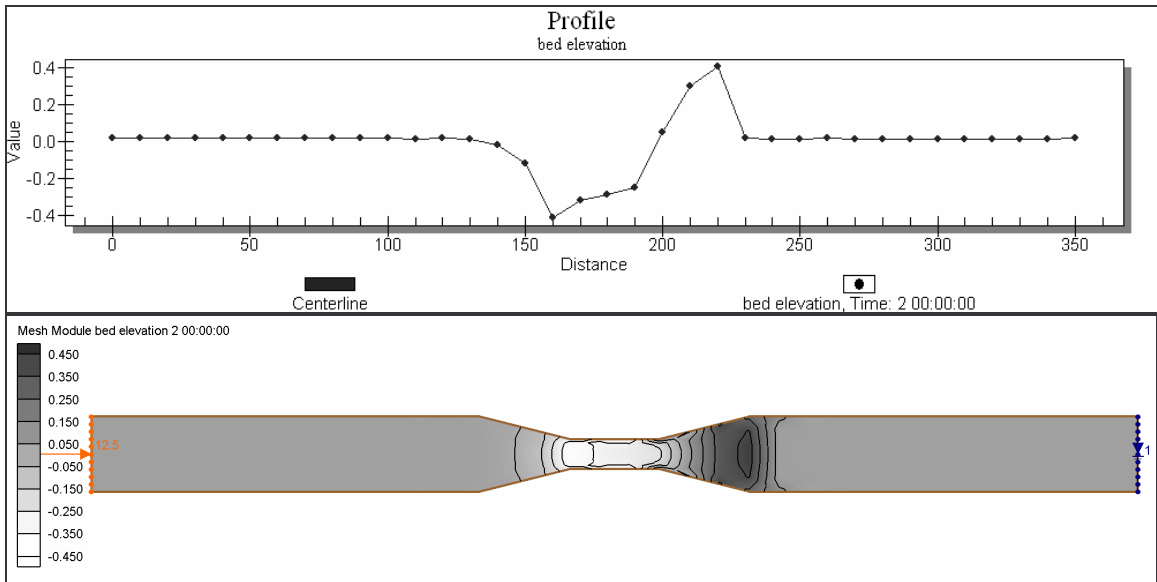


Figure 3-26: Centerline Profile and Plan View of the Final Bed Elevations for a 48 Hour Simulation of the Gradual Contraction Test Case with an Equilibrium Transport Rate at the Inflow Boundary and a Bed Particle Size of 2.0mm

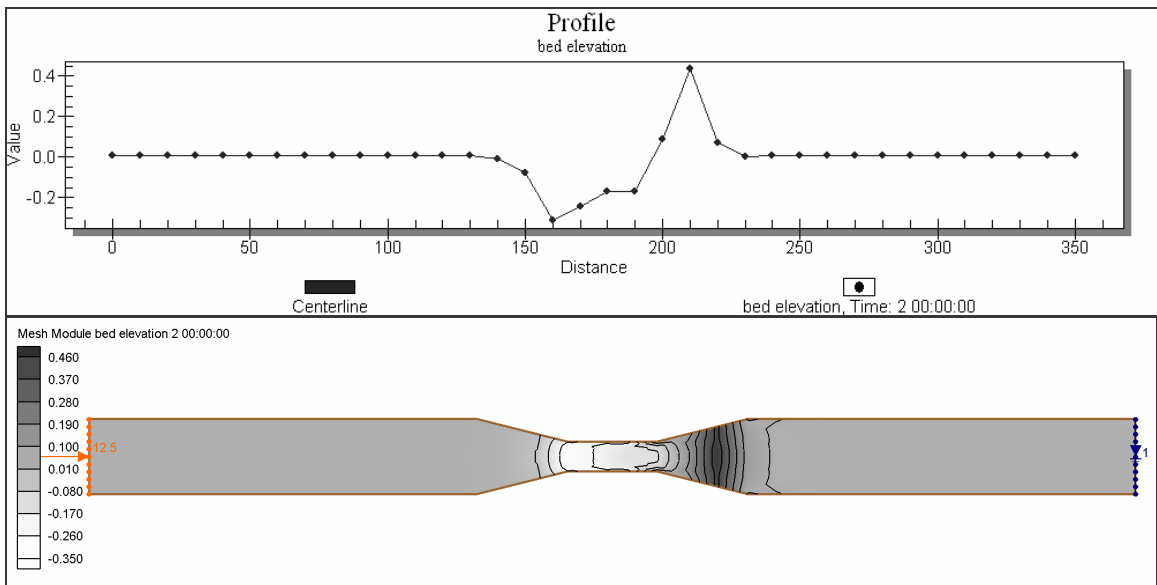


Figure 3-27: Centerline Profile and Plan View of the Final Bed Elevations for a 48-hour Simulation of the Gradual Contraction Test Case with an Equilibrium Transport Rate at the Inflow Boundary and a Bed Particle Size of 4.0mm

The change in the bed slope over time can best be seen in oblique view. Figure 3-28 on the next page shows an oblique view of the change in bed within the clear-water, 0.2mm test case for the flume with a gradual contraction. The contraction is shown from the upstream right side of the flume. As can be seen in these figures and in the ones given previously, the shape of the scour hole and central deposition location seem appropriate. The peaks within Figure 3-28 result from the low resolution of the grid used for this test case. A more-refined grid would provide a smoother surface for the bed, but the bed would still follow the general shape given in the figure.

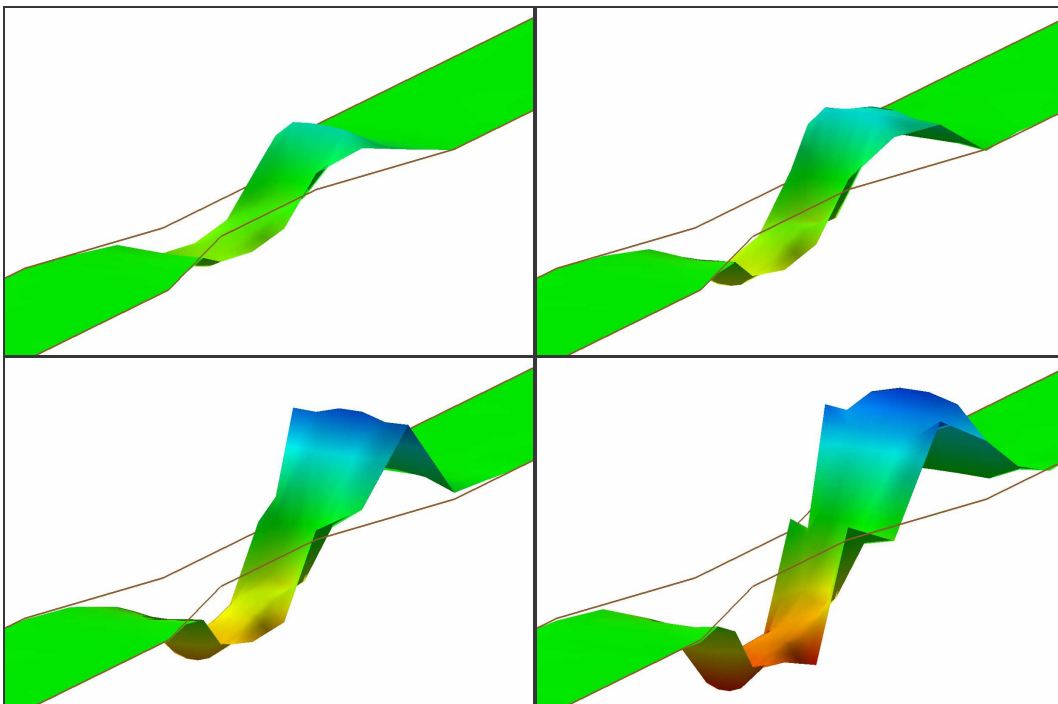


Figure 3-28: Oblique View of the Channel Bed after 6 Hours, 12 Hours, 24 Hours, and 48 Hours for the 2.0mm, Clear-Water Test Case for a Flume with a Gradual Contraction

Table 3-3 provides a summary of the locations and magnitudes of the points of maximum scour and deposition along the centerline of the channel for the test cases for

the flume with a gradual contraction. The table shows that as the particle size increases, the location of scour remains mostly constant, but the location of deposition moves upstream. Furthermore, the magnitude of scour generally decreases and the magnitude of deposition generally increases as the particle size increases.

Table 3-3: Locations and Magnitudes of the Points of Maximum Scour and Deposition for the Gradual Contraction Test Cases

<i>Particle Size (mm)</i>	<i>Location of Maximum Scour (m)</i>	<i>Magnitude of Maximum Scour (m)</i>	<i>Location of Maximum Deposition (m)</i>	<i>Magnitude of Maximum Deposition (m)</i>
0.08	170.0	0.64	230.0	0.09
0.2	160.0	0.67	230.0	0.20
2.0	160.0	0.43	220.0	0.39
4.0	160.0	0.32	210.0	0.43

3.3.2 Long Abrupt Contraction

Similar to the test cases for the flume with a gradual contraction, all but two of the test cases for the flume with a long abrupt contraction ran to completion—the tests with clear-water inflow and particle sizes of 0.08mm and 0.2mm. The tests for the flume with a long abrupt contraction were also similar to those for the flume with a gradual contraction in that for both cases, neither scour nor deposition occurred at the inflow boundary, regardless of whether the clear-water or equilibrium transport rate condition was applied.

The test cases for the long abrupt contraction showed that FST2DH predicts two main locations of scour within the contraction. The first scour hole extends slightly upstream from the point of sudden contraction and is contained mostly in the center

portion of the channel, and not along the banks. The second location of deepest scour occurs at the end of the contraction and the area of deposition is distributed around the downstream end of the scour hole and lies in the wider portion of the channel. The deposition is observed close to the contraction along the sides of the channel and further from it in the center of the channel. This pattern matches expectations, as the highest velocities caused by the contraction will lie in the center of the channel, which means that sediment will be carried further within the center of the channel. As the velocity slows down upon exiting the contraction, the highest velocity will remain in the center of the channel until the velocity across the channel becomes fairly uniform. These results are shown in Figure 3-29 for the equilibrium transport rate test case for a bed particle size of 0.2 mm.

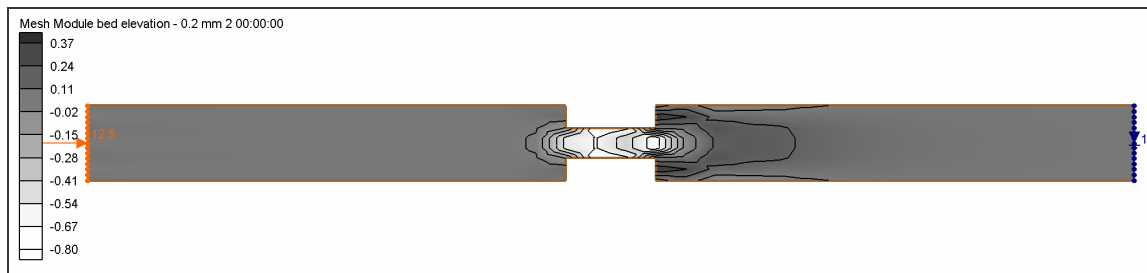


Figure 3-29: Plan View of the Bed Elevations after 48 Hours for the Equilibrium Transport Rate, 0.2mm Grain Size Test Case for a Flume with a Long Abrupt Contraction

The test cases for the long abrupt contraction show that as the bed particle size increases, the depth of the scour hole generally decreases. Also, as the particle size increases, the zone of deposition along the centerline of the channel decreases in length and increases in depth. The bed profiles for various particle sizes given in Figure 3-30 and Figure 3-31 illustrate these findings.

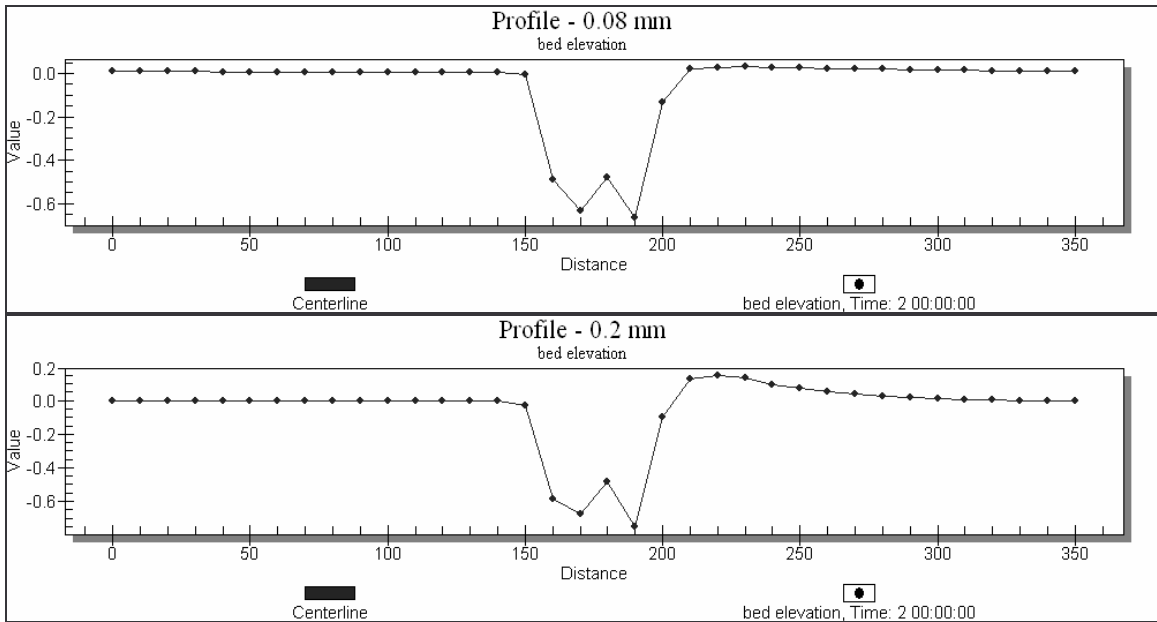


Figure 3-30: Centerline Profiles of Bed Elevation for a 48 Hour Simulation of a Flume with an Abrupt Long Contraction and an Equilibrium Transport Rate at the Inflow Boundary, with Particle Sizes of 0.08mm and 0.2mm

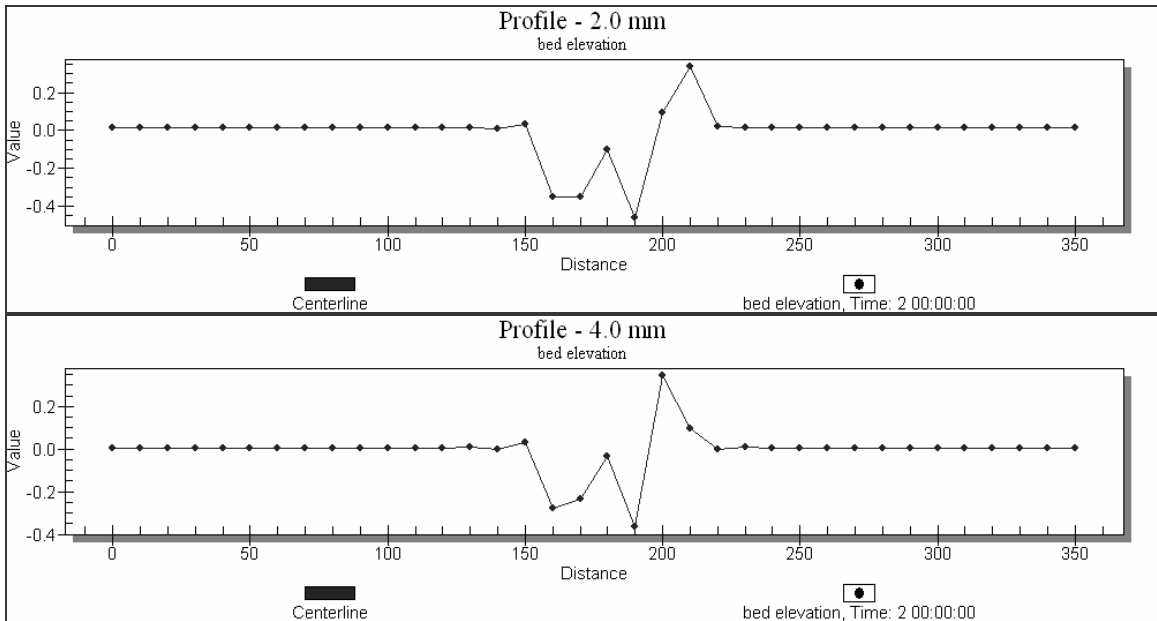


Figure 3-31: Centerline Profiles of Bed Elevation for a 48 Hour Simulation of a Flume with an Abrupt Long Contraction and an Equilibrium Transport Rate at the Inflow Boundary, with Particle Sizes of 2.0mm and 4.0m

The general shape of the regions of scour and deposition appear valid. Most scouring occurs within the contraction and along the center of the channel, where the highest velocities are observed. Figure 3-32 on the next page shows this pattern and also shows that the amount of scouring decreases towards the banks.

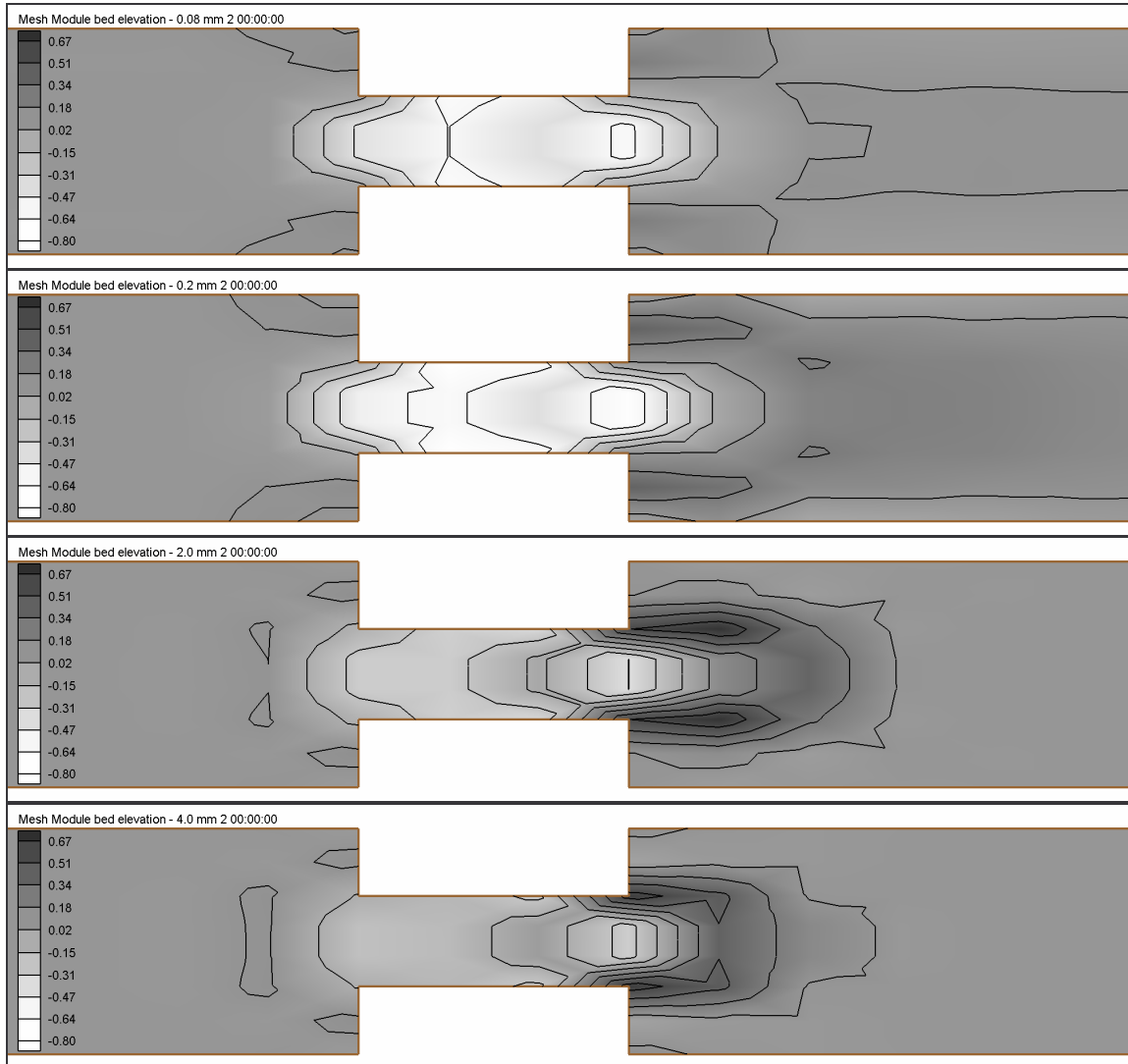


Figure 3-32: Close-up Plan View of the Final Bed Elevations for a 48 Hour Simulation of a Flume with an Abrupt Long Contraction with an Equilibrium Transport Rate at the Inflow Boundary and Bed Particle Sizes of 0.08mm, 0.2mm, 2.0mm, and 4.0mm

Table 3-4 provides a summary of the locations and magnitudes of the points of maximum scour and deposition along the centerline of the channel for the equilibrium transport rate test cases for the flume with an abrupt long contraction. The table reflects the same patterns shown in the results from the tests for the flume with a gradual contraction. As the particle size increases, the location of scour remains constant and the location of deposition moves upstream. Also, the magnitude of scour in the case for the largest particle size is much smaller and the magnitude of deposition for that case is much larger than that in the case for the smallest particle size.

Table 3-4: Locations and Magnitudes of the Points of Maximum Scour and Deposition for the Long Abrupt Contracion Test Cases

<i>Particle Size (mm)</i>	<i>Location of Maximum Scour (m)</i>	<i>Magnitude of Maximum Scour (m)</i>	<i>Location of Maximum Deposition (m)</i>	<i>Magnitude of Maximum Deposition (m)</i>
0.08	190.0	0.67	230.0	0.02
0.2	190.0	0.75	220.0	0.15
2.0	190.0	0.48	210.0	0.32
4.0	190.0	0.37	200.0	0.34

3.3.3 Short Abrupt Contraction

All the test cases for the short abrupt contraction ran to completion except for the clear-water case for a bed particle size of 0.08mm. The clear-water, 0.2mm particle size test case ran to completion but is unstable along the upstream boundary at the 48-hour mark (Figure 3-33). The remainder of the test cases ran to completion and were stable.

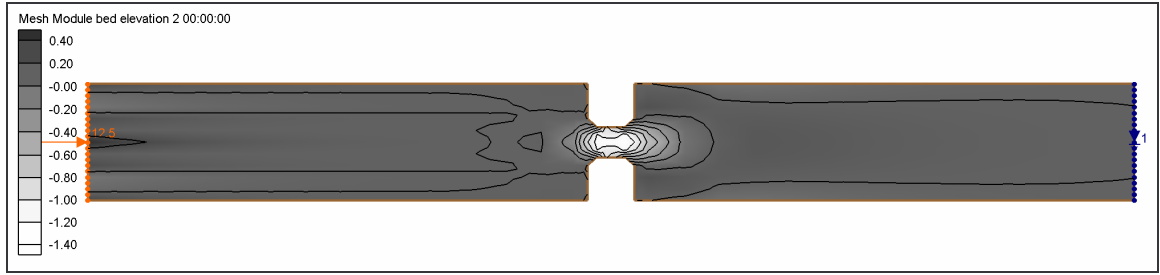


Figure 3-33: Bed Elevations at 48 Hours for the Clear-Water, 0.2mm Test Case for the Flume with an Abrupt Short contraction, Showing Instability at the Inflow Boundary

The steady-state solution for the water depth shows that the contraction creates a pool upstream. It also shows that the velocity is quite small upstream (0.27 m/s), rises dramatically through the contraction, where it peaks at 1.56 m/s, and then falls back down to 0.5 m/s downstream of the contraction. Longitudinal centerline profiles and plan views of the steady-state solutions for water depth and velocity magnitude are shown in the next two figures (Figure 3-34 and Figure 3-35, respectively).

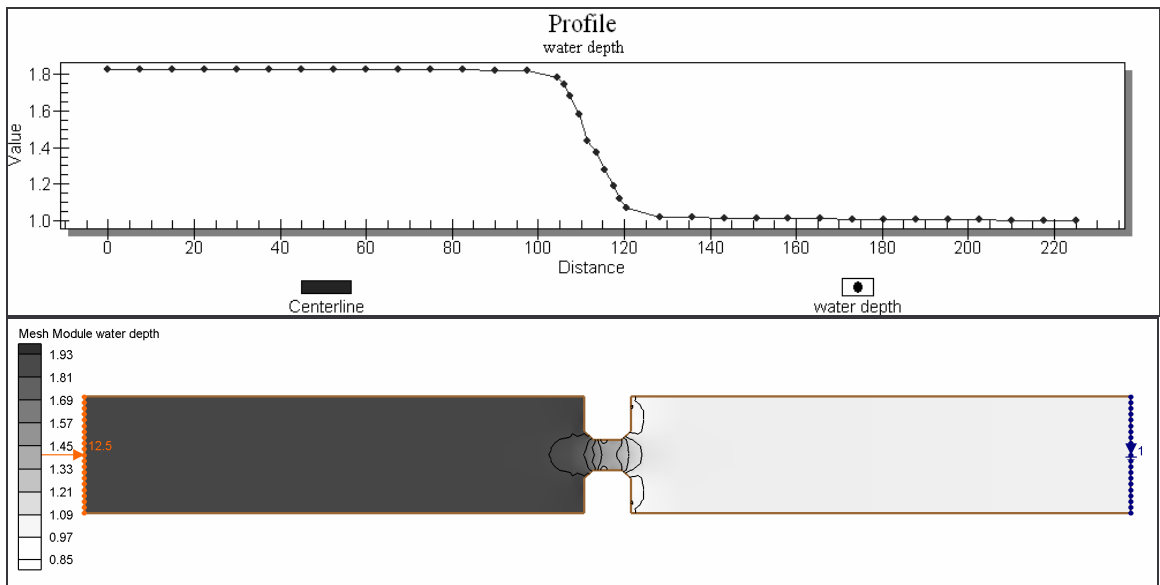


Figure 3-34: Centerline Profile and Plan View of the Steady-State Solution for Water Depth in the Flume with a Short Abrupt Contraction

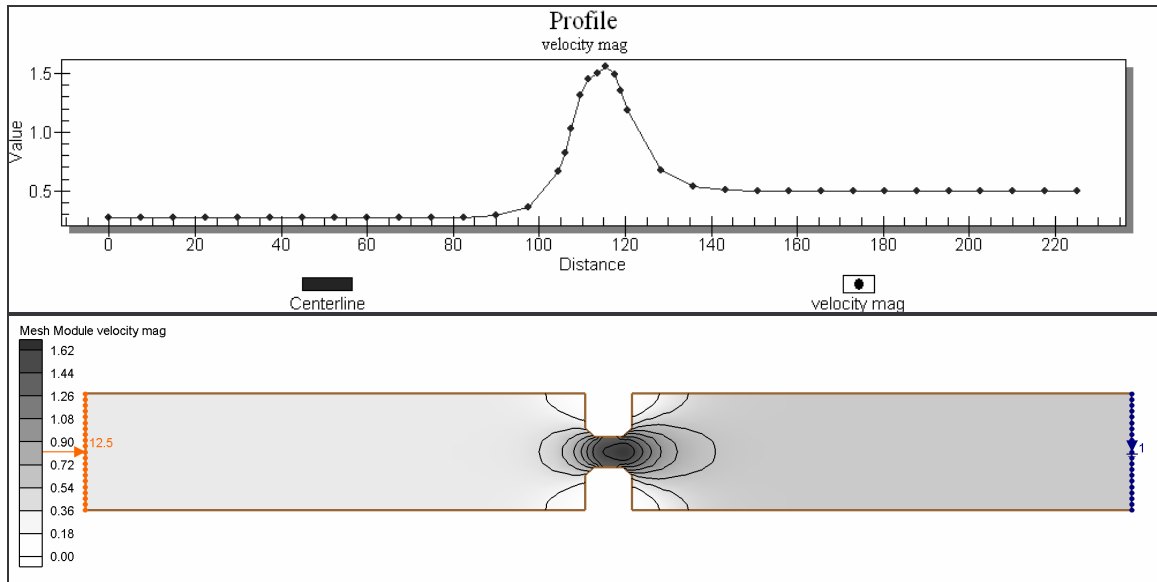


Figure 3-35: Centerline Profile and Plan View of the Steady-State Solution for Velocity Magnitude in the Flume with a Short Abrupt Contraction

The higher velocity that exists through the middle of the channel in the contraction suggests that the greatest amount of scour will occur in that same area. The sediment results from FST2DH show that this is accurately reflected by the model run. Figure 3-36 shows a close-up view of the contraction with an equilibrium transport rate assigned to the inflow boundary and uniform bed particle sizes of 0.08mm, 0.2mm, 2.0mm, and 4.0mm. The shapes of the regions of scour and deposition seem to be reasonable.

As was observed in the results from other runs, the results from the short abrupt contraction test cases showed that as the bed particle size increases, the area of scour decreases and the area of the deposition moves further upstream, towards the contraction. The decrease in scour depth is shown in Figure 3-37 with centerline profiles of bed elevation for increasing particle sizes.

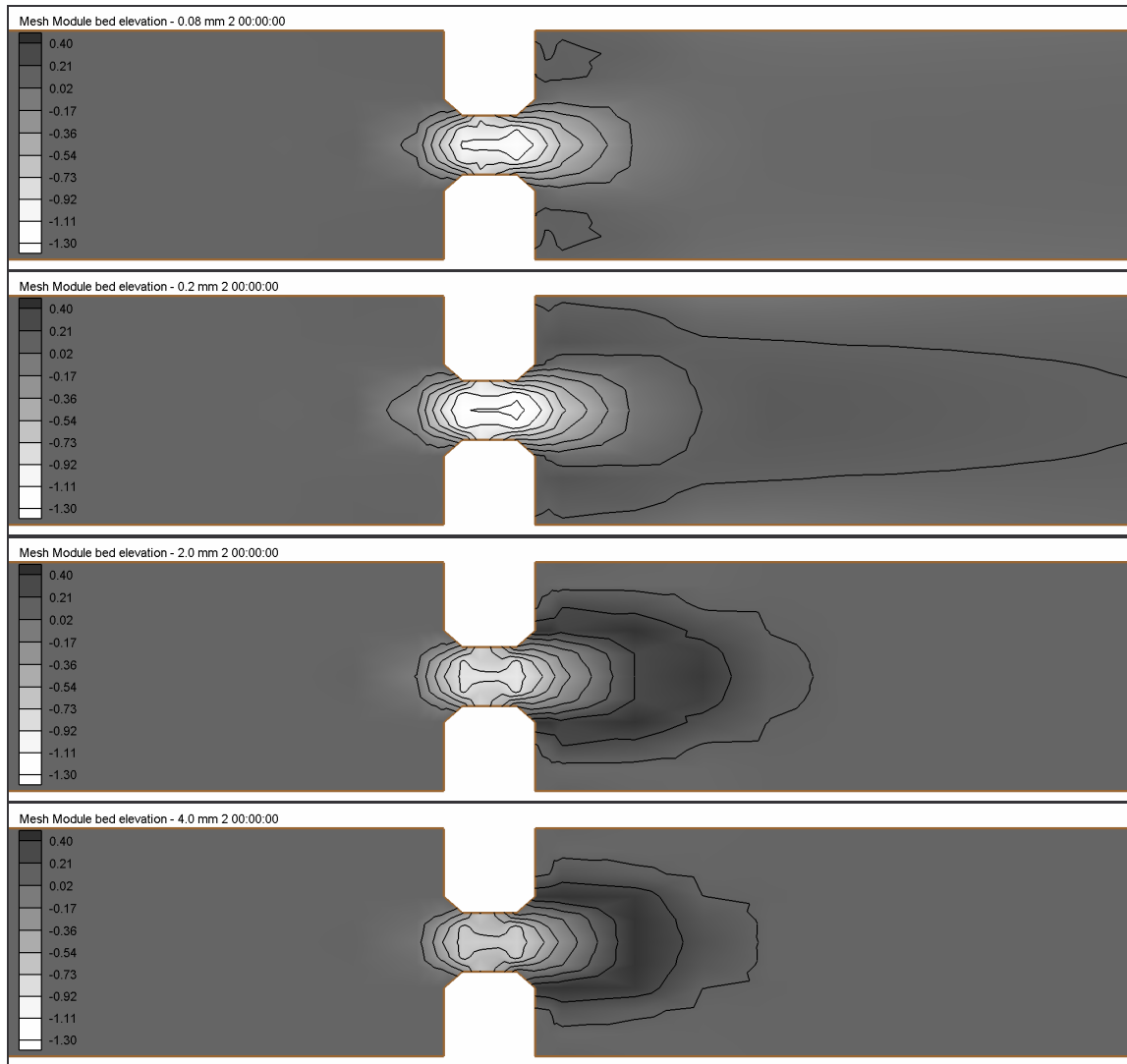


Figure 3-36: Bed Elevations after 48 Hours for the Short Abrupt Contraction Flume with an Inflow Equilibrium Transport Rate and Particle Sizes of 0.08mm, 0.2mm, 2.0mm, and 4.0mm

The sediment results from FST2DH also show that, as was observed in the test cases for the flumes with gradual and long abrupt contractions, the test cases for the short abrupt contractions have upstream velocities slow enough to eliminate the scour or deposition of the bed in that region. Therefore, the results from the clear-water test cases that ran to completion match the results of corresponding test cases with an equilibrium transport rate assigned to the inflow boundary.

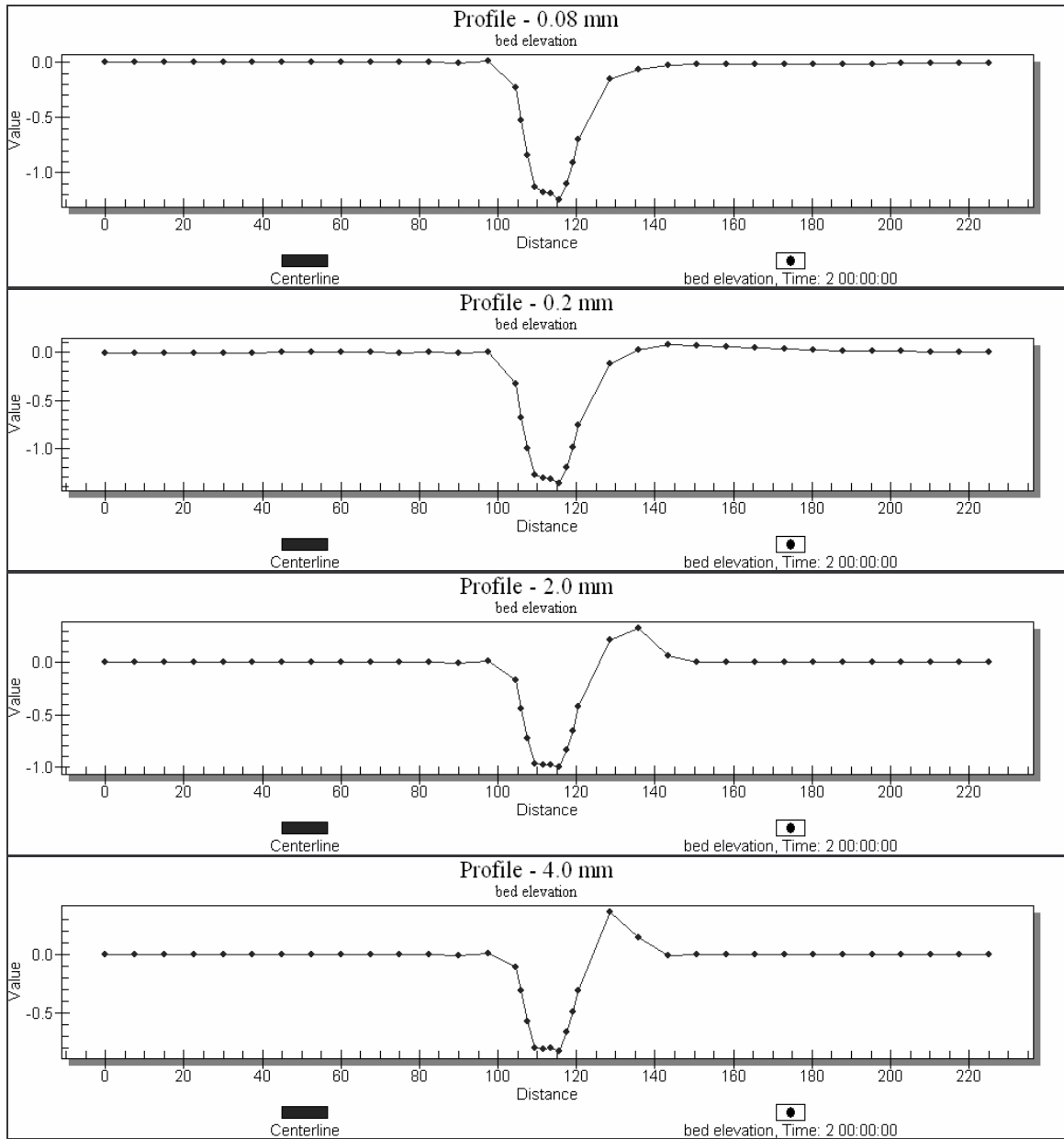


Figure 3-37: Centerline Profiles of Bed Elevations at 48 Hours for the Test Cases of a Short Abrupt Contraction with an Equilibrium Transport Rate Inflow and Bed Particle Size of 0.08mm, 0.2mm, 2.0mm, and 4.0mm

As the bed scours through the contraction, the cross-section area of flow through the contraction increases, which results in a decrease in velocity in that region over time.

The hydrodynamic and sediment solutions in Figure 3-38 show that FST2DH accurately portrays this scenario.

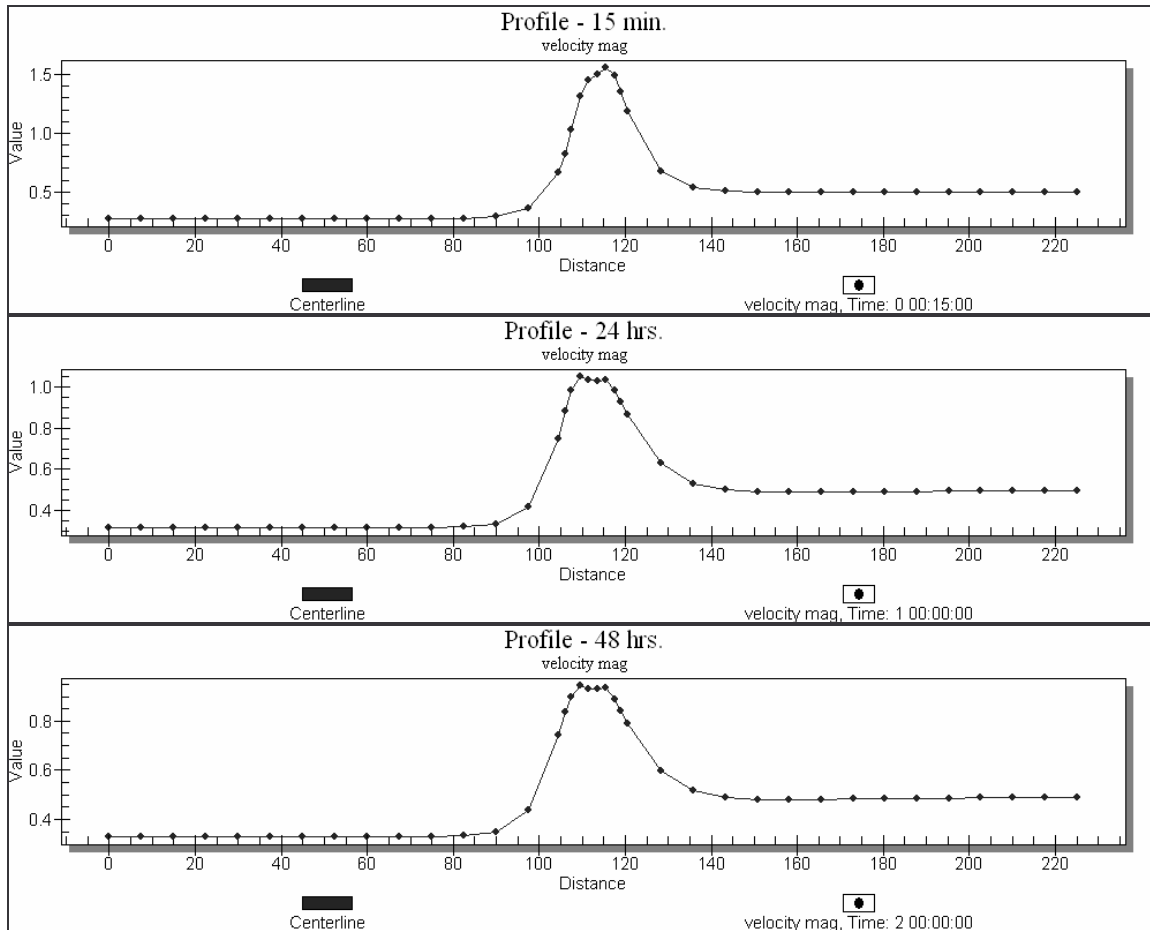


Figure 3-38: Centerline Profiles of Velocity Magnitude for the Equilibrium Transport Rate, 0.08mm Test Case at 15 Minutes, 24 Hours, and 48 Hours

Table 3-5 gives an overview of the locations and magnitudes of maximum scour and deposition for the abrupt contraction test cases. As with the other test cases for contraction, the table shows that the tests for the short abrupt contraction indicate that as the particle size increases, the location of scour remains constant and the location of

deposition moves upstream. Also, the magnitude of scour generally decreases and the magnitude of deposition generally increases as the particle size increases.

Table 3-5: Locations and Magnitudes of the Points of Maximum Scour and Deposition for the Short Abrupt Contracion Test Cases

<i>Particle Size (mm)</i>	<i>Location of Maximum Scour (m)</i>	<i>Magnitude of Maximum Scour (m)</i>	<i>Location of Maximum Deposition (m)</i>	<i>Magnitude of Maximum Deposition (m)</i>
0.08	115.5	1.24	97.5	0.01
0.2	115.5	1.37	143.3	0.08
2.0	115.5	1.00	135.9	0.33
4.0	115.5	0.82	128.4	0.37

4 Presentation of Results: Quantitative Analysis

The results given in chapter 3 identified the specific sediment transport options that are currently functional in FST2DH and also examined the degree to which the results obtained made sense intuitively. This chapter provides comparisons between the results from FST2DH and those from two other programs, SED2D WES and SAMwin. It also gives the results from several FST2DH test cases built with data from previous research with laboratory flumes and comments on those results. The last section in this chapter reviews the results from an FST2DH simulation modeling the deposition of sediment at a river's entrance into a reservoir.

4.1 SED2D WES

The test cases created for the comparison of FST2DH sediment results to those from SED2D WES provide insight pertaining to the advantages of using a semi-coupled model instead of an uncoupled one. The results from the test cases also illustrate that the general patterns seen in the changing bed elevations of an FST2DH sediment simulation are consistent with those predicted by SED2D WES.

Previous analysis suggested that currently the Ackers-White Formula in FST2DH does not work appropriately. Because SED2D WES only supports the Ackers-White Formula (USACE 2004), the simulations were created using different equations for the

two models. Originally, research attempted to manually couple the RMA2 and SED2D WES runs, but incomplete files generated inside one of the models made this attempt unsuccessful. Therefore, uncoupled results from SED2D WES (calculated with the Ackers-White formula) were compared to the semi-coupled results from FST2DH (calculated with the Engelund-Hansen formula). While this eliminated the possibility of making a direct quantitative evaluation, it did illustrate the advantage that FST2DH has over SED2D WES because of its automatic semi-coupling option.

4.1.1 Moderate Midsection Slope

The results from the test case in SED2D for a flume with a moderate midsection slope illustrate that a new hydrodynamic solution should be obtained as a channel's geometry undergoes dramatic changes. The steady-state hydrodynamic solutions for FST2DH and SED2D WES provided fairly identical profiles for water surface elevation and velocity magnitude. In both cases, the peak velocity occurred just downstream of the first break in slope. In SED2D WES, the velocity reached a maximum of 1.58 m/s and in FST2DH, it reached a maximum of 1.53 m/s.

The hydrodynamics for the FST2DH simulation gradually changed over time as the channel flattened. The velocity through the middle segment decreased greatly over time. This resulted in less scour through the middle segment of the channel. This expected trend was modeled well with semi-coupling. In the uncoupled situation, SED2D WES applied the same initial hydrodynamics to the middle portion of the channel even after its geometry changed significantly. Because the hydrodynamics did not change as the channel flattened, the middle segment continued to scour dramatically, as shown in Figure 4-1.

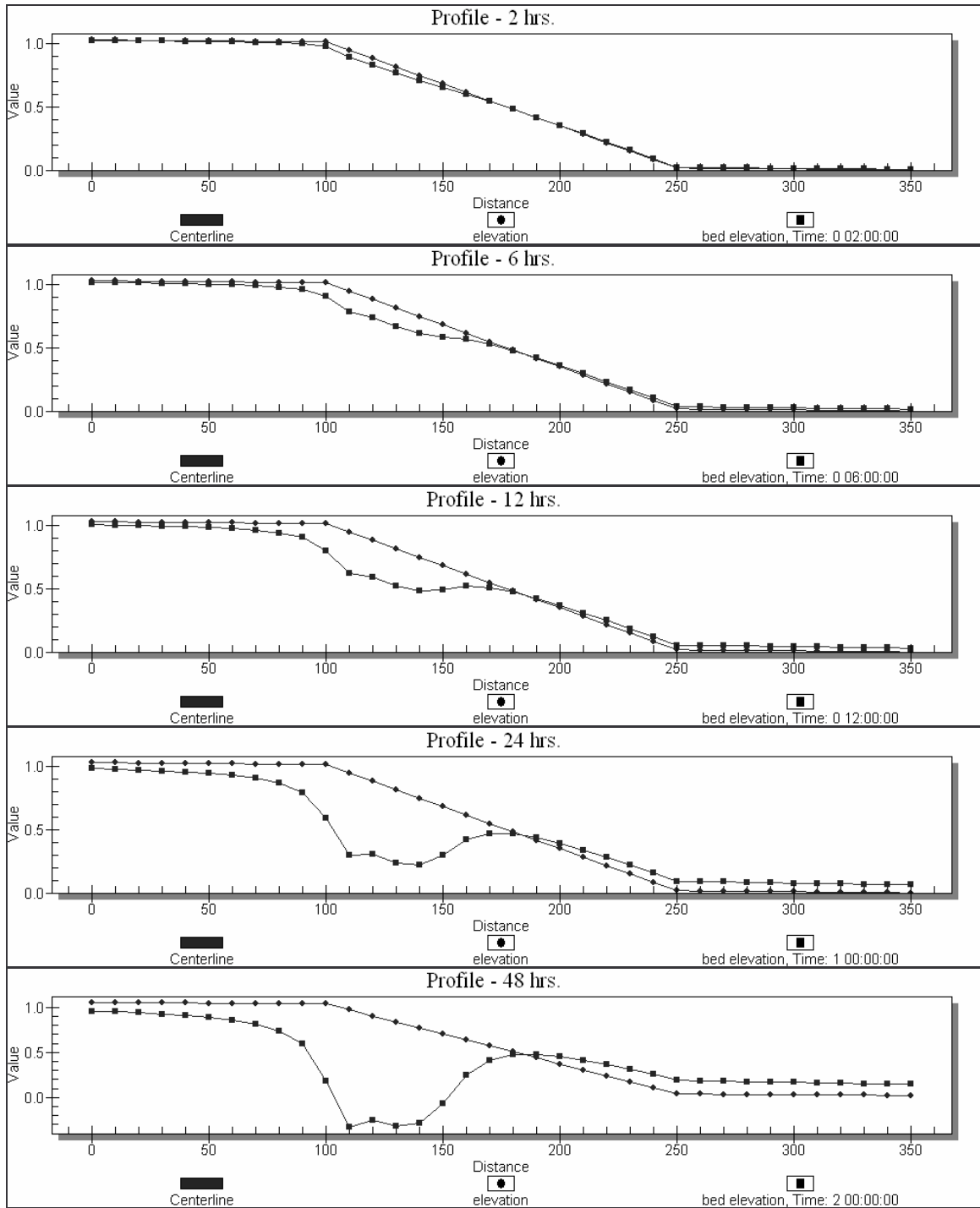


Figure 4-1: Bed Elevations from SED2D for the Clear-Water, 0.2mm Test Case for the Flume with a Moderate Midsection Slope after 2 Hours, 6 Hours, 12 Hours, and 24 Hours

The final bed from the SED2D run does not reflect scour patterns expected for this flume. A comparison of the final bed profiles after a 48-hour simulation in FST2DH and SED2D WES (Figure 4-2) shows that SED2D WES predicted a much different scour pattern than did FST2DH because of its uncoupled nature. The bed profile found with FST2DH seems more appropriate for the given case. The figure also shows that the point separating scour and deposition falls at the same location for both cases—halfway down the sloped midsection.

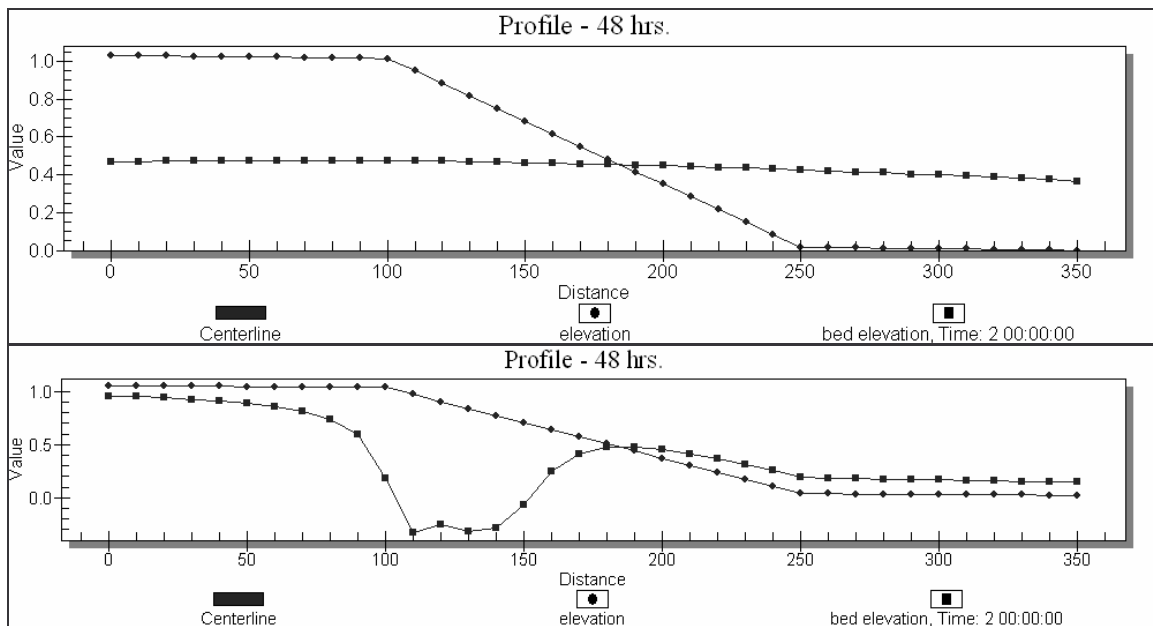


Figure 4-2: Final Bed Profiles for SED2D and FST2DH for a 48 Hour Simulation of the Clear-Water, 0.2mm Test Case for the Flume with a Moderate Midsection Slope

4.1.2 Gradual Contraction

The second set of tests created for the comparison of FST2DH and SED2D WES consisted of simulations for various particle sizes in a flume with a gradual contraction.

The steady-state hydrodynamic solutions from SED2D WES and FST2DH were very similar. When compared to the FST2DH sediment results, the SED2D WES solution for the 0.08 mm test case showed that when a large amount of scour or deposition occurred during a simulation, the uncoupled model does not provide appropriate bed elevations. Figure 4-3 gives the final bed elevations from FST2DH and SED2D WES for this case. The bed scoured ten times deeper with SED2D WES because the hydrodynamics used in the sediment calculation didn't change to reflect the new geometry in the contraction. Also, SED2D WES did not predict any deposition downstream. These results show that FST2DH more closely represents the expected scour and deposition than does SED2D WES. Although an equilibrium transport rate was used in FST2DH and clear water was used in SED2D, the results from the two cases were comparable because neither scour nor deposition occurred upstream in either setup, suggesting a state of equilibrium.

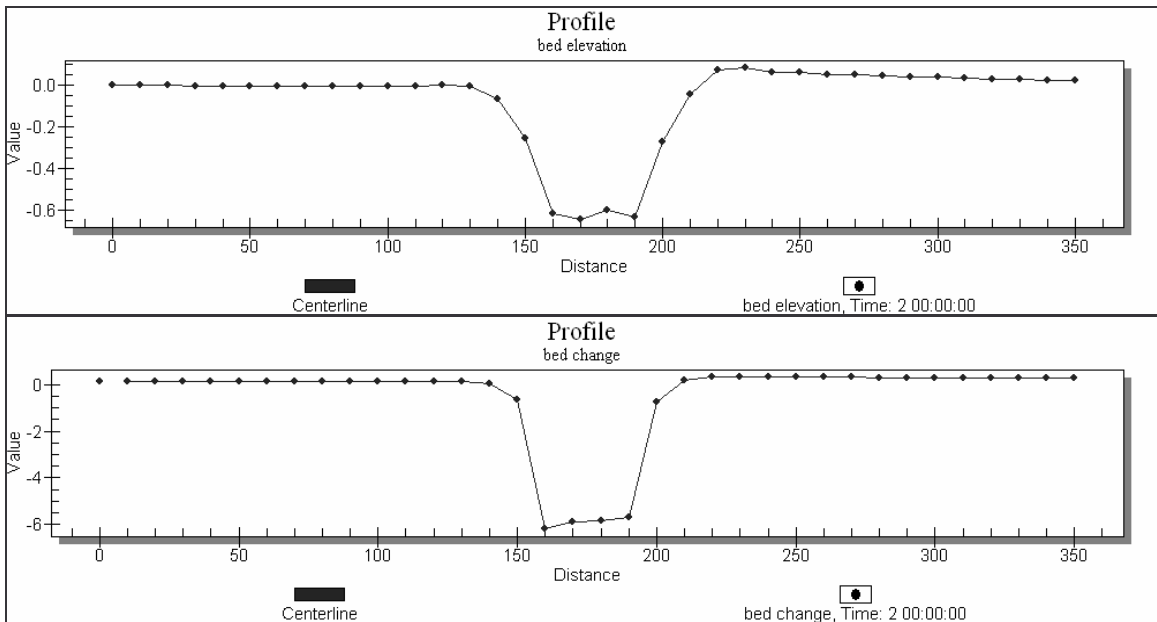


Figure 4-3: Final Bed Elevations from FST2DH and SED2D for the 0.08mm Test Case for the Flume with a Gradual Contraction

As the sediment size modeled in SED2D WES increased, the bed scoured less through the contraction (Figure 4-4). FST2DH showed this same pattern and it makes sense intuitively.

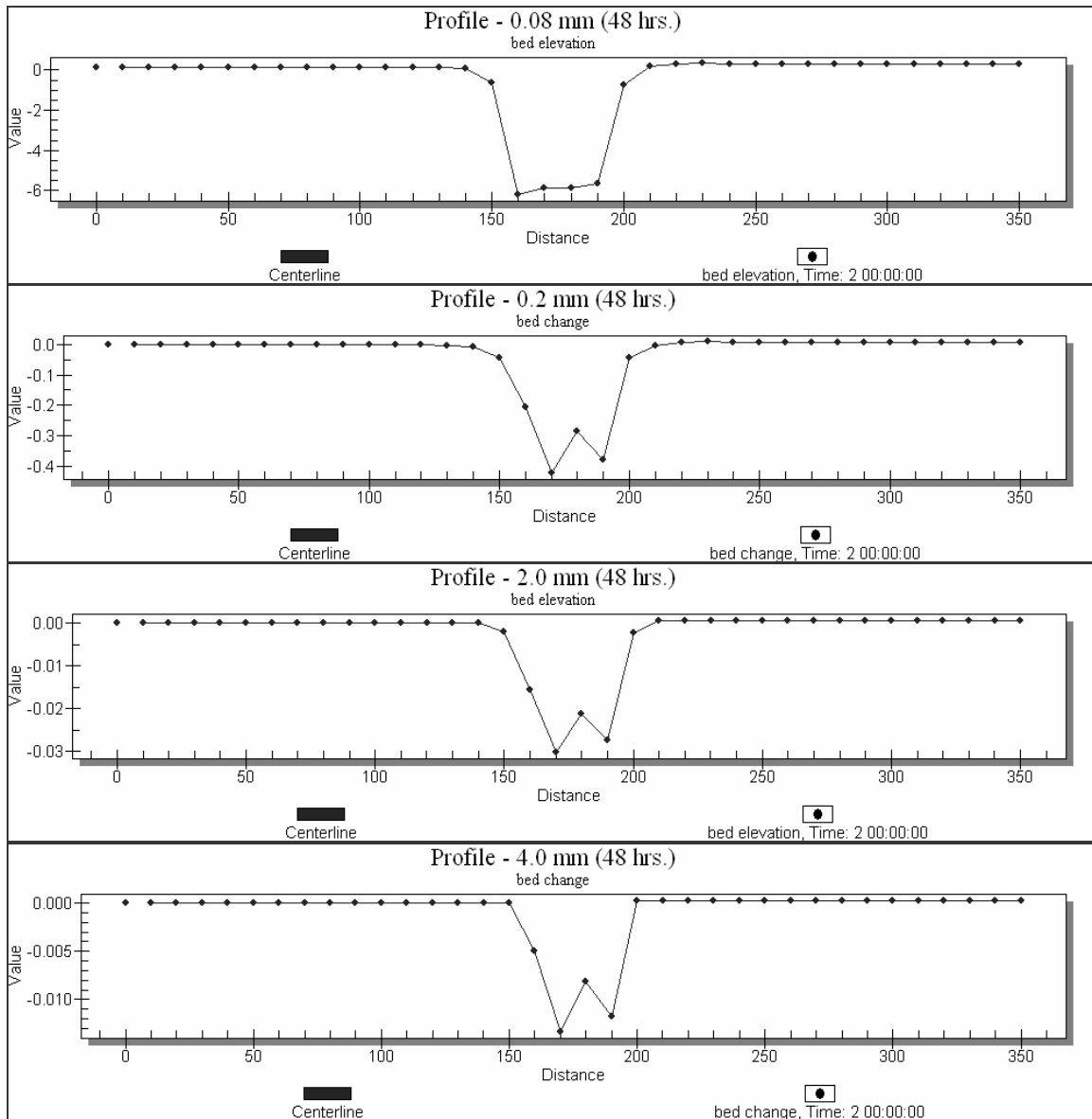


Figure 4-4: Final Bed Elevations from SED2D for the Test Cases for the Flume with a Gradual Contraction with Particle Sizes of 0.08mm, 0.2mm, 2.0mm, and 4.0mm

The results from SED2D WES suggest that less scour occurs for larger particle sizes than FST2DH predicted. There is no documentation that verifies appropriate implementation or testing of the Ackers-White formula in SED2D WES. The SED2D WES User's Manual does, however, state that the appropriateness of its use with the Ackers-White formula diminishes as the coarseness of the modeled sediment increases (USACE 2004).

Although the results from the SED2D WES test cases don't provide reasonable comparison to FST2DH results for a quantitative analysis, they still effectively illustrate the importance of running hydrodynamic and sediment calculations in a semi-coupled mode. The tests specifically showed that coupling is a critical part of obtaining an appropriate solution, especially when the geometry of a channel changes significantly. Furthermore, the test cases for SED2D WES demonstrated that once all the options for sediment transport in FST2DH are completely functional, FST2DH will be even more advantageous over SED2D WES for the modeling of sediment transport because of the limitations of SED2D WES.

4.2 SAMwin

SAMwin applies sediment transport capacity equations to calculate the sediment transport capacity of a river that is in general equilibrium (Thomas 2002). When an equilibrium transport rate is specified for the inflow boundary in an FST2DH model, FST2DH calculates the concentration of sediment required to create an equilibrium condition at the inflow boundary so that the amount of sediment entering the model is

equal to the carrying capacity of the channel. In such a case, neither deposition nor erosion occurs.

Each of the test cases used for SAMwin-FST2DH comparison ran in SAMwin first and then in FST2DH. This allowed for the default input parameters for SAMwin to be identified and entered into FST2DH. After the completion of both models runs, the equilibrium concentrations calculated at the inflow boundary of the FST2DH model were converted to units of parts per million (ppm) for comparison to the concentrations output by SAMwin. Two different particle sizes and three different transport equations with six different flowrates were tested. The transport equations included three of those that earlier research found to be functional in FST2DH: the Yang Sand and Gravel formula, the Engelund—Hansen formula, and the Laursen equation. The next two figures show the comparison of results from the runs for each of the flowrates and transport equations for the 0.177mm case (Figure 4-5) and the 1.414mm case (Figure 4-6).

The results suggest that for the smaller particle size (0.177mm), the equilibrium concentrations calculated in FST2DH best match those from SAMwin when using the Engelund—Hansen equation. The concentrations for the Engelund—Hansen case match quite well, with those output by FST2DH being 105 percent of the value of those output by SAMwin. The application of the Yang equation in both models also provided resulting equilibrium concentrations that are comparable, with the concentrations output by FST2DH with values that are about 84 percent of those output by SAMwin.

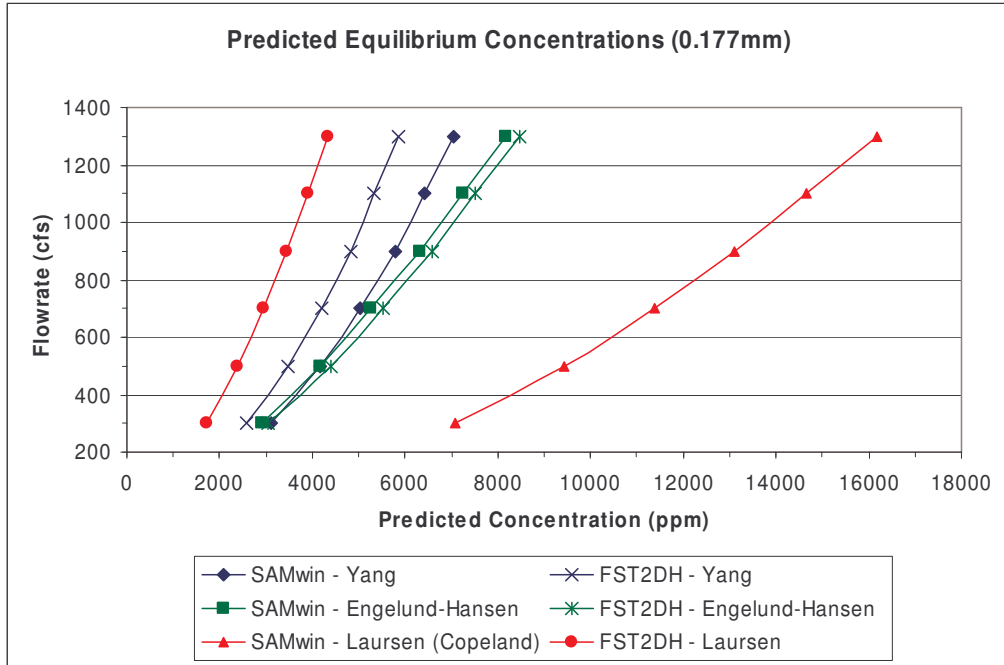


Figure 4-5: Equilibrium Transport Concentrations Predicted by FST2DH and SAMwin for Varying Flowrates and Transport Equations for Test Cases with a 0.177mm Particle Size

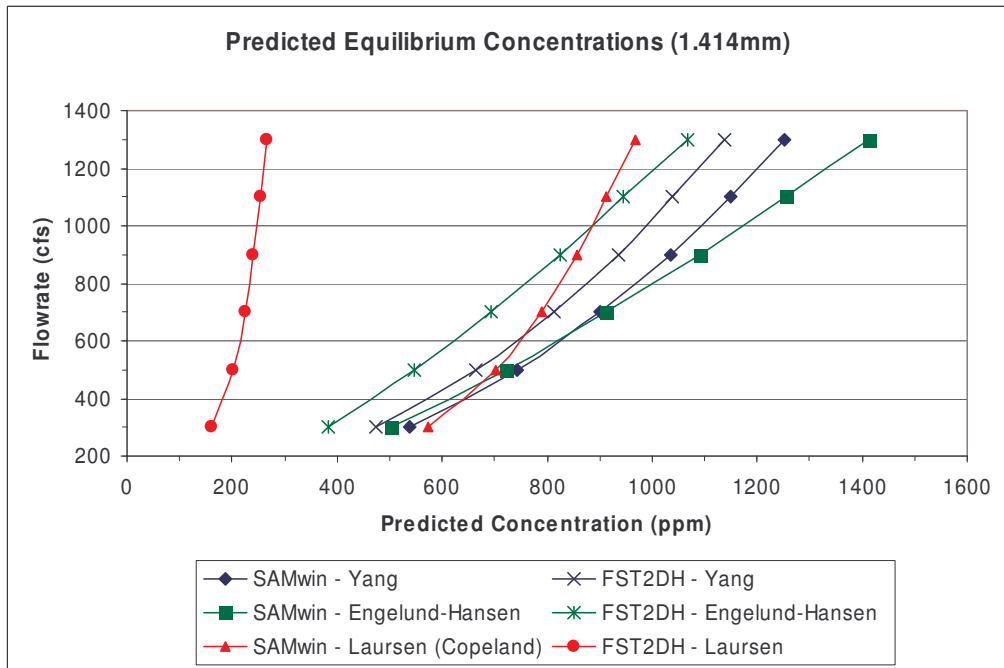


Figure 4-6: Equilibrium Transport Concentrations Predicted by FST2DH and SAMwin for Varying Flowrates and Transport Equations for Test Cases with a 1.414mm Particle Size

The Laursen (Copeland) equation provided in SAMwin is a modification to the Laursen equation used in FST2DH, as it extends the applicability of the Laursen equation to larger gravel sizes (Thomas 2002). Because the grain sizes used in the test cases for FST2DH and SAMwin are smaller, a reasonable comparison could be made between the two models using the Laursen and the Laursen (Copeland) formulas. The resulting equilibrium concentrations from FST2DH (using the Laursen equation) and SAMwin (using the Laursen (Copeland) formula) provided a relatively poor agreement between the concentrations output from each model. The concentrations reported by FST2DH for this case are only 24 percent of those found with SAMwin.

The test cases with the 1.414 mm grain size showed that when larger particles were used, the tests for the Yang equation provided a closer match for the equilibrium concentrations output by each model than the Engelund—Hansen formula. The FST2DH concentrations from models using the Yang Equation fell at about 90 percent of the values of those predicted by SAMwin with the same equation. With the Engelund—Hansen equation, FST2DH gave concentrations that were about 76 percent of the value of those found with SAMwin. The Laursen and Laursen (Copeland) equations again provided the poorest agreement of concentration, with those calculated by FST2DH being only 28 percent of the value of those obtained with SAMwin.

The Engelund—Hansen equation appears to be implemented fairly well in FST2DH. The model does a good job of calculating appropriate equilibrium concentrations when the Engelund—Hansen equation is used with smaller sediment sizes. As the sediment size increases, the appropriateness of the application of

Engelund—Hansen equation in an FST2DH model decreases and the appropriateness of Yang's Sand and Gravel formula increases.

4.3 Laboratory Models

The test cases for the simulation of several different laboratory flumes provided additional information about the modeling of sediment transport in FST2DH. Research included the setup for simulations of five different laboratory flumes in FST2DH. Each of the test cases illustrated that although FST2DH provides logical and intuitive results for general and hypothetical sediment transport analysis, difficulty arises when specific laboratory models are to be simulated. Some of the difficulties encountered in this portion of the research are explained in the next few paragraphs. The sections that follow provide an overview of the modeling attempts made and possible reasons for their failure.

One of the main difficulties experienced while modeling the small laboratory flumes in FST2DH was that when the elements represented small areas, the resulting model runs were unstable. The research enlarged one of the models to determine if FST2DH would be more stable with elements that represented larger areas and found that that was the case. Others have experienced similar difficulty in modeling small channels with elements that represented very small areas (Barton 2001). While a larger-scaled model of a laboratory flume can be created, doing so may introduce other errors into the simulation and it would thus not represent the actual conditions in the laboratory.

A second difficulty arose when modeling laboratory flumes in FST2DH because of the limitations in the current functionality of the sediment transport options in FST2DH. Most of the laboratory models described in various journal articles included the inflow of

sediment at specific transport rates or concentrations. Since the options for applying an incoming sediment transport rate or sediment concentration to the inflow boundary do not currently work in FST2DH, the studies with such boundary conditions could not be modeled completely as they were in the laboratory. A couple of the test cases given below attempted to replicate an inflow transport rate by applying an equilibrium flowrate to an extended, sloped upstream addition to the flume. Although the exact laboratory conditions could not be replicated, the test cases did illustrate patterns of deposition that make sense intuitively. These tests are described in more detail in are described in sections 4.3.4 and 4.3.5.

Other difficulties arose because some of the steady-state hydrodynamic runs failed and others did not reflect the flow conditions observed in the laboratory. Investigation was not able to find the exact causes for the failure. Information about the flow characteristics and associated parameters beyond that given in the journal articles is needed to create models that better replicate the observed flow conditions. The flow regime for such cases must be identified before sediment analysis can be completed for these laboratory test cases.

The following sections provide a general overview of the models and results from the five specific laboratory flume test cases developed in FST2DH. Because of the difficulties described above, most of the test cases failed to provide sediment results. Therefore, the main purpose for the following sections is to provide a general overview of the research's attempts and a brief summary of each model for future reference.

4.3.1 Scour Patterns and Depths Around a Pier

The first laboratory flume test case consisted of an FST2DH model of one the experiment runs (experiment 10) from a set of clear-water scour tests for flow around piers of various sizes (Sheppard 2004). The full set of laboratory tests included representation of three differently-sized piers. Experiment 10 provided analysis of the scour that occurred around a pier with a diameter of 0.91 meters. Figure 4-7 shows the grid created for this test case.

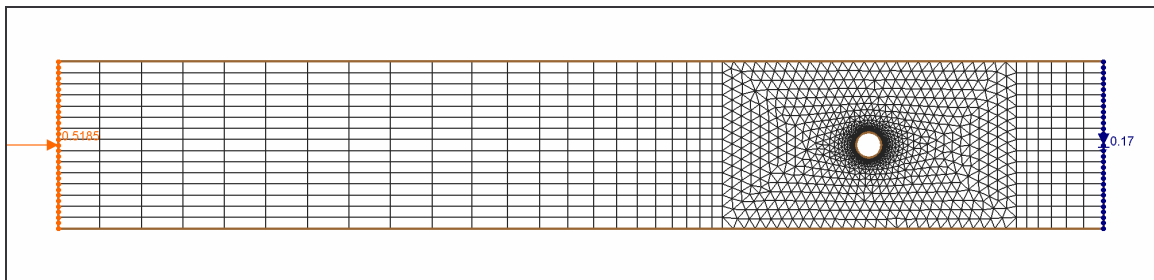


Figure 4-7: Grid for Experiment 10 from Sheppard's Experiments

The steady-state hydrodynamic run for this test case would not run to completion. Although many attempts were made and the input parameters were all checked for reasonableness, the steady-state run continued to fail. With the aid of the spin-down steering option in the Surface-Water Modeling System (SMS), the simulation still only ran to about 50% completion. The purpose for the failure remains unclear, and a sediment transport simulation could not be carried forward.

4.3.2 Narrow Contraction Flume with Varying Entrance and Exit Angles

A series of laboratory experiments performed by Dey et al. illustrated the different maximum scour depths that resulted from the variation of the width of a long contraction (Dey 2005). The widest portion of the flume was 0.6 meters wide and the entire flume was 12.0 meters long. The journal article provided measurements of upstream velocity and water depth for each experiment, but only mentioned that the flume was “tilting” and did not give a specific slope or flowrate. The current research made several attempts to match the hydrodynamic conditions of the laboratory flume in FST2DH, but was unsuccessful at doing so. More detail about the specific flowrates and downstream water surface elevations observed in each of the test cases would be beneficial. Figure 4-8 shows the grid for the flume with the widest contraction (0.42 m).

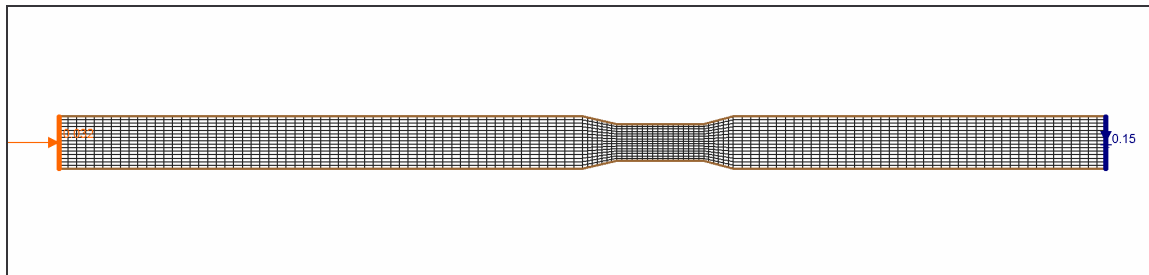


Figure 4-8: Grid for Dey’s Experiment for the Flume with the Largest Contraction

4.3.3 Scour at a Basin’s Entrance

Two papers found during the research process referred to experiments completed by Thuc (Thuc 1991) in which Thuc examined the erosion in a basin due to clear-water inflow (Duc 2004, Wu 2004). Journal articles by Duc and Wu provided the dimensions

for the experimental basin, as well as the velocity for the inflow channel and the water surface elevation for the outflow channel. The slope was assumed to be zero, based on the elevations along the beginning and ending segments of the bed elevation curves given in a plot in Duc's paper (Duc 2004). Because the papers by Duc and Wu provide no further information about the flow regime, it remains unknown whether a hydraulic jump occurred near the basin opening. Without more information about the flow regime, the research was unable to create a reasonable hydrodynamic solution and the sediment transport could not be modeled accurately in FST2DH. More specific data needs to be obtained directly from Thuc's dissertation (Thuc 1991) before an appropriate model can be created. Figure 4-9 shows the grid created for Thuc's Experiment.

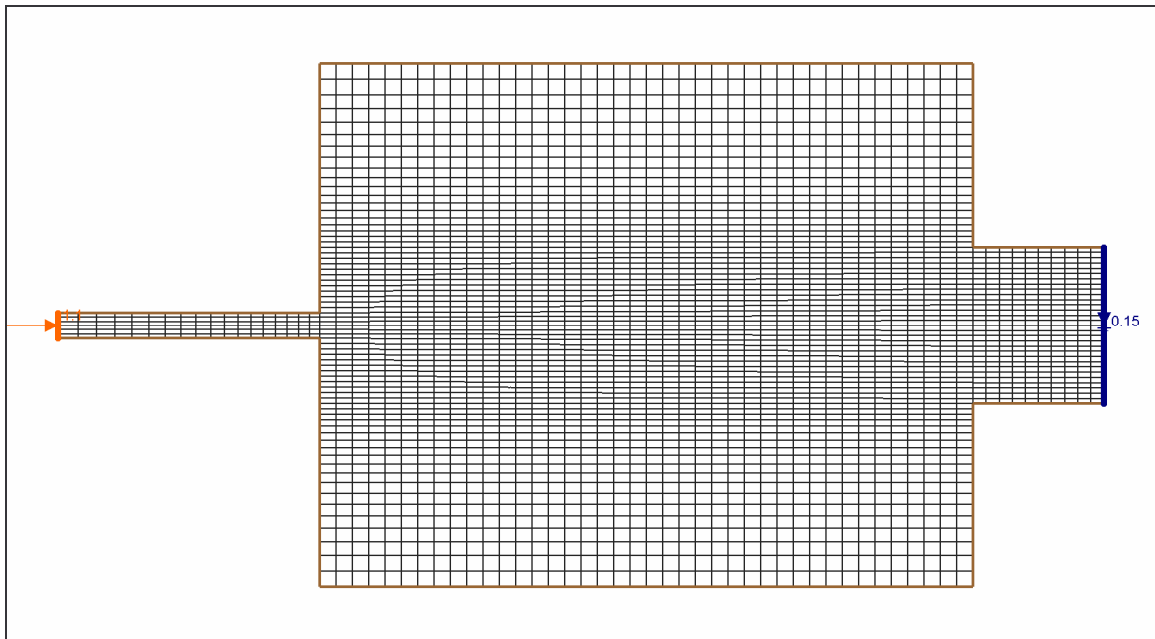


Figure 4-9: Grid for Thuc's Experiment

4.3.4 Narrow Flume with Downstream Fining

Seal et al. modeled downstream fining in a long, narrow (0.3 meters wide) rectangular flume with smooth walls and floor (Seal 1997). A flowrate of 0.049 cms carried sediment fed to the flume at its upstream end down the flume. Some of the larger sediment deposited fairly quickly and the smaller sediment was carried further downstream. Because the option for specifying an inflow sediment concentration or transport rate in FST2DH does not work properly, a steeper-sloped segment was added to the upstream end of the modeled flume and an equilibrium transport rate was applied to the upstream boundary. Manipulation of the slope of the upstream portion attempted to match the sediment feed rate from the laboratory experiment. While the steady-state hydrodynamic runs succeeded, each of the sediment runs attempted failed after a few timesteps. It is believed that the failure resulted from the narrow width of the flume. Each element only covered a very small area, and in such cases, the model seemed to be unstable. This reason for failure is supported by the results of the test case described in the next section, in which a sediment model of a similar, yet wider channel ran successfully.

4.3.5 Wide Flume with Downstream Fining

Toro-Escobar et al. performed several experiments on downstream fining in flumes with a width of 2.7 meters (Toro-Escobar 2000). One of their experiments, labeled Run 5 in the Toro-Escobar paper, examined the downstream fining of sandy sediment along the length of the flume. Similar to Seal's experiment, Toro-Escobar's experiment included an inflow sediment rate, which FST2DH cannot currently replicate appropriately. Therefore, the model was modified by adding an extension with a slightly steeper slope

to the upstream boundary of the model. The inflow boundary's flowrate and the outflow boundary's water surface elevation were set to match the data from the Toro-Escobar experiment and an equilibrium sediment transport rate was assigned to the inflow boundary. The bed consisted of a single grain size of 2.0 mm, representing the geometric mean grain size from the Toro-Escobar paper.

Research adjusted the slope of the upstream segment until a sediment concentration of approximately 20 kg/min entered the mesh. This rate (two-thirds of that given by Toro-Escobar et al.) was chosen arbitrarily but still provided results that showed an appropriate trend. Even if the inflow rate of sediment matched that given in the Toro-Escobar paper, the resulting bed profile would not be the same as that observed in the laboratory. This happens because the sediment entering the domain deposits upstream from the break in slope and thus, less sediment enters the region modeled in the laboratory.

Figure 4-10 shows the change in the bed over time for the Toro-Escobar test case, modified slightly due to the limitations in the functionality of the FST2DH sediment transport options. The pattern of deposition shown in the figure makes sense intuitively. It begins near the break in slope, where the velocity of the flow slows dramatically. The volume of deposited material increases throughout the entire simulation and the front of the zone of deposition gradually moves downstream.

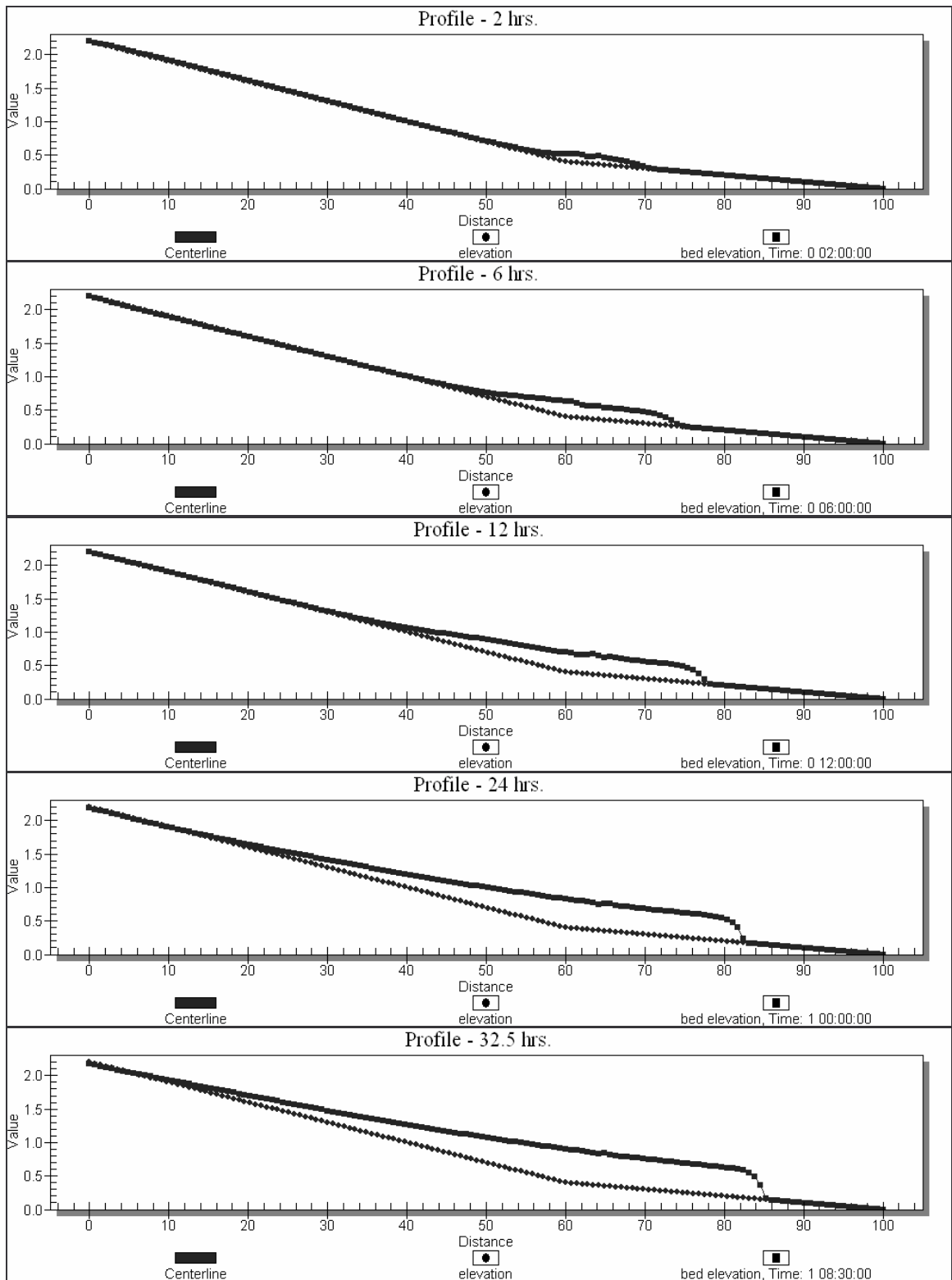


Figure 4-10: Bed Elevations for the Modified Toro-Escobar Test Case after 2 Hours, 6 Hours, 12 Hours, 24 Hours, and 32.5 Hours

4.4 Deposition in a Reservoir

The test case for the flume entering into the reservoir only completed 144 days out of the full 180-day simulation. A message provided upon the model run's failure stated that an access violation had occurred. The solution suggests that the model was stable up to the 70-day mark, as the volume of material being deposited over time closely matched the volume available for deposition (the volume of material entering the domain for equilibrium conditions minus the volume of material exiting the domain through the downstream boundary). Figure 4-11 shows that the volume of sediment available for deposition and the volume of sediment actually being deposited match well until about the 70-day mark.

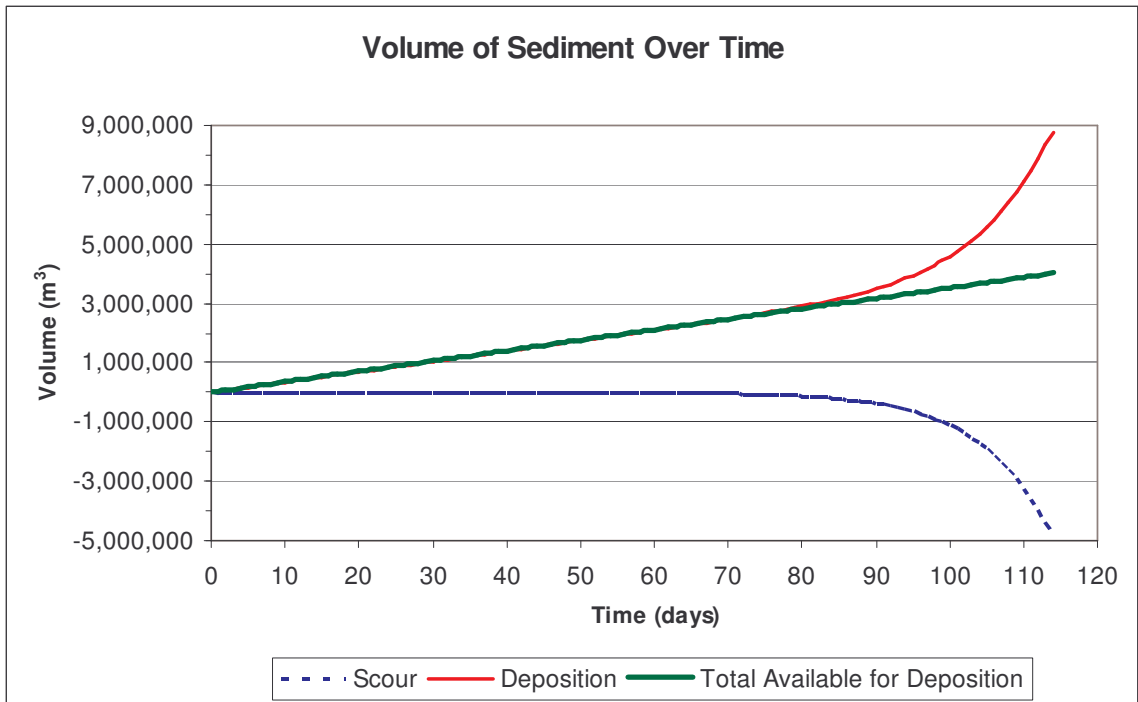


Figure 4-11: Volumes of Sediment Deposited, Scoured, and Available for Deposition

The divergence of the scour and deposition volumes that occurs after the 70-day mark suggests that the model started showing instability just after that time. The cause for the instability that resulted in the run's failure at the 144-day mark could not be determined and should be investigated by the model developers. Figure 4-12 provides a closer view of the stable portion of the model run, showing the close correlation of the volumes of sediment available for deposition and the sediment actually being deposited.

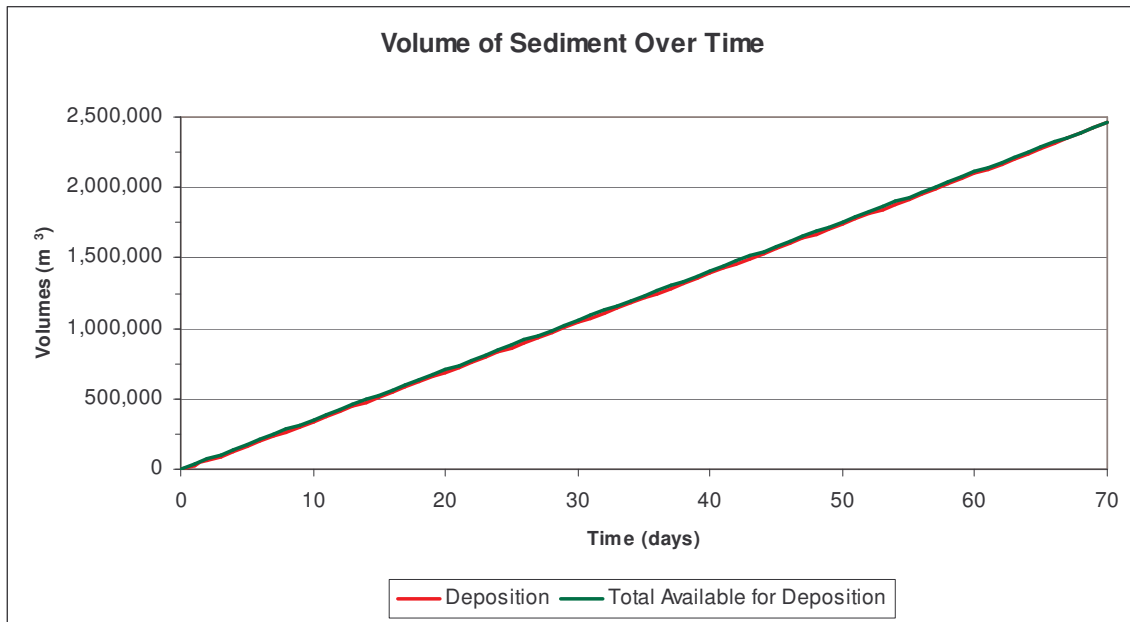


Figure 4-12: Volumes of Sediment Deposited and Available for Deposition

The resulting bed profiles from the stable portion of the model run show that a delta appropriately forms due to backwater. The location of the delta was appropriate—it formed at the location where the velocity quickly decreased due to the changing cross-section. This is shown in the close-up view of the 30-day bed and water surface profiles given in Figure 4-13.

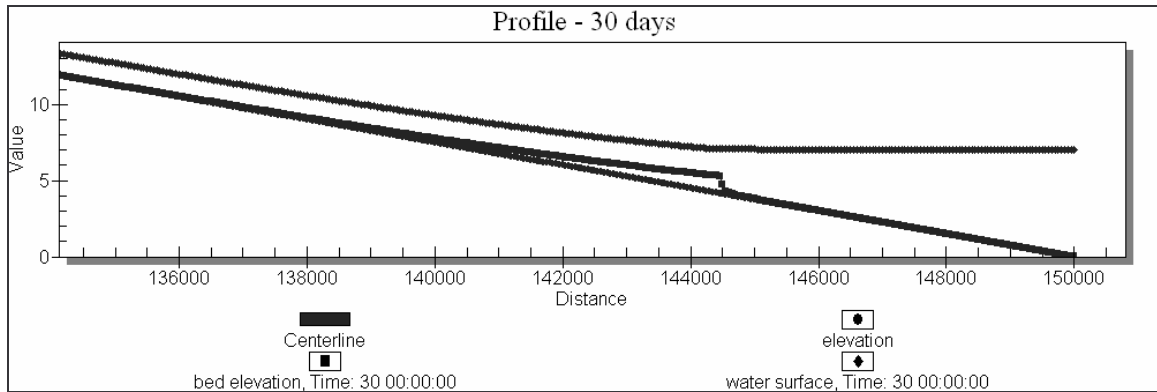


Figure 4-13: Profiles for the Water Surface Elevation, Original Bed Elevations, and Bed Elevations after 30 Days

The delta that formed over time gradually increased in depth and gradually moved downstream. The steepness of the downstream face of the delta increased as well. This pattern of aggradation that occurred as a result of a backwater appropriately followed that described generally by Hotchkiss (1991). Figure 4-14 shows the bed profiles for several different timesteps from the FST2DH simulation.

Research found that a large amount of material deposited over a relatively short amount of time. It further discovered that the volumes of sediment available for deposition (the volume of sediment inflow minus outflow) matched closely with the volume of sediment deposited for each timestep in the first 70 minutes of simulation. To verify that the equilibrium inflow concentration calculated by FST2DH was appropriate, research modeled the upstream portion of the channel in SAMwin. SAMwin gave an equilibrium concentration of 1,146 ppm. The concentration predicted by FST2DH (1,070 ppm) closely matched that obtained from SAMwin, falling at about 93 percent of its value (a difference of only 76 ppm). This suggests that correct sediment equilibrium conditions were calculated in the FST2DH test case. Thus, although it was quite large,

the volume of material deposited during the 70-day simulation in FST2DH was appropriate.

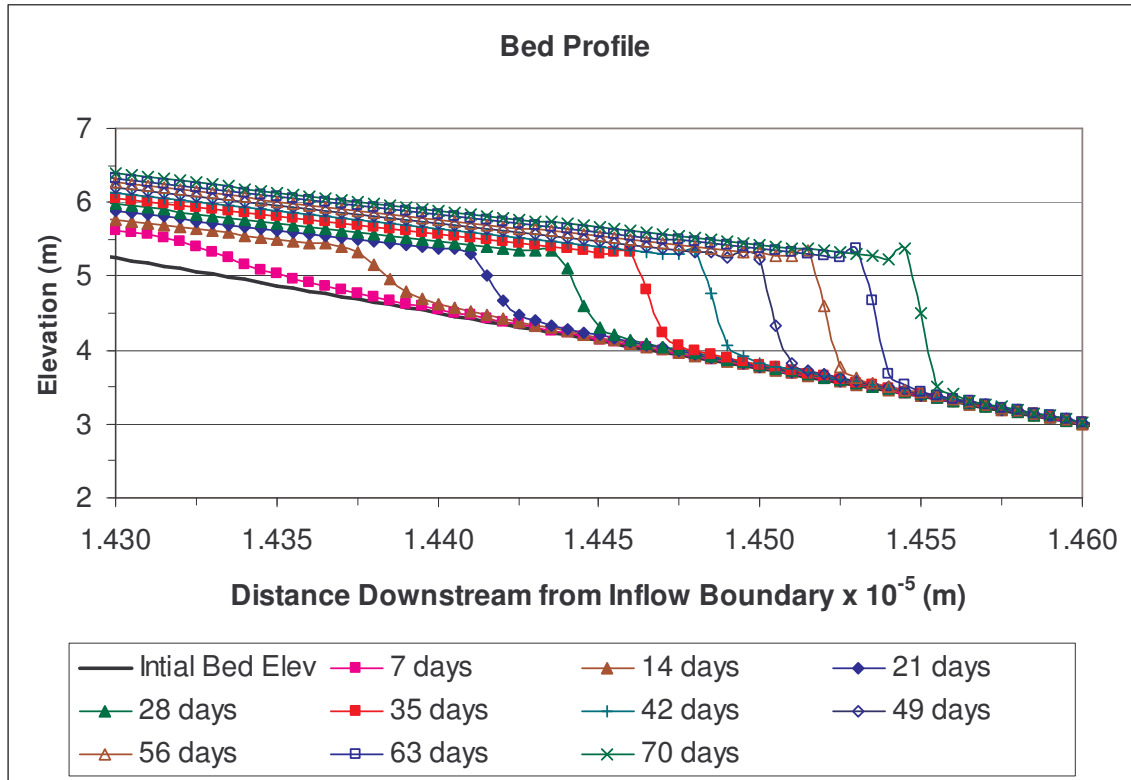


Figure 4-14: Change in Bed Profile over Time Due to Backwater

The flume used in the first test case utilized a single sediment size of 0.5mm for analysis. A second simulation of the same flume with two grain sizes (0.5mm and 2.0mm) failed at 39 days, with instability beginning just after 23 days, as shown in Figure 4-15. In this case, the model demonstrated instability in the sediment inflow (sediment available for deposition) rather than in the volume of sediment deposited, as occurred in previous cases. The model developers should investigate why the model failed sooner when two particle sizes were specified instead of only one.

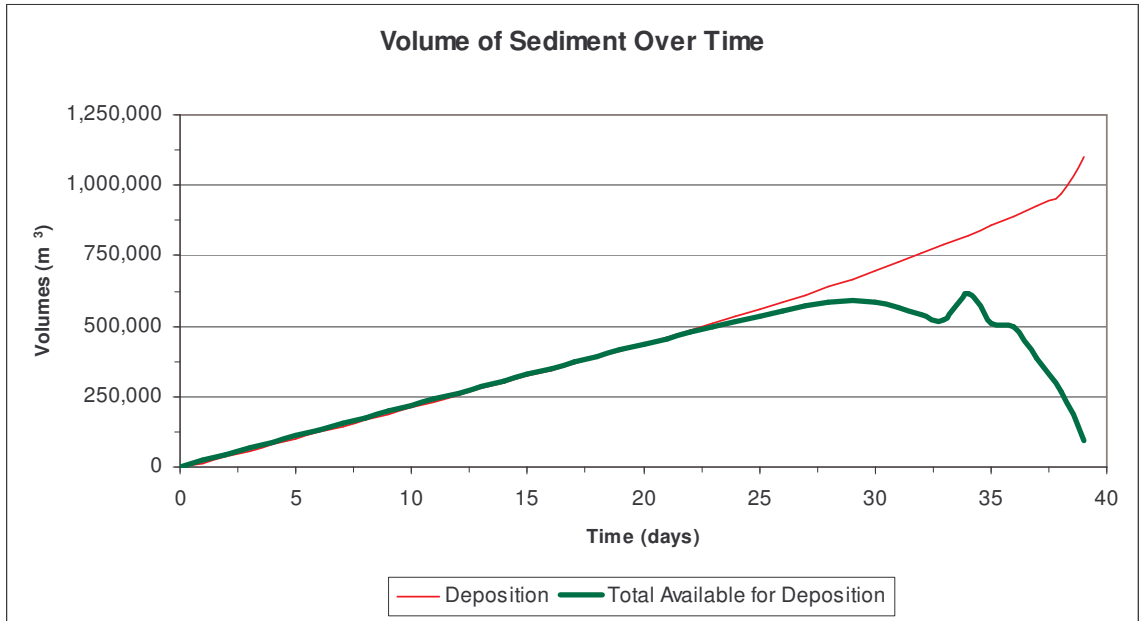


Figure 4-15: Volumes of Deposition and Material Available for Deposition for the Reservoir Test Case with Two Grain Sizes (0.5mm and 2.0mm)

Figure 4-16 shows a plot comparing the resulting bed elevations at 23 days for the single and multiple grain size simulations.

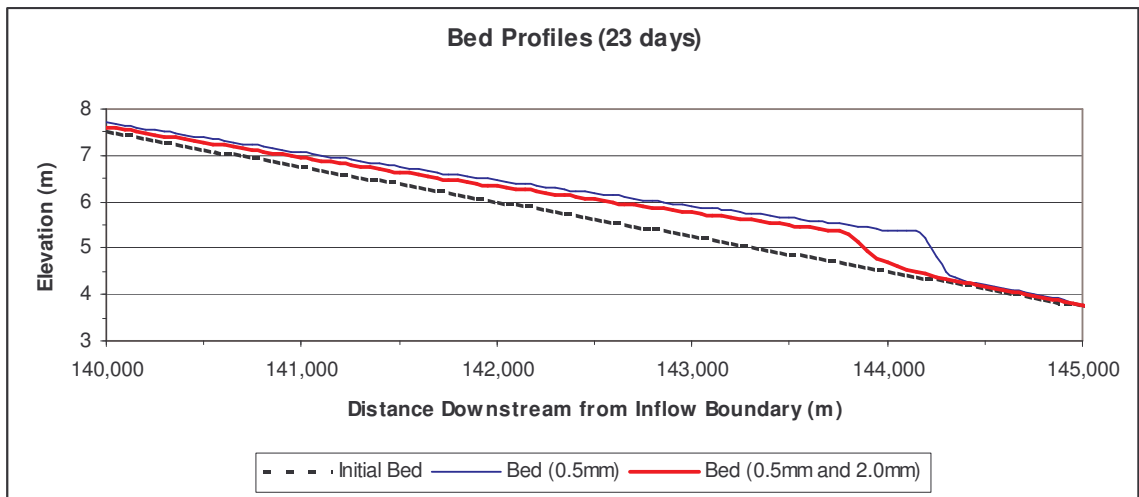


Figure 4-16: Bed Profiles for the Reservoir Test Case with a Single Grain Size and the Test Case with Two Grain Sizes (0.5mm and 2.0mm)

The profiles in Figure 4-16 suggest that deposition occurred furthest upstream in the test case with two particle sizes. They also show that the delta that formed had a flatter downstream slope when two particle sizes were specified. The difference in delta's location, magnitude, and downstream slope for the two cases results from the fact that as the river slows down upon entering the zone of backwater, larger sediment stops moving sooner than smaller sediment comprised of the same type of material (e.g.- sand).

Two of the test cases developed for a longer flume with different element sizes failed to run to completion (runs C and D). Another test case (run A) showed erosion throughout the run, which is indicative of other problems in the model, as no scour should occur in any of the cases. Run B showed an appropriate amount of deposition and erosion (close to no erosion) and ran to completion. The plots relating the volumes of material eroded, deposited, and the material available for deposition are shown in the next four figures (Figure 4-17, Figure 4-18, Figure 4-19, and Figure 4-20). For the two cases of divergence (run C and run D), the divergence occurred at different times. This may be due to their different element sizes, but further investigation by model developers is needed to determine if this is in fact the case. It remains unknown why the volumes for deposition didn't match for any of run A. While run B provided some deposition, the small delta that was formed in the region of backwater did not show up in the bed profile as being anything more than a small mound, without a steep front edge. A much longer model run needs to be completed to determine if the delta grows and moves in a manner similar to that observed in the first test case. However, FST2DH limits the total allowable simulation time to 9,999 hours (416.6 days), so such a model cannot be created at the current time.

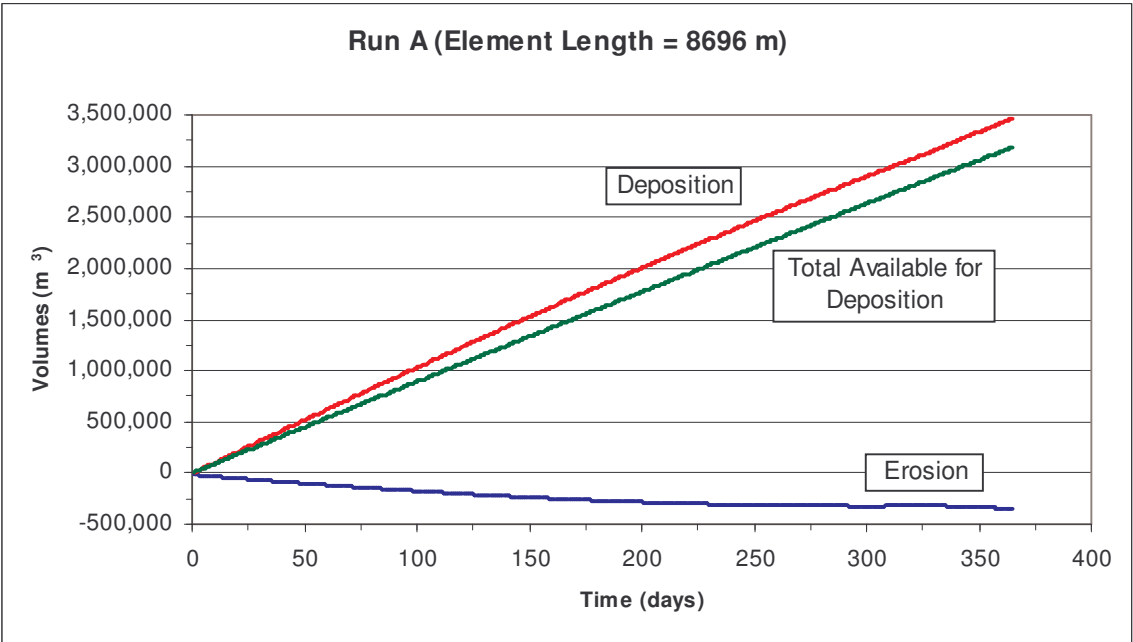


Figure 4-17: Volumes of Erosion, Deposition, and Material Available for Deposition for Run A

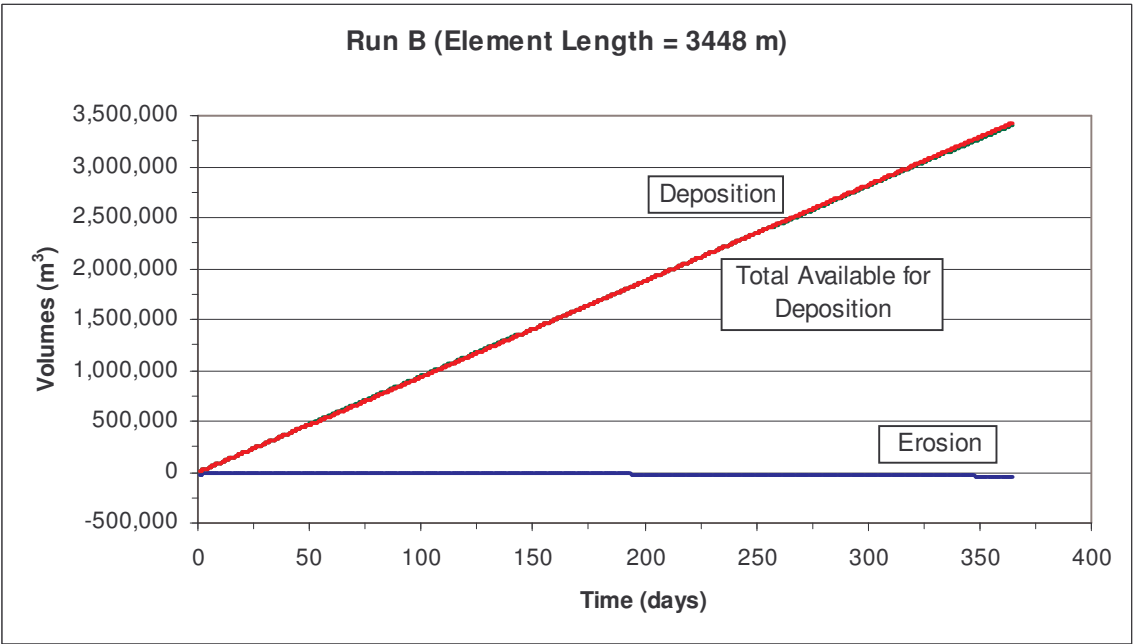


Figure 4-18: Volumes of Erosion, Deposition, and Material Available for Deposition for Run B



Figure 4-19: Volumes of Erosion, Deposition, and Material Available for Deposition for Run C

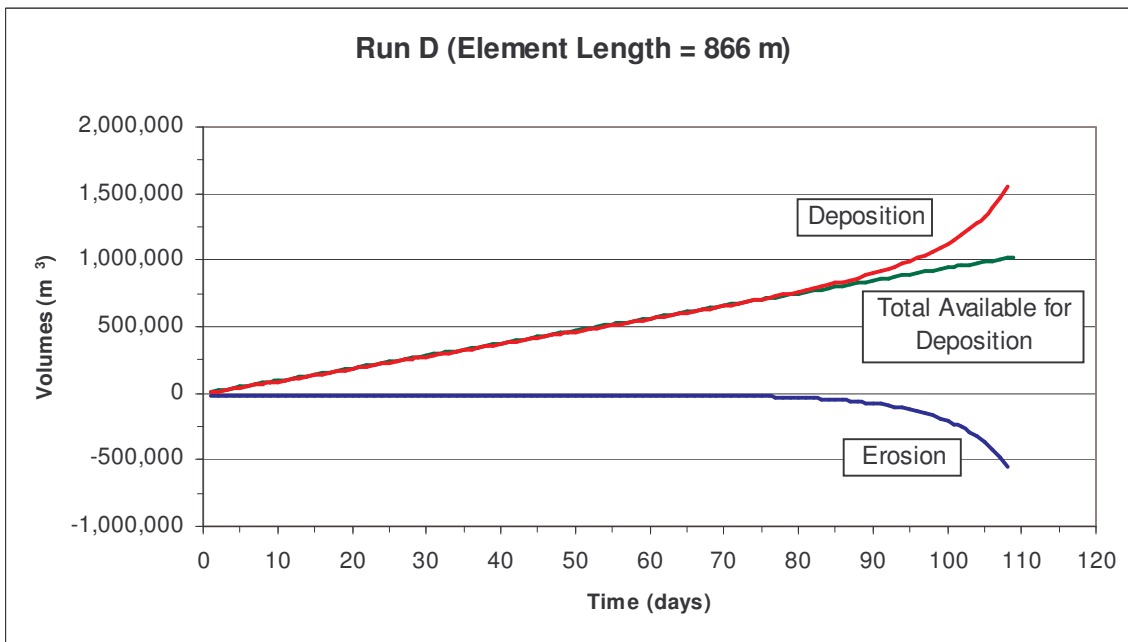


Figure 4-20: Volumes of Erosion, Deposition, and Material Available for Deposition for Run D

The next figure (Figure 4-21) shows a plot relating the time of model stability to the element sizes tested for the four test cases studied. Because runs A and B ran to completion and did not show a pattern of instability consistent with that seen in runs C and D, a trend line relating the element size to the beginning time of instability could not be created. From the trend seen in runs C and D, however, it appears that the larger the element length, the longer the model used in these test cases is stable.

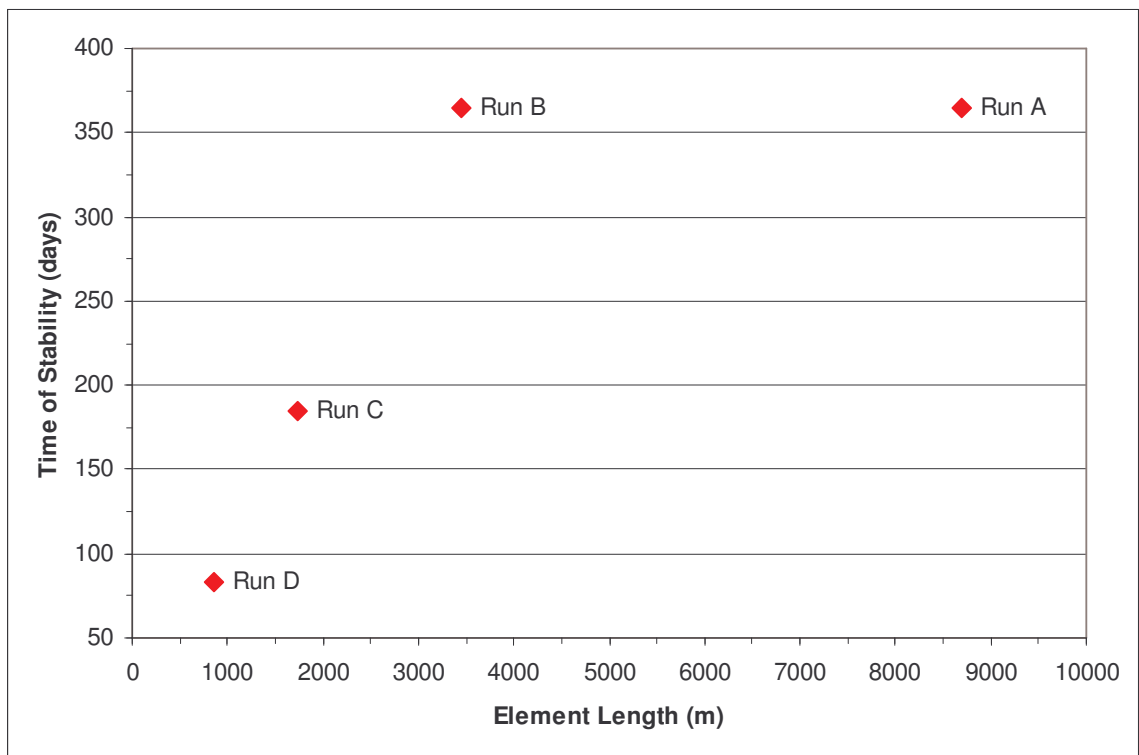


Figure 4-21: Element Length and Time of Stability for the Long Flume Emptying into a Reservoir

The test cases representing a river with backwater due to a downstream obstruction showed that FST2DH is capable of modeling the formation of a delta due to backwater. The downstream slope of the modeled delta grows steeper and moves

downstream slowly with time, which makes sense intuitively. When two material sizes are specified, FST2DH shows the formation of a smaller delta further upstream and with a shallower downstream slope than a delta formed when only a single particle size is used. Further, the test cases showed that FST2DH has some difficulty in maintaining stability when modeling sediment movement in large, shallow-sloped models with small element lengths. It further cannot appropriately simulate sediment transport that occurs over many years' time, as it restricts the maximum time of a model run to 9,999 hours (416.6 days).

5 Conclusions

The following sections give an overview of the results of this research and provide suggestions for possible future research of the sediment transport capabilities of FST2DH.

5.1 Conclusions

Numerous test cases allowed for the identification of the current functionality of the sediment transport options in FST2DH. The findings from these tests are given in section 5.1.1. The other two sections summarize the changes made to SMS to support FST2DH sediment transport (section 5.1.2) and the suggested changes for the improvement of the FST2DH sediment transport capabilities (section 5.1.3).

5.1.1 Test Case Results and Observations

Each set of tests included several cases that ran to completion and provided resulting bed elevations that were reasonable and made sense intuitively. However, every set of tests also contained at least one case that became unstable and failed. The first set of tests examined the functionality of each of the sediment inflow options offered by FST2DH (Table 5-1). Research found that tests using either clear-water or equilibrium transport rate boundary conditions along the inflow boundary ran to completion and gave

results that are reasonable. Inflow specifications of specific concentrations and transport rates for essential conditions provided models that ran to completion, but the results from those models were identical, regardless of the amount of sediment entering the mesh. A concentration of 0 ppm and a transport rate of 0.0 cms do not provide the same result as the clear-water case (no inflow specification). Furthermore, the options for assigning concentrations or transport rates at the inflow boundary as natural conditions caused an internal error in FST2DH. Research thus found that the only inflow options currently functional in FST2DH are the clear-water and equilibrium transport rate conditions.

Table 5-1: Summary of Results for the Variation of Sediment Inflow Types

<i>Inflow Type</i>	<i>Parameter</i>	<i>Did the Model Run to Completion?</i>	<i>Are the Results Reasonable?</i>
Clear-Water	---	Yes	Yes
Concentrations (Essential Conditions)	0 ppm	Yes	No
	10 ppm	Yes	No
	100 ppm	Yes	No
	1,000 ppm	Yes	No
	10,000 ppm	Yes	No
Concentrations (Natural Conditions)	0 ppm	No	---
	10 ppm	No	---
	100 ppm	No	---
	1,000 ppm	No	---
	10,000 ppm	No	---
Transport Rate (Essential Conditions)	0 cms	Yes	No
	1 cms	Yes	No
	5 cms	Yes	No
	10 cms	Yes	No
Transport Rate (Natural Conditions)	0 cms	No	---
	1 cms	No	---
	5 cms	No	---
	10 cms	No	---
Equilibrium Transport Rate	---	Yes	Yes

The results from the second set of tests identified the transport equations that, when used, provide a model that runs to completion. Research found that five of the eight transport equations provided runs that were successful (Table 5-2). The equations found to be functional in FST2DH include the Engelund—Hansen, Yang Sand and Gravel, and the Meyer-Peter—Mueller formulas. The test cases for the Laursen and the Ackers—White—Day equations ran to completion but they also provided identical results, suggesting that the validity of their implementation should be investigated by model developers. The transport equations used in tests that ran to completion provided appropriate bed profiles for both clear-water and equilibrium transport rate inflow conditions. Research also found that the tests that failed did so regardless of the sediment inflow type specified. While any of the transport equations that are functional may be used in an FST2DH simulation, the Engelund—Hansen equation proved to be adequate for the many other test cases examined by research.

Table 5-2: Summary of Test Cases that Ran to Completion and Test Cases that Failed with the Variation of Sediment Transport Equations

<i>Transport Equation</i>	<i>Clear-Water Inflow</i>	<i>Equilibrium Transport Rate Inflow</i>	<i>Are the Results Reasonable?</i>
Power (a = 1.0, b = 1.0)	No	No	---
Power (a = 0.5, b = 0.75)	No	No	---
Engelund—Hansen	Yes	Yes	Yes
Ackers—White	No	No	---
Laursen	Yes	Yes	No
Yang Sand and Gravel	Yes	Yes	Yes
Meyer-Peter—Mueller	Yes	Yes	Yes
Ackers—White—Day	Yes	Yes	No
Garbrecht et al. (combination)	No	No	---

The third set of test cases used in the examination of the functionality of sediment transport in FST2DH included channels with varying midsection slopes and contractions. Table 5-3 gives a summary of the test cases that failed and the ones that ran to completion. All tests that ran successfully provided reasonable results that were intuitive. They appropriately defined the location and magnitude of both scour and deposition over time.

Successful runs showed several expected trends. As the particle size in each case increased, the amount of scour and deposition in the channel generally decreased and the deposition occurred further upstream. Cases with an equilibrium transport rate assigned to the inflow boundary appropriately showed that the bed elevations at the inflow boundary remained constant over time. All successful tests showed scouring in areas of higher velocity and deposition in areas where the water slowed down. Another trend observed by research was that the hydrodynamic solution changed as the geometry of the channel changed with scour and deposition over time. Specifically, as the bed scoured, the solution showed an increase in water depth and a decrease in velocity. Over time, as the highest velocities in the channel decreased, less sediment movement occurred. These trends suggest that the semi-coupling mode in FST2DH works appropriately.

FST2DH was unstable when small particle sizes (fine sand) were used for the clear-water inflow condition. The equilibrium inflow condition proved to provide more stability. Instability also occurred for all test cases run on the channel with a steep midsection slope. Research found that instability also occurred in the region of the hydraulic jump modeled in the test cases for the channel with a steep midsection slope. The complex flow and energy conditions associated with hydraulic jumps most likely

caused that instability. The causes for the instability observed in each of the test cases should be investigated by model developers.

Table 5-3: Identification of the Midsection Sloped and Contraction Test Cases that Ran to Completion and Test Cases that Failed

<i>Channel</i>	<i>Sediment Inflow</i>	<i>0.08 mm Particle Size</i>	<i>0.2 mm Particle Size</i>	<i>2.0 mm Particle Size</i>	<i>4.0 mm Particle Size</i>
Steep Midsection Slope	Clear-Water Equilibrium	No	No	No	No
Moderate Midsection Slope	Clear-Water Equilibrium	No	Yes	No	No
Shallow Midsection Slope	Clear-Water Equilibrium	Yes	Yes	Yes	Yes
Gradual Contraction	Clear-Water Equilibrium	No	No	Yes	Yes
Long Abrupt Contraction	Clear-Water Equilibrium	Yes	Yes	Yes	Yes
Short Abrupt Contraction	Clear-Water Equilibrium	No	Yes	Yes	Yes
		Yes	Yes	Yes	Yes

Comparison of FST2DH sediment results to those from SED2D WES illustrated that semi-coupling is essential for obtaining an appropriate sediment solution when large changes in the channel geometry occur. Without semi-coupling, the SED2D WES results did not make sense and didn't reflect the effects that the change in geometry would have on the flow condition and vice-versa. Thus, FST2DH results could not really be compared to those from SED2D WES. However, a couple of similar trends were observed in the results from each model. Both models predicted similar shapes and locations of scour and deposition in the flume with a gradual contraction. The results also showed that for both models, as the particle size increased, the depth of the scour

generally decreased. Finally, results from the SED2D WES test cases illustrated several advantages that FST2DH currently has over SED2D WES, including the following:

- Semi-coupling of hydrodynamic and sediment calculations
- Choice of several transport capacity equations
- Ability to model larger particle sizes, such as gravels
- Ability to model equilibrium sediment inflow transport rate with ease

The equilibrium concentrations calculated with FST2DH for the Engelund—Hansen equation and the Yang formula match closely with those found with the same two equations in SAMwin. The concentrations calculated by the two programs for models with smaller particle sizes matched better when the Engelund—Hansen equation was used and concentrations calculated for models with larger particle sizes matched better with the application of the Yang equation.

The laboratory flume test cases illustrated that FST2DH has some difficulty in modeling laboratory flumes. Table 5-4 provides the results from the several models created for different laboratory flumes and for the formation of a delta due to backwater as a river enters a reservoir. One of the difficulties listed in the table for some of the experiments is that of obtaining stability for models of narrow channels. FST2DH seems to have more difficulty running models with elements representing small areas than it does in running models with larger elements. Another difficulty listed in the table is that of accurately representing conditions seen in the laboratory because of the limited functionality of the sediment options in FST2DH. Research generally found that the instabilities encountered with some of the models require users to spend unnecessary effort and time manipulating the model to make it work.

Table 5-4: Summary of the Laboratory Flumes Attempted in FST2DH

<i>Laboratory Flume</i>	<i>Results / Reason for Failure</i>
Clear-Water Scour Around Piers of Various Sizes	Unstable hydrodynamic run, possibly due to the narrow channel width
Contractions with Varying Entrance and Exit Angles	Flow conditions given in journal article could not be reproduced
Thuc's Basin	More information is needed about the flow regime near the entrance to the basin
Seal's Experiment (downstream fining)	Limitations in FST2DH functionality prohibit modeling of lab conditions and the model seemed to be unstable (possibly due to the narrow width of the channel)
Toro-Escobar Experiment (downstream fining)	Limitations in FST2DH functionality prohibit modeling of actual laboratory conditions but trends can still be analyzed
Formation of a Delta due to Backwater	The first flume showed the appropriate formation and movement of a delta over time. The second set of flumes showed difficulty in obtaining model stability due to element size

The test cases for the flume representing deposition at the entrance to a reservoir appropriately represented the formation of a delta due to backwater when an obstruction is placed downstream. The volumes of sediment inflow and deposition were consistent and matched equilibrium conditions predicted by SAMwin. When multiple particle sizes are specified, the downstream slope of the delta flattens slightly and the delta moves upstream.

5.1.2 Changes to the SMS Interface

In addition to the test cases described in this report, research included changes to the Surface-Water Modeling System (SMS) code to fully support the sediment options offered by FST2DH. A review of the files output by SMS for FST2DH sediment transport allowed research to find and fix several incorrect parameters. Research further added code to SMS for reading the sediment data solution files output by FST2DH so

that the sediment results could be analyzed inside SMS. Finally, research involved the creation of a tutorial that outlines the steps for setting up and running an FST2DH sediment simulation. The tutorial is included in the appendix of this report.

5.1.3 Suggested Improvements for FST2DH

While many of the sediment options offered by FST2DH are functional, many options should be fixed. FST2DH developers should examine the algorithms used in modeling inflow concentrations and flowrates. The implementation of the Power equation, the Ackers—White equation, and Garbrecht et al. approach should be reviewed and code should be changed to provide model stability for these cases. Other changes should be implemented to make FST2DH more stable for models with smaller particle sizes, hydraulic jumps, and small element sizes.

5.2 Future Work

In order to verify that the sediment transport options in FST2DH work appropriately after the suggested changes are made to the source code, the test cases that failed in this research should be run again in FST2DH. Results from those runs should be evaluated again for reasonableness and to see if they follow the trends established by the results presented in this report. Additional models that represent simple changes in geometry should also be evaluated. Furthermore, after research was completed, investigation of the power equation suggested that the values used in that equation provided an unfair evaluation of the formula's functionality (solid sediment flow is represented when $a = 1.0$). The power equation should thus be reevaluated using smaller values for its "a" coefficient once changes are made to the FST2DH code.

Because the scope of this thesis involved the identification of the general functionality of the FST2DH sediment transport options, research has only examined simple test cases. As model developers fix the faulty sediment transport options in FST2DH, more complex analysis should be completed to determine the full extent of the model's applicability. This analysis would include models of hypothetical and laboratory flumes, as well as models of real rivers. Examples of hypothetical models may include s-shaped flumes, flumes with strings of differing contractions and changes in bed, and flumes with complex cross-sections. Examples of laboratory flumes may include those given in this report, those found by the current research and not detailed in this report, and many others (see, for example, Gaudio 2003, Lim 1997, and Yanmaz 1991).

Currently, sediment data files are output by FST2DH in ASCII format. This results in output files that require a lot of memory and take a lot of time to open in SMS. Future work may include modification to FST2DH and SMS to write and read sediment solution files in a compressed X MDF format, which requires less memory and decreases the amount of time required to read the file into SMS for post-processing.

A final recommendation for future work involves the creation of a standard suite of tests to be used in the verification process of newly-developed sediment transport models. The suite would include all data and results from several different laboratory and field studies that are required for a sediment transport simulation. The hypothetical models contained in this report may also be included in that suite. Such a collection of tests would not only benefit further research of sediment transport in FST2DH, but would also benefit developers of other transport models.

References

- Barton, C. L. (2001). "Flow Through an Abrupt Constriction – 2D Hydrodynamic Model Performance and Influence of Spatial Resolution." Master's Thesis, Griffith University, School of Environmental Engineering.
- Brush, L. M., Jr. and Wolman, M. G. (1960). "Knickpoint Behavior in Noncohesive Material: A Laboratory Study." *Bulletin of the Geological Society of America*. Volume 41, pp. 59-74.
- Cancino, L. and Neves, R. (1999). "Hydrodynamic and Sediment Suspension Modelling in Estuarine Systems, Part I: Description of the Numerical Models." *Journal of Marine Systems*. Volume 22, pp. 105-116.
- Chang, H. H. *Fluvial Processes in River Engineering*. Malabar, FL: Krieger, 1992.
- Dey, S. and Raikar, R. V. (2005). "Scour in Long Contractions." *Journal of Hydraulic Engineering*, ASCE, Volume 131, Issue 12, pp. 1036-1049.
- Duc, B. M., Wenka, T., and Rodi, W. (2004). "Numerical Modeling of Bed Deformation in Laboratory Channels." *Journal of Hydraulic Engineering*. Volume 130, Issue 9, pp. 894-904.
- Froehlich, D. C. (2003). "User's Manual for FESWMS FST2DH, Two-dimensional Depth-averaged Flow and Sediment Transport Model." U.S. Department of Transportation, Federal Highway Administration, McLean, Virginia.
- Gaudio, R. and Marion, A. (2003). "Time Evolution of Scouring Downstream of Bed Sills." *Journal of Hydraulic Research*. Volume 41, Number 3, pp. 271-284.
- Hotchkiss, R. H. and Parker, G. (1991). "Shock Fitting of Aggradational Profiles Due to Backwater." *Journal of Hydraulic Engineering*. Volume 117, Issue 9, pp. 1129-1144.
- Kassem, A. A. and Chaudhry, M. H. (1998). "Comparison of Coupled and Semicoupled Numerical Models for Alluvial Channels." *Journal of Hydraulic Engineering*. Volume 124, Issue 8, pp. 794-802.

- Lagasse, P. F., Zevenbergen, L. W., Schall, J. D., and Clopper, P. E. (2001). "Bridge Scour and Stream Instability Countermeasures: Experience, Selection and Design Guidance, Second Edition." U.S. Department of Transportation, Federal Highway Administration, National Highway Institute, Arlington, Virginia.
- Lim, S-Y (1997). "Equilibrium Clear-Water Scour Around An Abutment." *Journal of Hydraulic Engineering*. Volume 123, Issue 3, pp. 237-243.
- Molinas, A. (2000). "User's Manual for BRI-STARS (Bridge Stream Tube Model for Alluvial River Simulation)." U.S. Department of Transportation, Federal Highway Administration, McLean, Virginia.
- Nakato, T. (1990). "Tests of Selected Sediment-Transport Formulas." *Journal of Hydraulic Engineering*. Volume 116, Issue 3, pp. 362-379.
- Richardson, E. V., Simons, D. B., and Lagasse, P. F. (2001). "River Engineering for Highway Encroachments: Highways in the River Environment, Hydraulic Design Series Number 6." U.S. Department of Transportation, Federal Highway Administration, National Highway Institute, Arlington, Virginia.
- Seal, R., Paola, C., Parker, G., Southard, J. B., and Wilcock, P. R. (1997). "Experiments on Downstream Fining of Gravel: I. Narrow-Channel Runs." *Journal of Hydraulic Engineering*. Volume 123, Issue 10, pp. 874-884.
- Shams, M., Ahmadi, G., and Smith, D. H. (2002). "Computational Modeling of Flow and Sediment Transport and Deposition in Meandering Rivers." *Advances in Water Resources*. Volume 25, pp. 689-699.
- Sheppard, D. M., Odeh, M., and Glasser, T. (2004). "Large Scale Clear-Water Local Pier Scour Experiments." *Journal of Hydraulic Engineering*. Volume 130, Issue 10, pp. 957-963.
- Thomas, W. A., Copeland, R. R., and McComas, D. N. (2002). "SAM Hydraulic Design Package for Channels." U.S. Army Corps of Engineers, Engineer Research and Development Center, Coastal and Hydraulics Laboratory, Vicksburg, Mississippi.
- Thuc, T. (1991). "Two-dimensional morphological computations near hydraulic structures." Doctoral dissertation. Asian Institute of Technology, Bangkok, Thailand.
- Toro-Escobar, C. M., Paola, C., Parker, G., Wilcock, P. R., and Southard, J. B. (2000). "Experiments on Downstream Fining of Gravel. II: Wide and Sandy Runs." *Journal of Hydraulic Engineering*, Volume 126, Issue 3, pp. 198-208.

- U.S. Army Corps of Engineers (USACE), (2004). "User's Guide to SED2D WES Version 4.5." U.S. Army Corps of Engineers, Engineer Research and Development Center, Waterways Experiment Station, Coastal and Hydraulics Laboratory, Vicksburg, Mississippi.
- U.S. Army Corps of Engineers (USACE), (1991). "HEC-6, Scour and Decomposition in Rivers and Reservoirs, User's Manual." U.S. Army Corps of Engineers, Hydrologic Engineering Center, Davis, California.
- Wu, W. (2004). "Depth-Averaged Two-Dimensional Numerical Modeling of Unsteady Flow and Nonuniform Sediment Transport in Open Channels." *Journal of Hydraulic Engineering*, Volume 130, Issue 10, pp. 1013-1024.
- Yang, C. T., Simões, F. J. M., Huang, J., and Greimann, B. (2005). "Generalized Sediment Transport Models for Alluvial Rivers and Reservoirs." US-China Workshop on Advanced Computational Modelling in Hydroscience & Engineering. September 19-21, Oxford, Mississippi, U.S.A.
- Yang, C. T. and Wan, S. (1991). "Comparisons of Selected Bed-Material Load Formulas." *Journal of Hydraulic Engineering*. Volume 117, Issue 8, pp. 973-989.
- Yanmaz, A. M. and Altmbilek, H. D. (1991). "Study of Time-Dependent Local Scour Around Bridge Piers." *Journal of Hydraulic Engineering*. Volume 117, Issue 10, pp. 1247-1268.
- Zeng, W., and Beck, M. B. (2003). "STAND, A Dynamic Model for Sediment Transport and Water Quality." *Journal of Hydrology*. Volume 277, Issues 1-2, pp. 125-133.

Appendix A. FST2DH Sediment Transport Tutorial

The research outlined in this report included changes to the Surface-Water Modeling System (SMS) software package source code to enable users to set up a FST2DH sediment run and graphically view and analyze the simulation's results within the SMS interface. As part of that update, a new tutorial was created to teach SMS users how to set up and run a basic FST2DH sediment analysis in SMS. The pages that follow contain that tutorial.

Introduction

In this lesson you will learn how to set up and run a sediment transport simulation in FST2DH. The run will be semi-coupled, meaning that once a steady-state hydrodynamic solution is obtained, sediment and hydrodynamic calculations will be completed iteratively for all timesteps in the simulation.

Because the sediment transport options in FST2DH are fairly new, some of the options are not yet fully functional. Information about the current functionality of specific options can be found in the report accompanying this tutorial.

The first part of this tutorial outlines the setup for a steady-state hydrodynamic run and the remainder of the tutorial focuses on setting up, running, and interpreting results for a semi-coupled sediment run. Because FST2DH only supports the non-

cohesive sediments, sand with a uniform grain size of 0.5 mm will be used in this tutorial. While FST2DH supports both English and Scientific units, the data for this tutorial will be entered using scientific.

Opening the Mesh

The grid for this tutorial has already been generated and includes a representation of a contraction for a highway crossing. To open the grid file, select **File|Open**. Browse to the `fst2dh_sediment` folder and open the file named “`hwy_cross.sms`”. The main display window should appear similar to that given in Figure A-1.

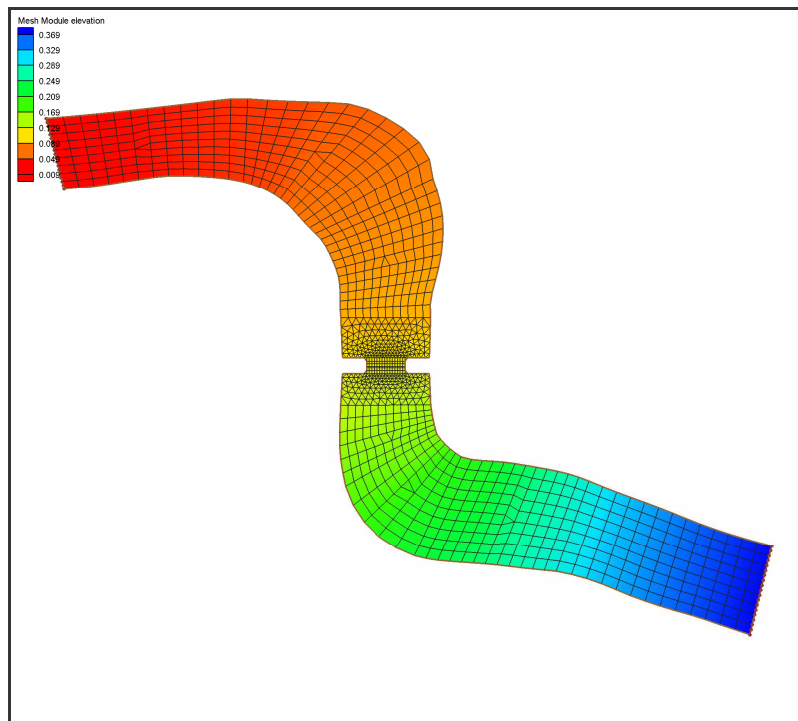


Figure A-1: Screen Shot of the Initial Mesh

Assigning Boundary Conditions

The channel you are modeling will have a flowrate of 60.0 cms and a downstream water surface elevation of 1.7 m, representing a depth of that same magnitude. To assign these boundary conditions:

1. Click on the “Select Nodestring”  tool.
2. Select the nodestring representing the inflow boundary, located to the lower right hand end of the mesh.
3. Select **FESWMS | Assign BC...**
4. Check the Flow toggle, enter a flowrate of 60.0 (cms), and click OK.
5. Select the nodestring representing the outflow boundary, located at the upper left hand corner of the mesh.
6. Open the boundary conditions dialog again (**FESWMS|Assign BC...**) and select the Water surface elevation toggle.
7. Specify a constant water surface elevation (WSE) of 1.7 (m) and click OK to exit the dialog.

Material Properties

For simplicity, the channel being modeled in this tutorial contains a single material type—sand. To assign a Manning’s n value for sand to the entire mesh:

1. Select **FESWMS | Material Properties...**
2. Assign a value of 0.025 for Manning’s roughness (n1 and n2)
3. Click OK to exit the FESWMS Material Properties dialog.

Model Control

Most of the parameters used as input for FST2DH simulations are defined in the FESWMS Model Control dialog. To set up the parameters for a steady-state hydrodynamic simulation:

1. Select **FESWMS | Model Control...**
2. In the FESWMS Model Control dialog, select the General Tab, make sure the **Run Type** is set to “Hydrodynamic” and the **Solution Type** is set to “Steady State”.
3. Select the Timing Tab and set the number of **Iterations** to 10.
4. Select the Parameters Tab. Assign the **Water-surface elevation** a value of 1.7 (m), and the **Unit flow convergence** and **Water depth convergence** a value of 0.01.
5. Select OK to exit the FESWMS Model Control.

Renumbering the Mesh

Before a hydrodynamic solution is run, the mesh should be renumbered. To renumber the mesh:

1. Click the “Select Nodestring” tool  and select the inflow boundary (at the lower right end of the mesh).
2. Select **Nodestrings | Renumber...**

Obtaining the Steady-State Hydrodynamic Solution

Before running FST2DH, you will need to save the file:

1. Select **File|Save As...**
2. Browse to the “fst2dh_sediment\output” folder and save the project file (*.sms) as “hwy_cross_out.sms”.

Now that the parameters for the steady-state hydrodynamic run have been saved, you are ready to run FST2DH. Select **FESWMS | Run FST2DH** to start the simulation. The model will take a few seconds to run. Once it is complete, make sure the “Load solution” toggle box is checked and click on the Exit button. The steady-state hydrodynamic solution opens in SMS.

Some models require the use of incremental loading in order to reach a solution. In those cases, the hydrodynamic solution serves as a hotstart file for a subsequent semi-coupled hydrodynamic and sediment simulation. Although the channel in this tutorial did not require incremental loading, the hydrodynamic solution will still be used as a hotstart for the semi-coupled simulation so that you can see how it is done.

Creating a Sediment Simulation

You are now ready to set up the sediment simulation. In order to use the hydrodynamic solution just created by FST2DH as a hotstart for the sediment run, you must rename the project so the new hydrodynamic output file does not overwrite the steady-state one. To save the project with a different name:

1. Select **File | Save As...**
2. Change the File name to “hwy_cross_sed_out.sms” and click Save.

Setting the Sediment Parameters in Model Control

You will now set up the appropriate options for the sediment transport simulation. As was the case for the hydrodynamic run, most of the sediment parameters will be set in the FESWMS Model Control dialog. To set the parameters:

1. Select **FESWMS | Model Control**
2. In the General Tab, change the **Run Type** to “Semi-coupled” to tell FST2DH to run the hydrodynamic and sediment calculations iteratively for each timestep.
3. Change the **Solution Type** to “Dynamic” to have FST2DH simulate the movement of sediment over time
4. Select the **Sediment Transport Solutions** toggle, click the file macro, and enter “hwy_cross_sed_out.sed” for the name of the sediment data output file to be created by FST2DH during the sediment simulation. Click Save.
5. Select the **INI file** toggle in the FST2DH Input section of the General Tab, click the file macro, and open the file called “hwy_cross_out.flo” from the fst2dh_sediment\output folder. This tells FST2DH that the output file from the steady-state hydrodynamic run will be used as a hotstart for the sediment simulation.
6. Select the Timing Tab in the FESWMS Model Control dialog. Set the **Starting time** to 0.0 (hours), the **Run time** to 48.0 (hours), and the **Time step size** to 0.25 (hours). The simulation will run for 48 hours, with a 15-minute timestep.
7. Select the Sediment Control Tab. In this tab, you enter the sediment parameters for the model run. The options in the **Report Options** section allow you to specify which information is included in the *.prt informational text file output by

FST2DH while completing a simulation. More information about these options can be found in the User's Manual for FESWMS FST2DH. For this simulation, FST2DH will not write any sediment data to the informational text file. Make sure all three toggle boxes in the **Report Options** section are unchecked.

8. The fields in the **Control Options** section of the Sediment Control tab allow for the specification of other sediment parameters. Select the **Parameters...** button. This opens the FESWMS Sediment Parameters dialog (Figure A-2). In this dialog, a user can specify the sediment transport equation desired and can also set specific properties for the bed sediment being modeled. Select the **Engelund-Hansen** formula and click OK.

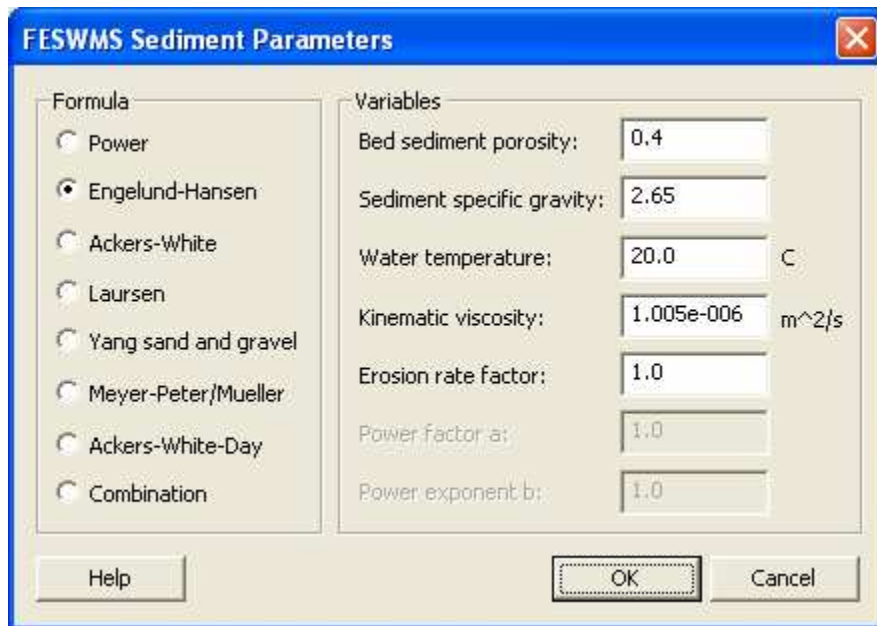


Figure A-2: FST2DH Sediment Parameters Dialog

9. Select the **Bed Control...** button to open the Global Bed Control dialog shown below in Figure A-3. This dialog allows you to enter the grain size distribution for the bed. The particle sizes are specified in the top row of the spreadsheet and the percentage (in decimal form) of each bed layer made up of the particles is specified in the lower three rows. Up to eight (8) different particle sizes may be specified. This first sediment run will model a sand bed with a uniform particle size of 0.5 mm. To define the bed:
 - a. Set the Active bed-layer, Deposition bed-layer, and Original bed-layer thicknesses to 0.001 m, 0.5 m, and 2.0 m, respectively. (More information about the values that are acceptable for layer thicknesses can be found in the FESWMS FST2DH User's Manual).
 - b. In the first column of the spreadsheet:
 - i. Set the **Particle Size** to 0.5 (mm).
 - ii. Specify a value of 1.0 (100%) for the remaining rows in the first column. This tells FST2DH that each layer is composed entirely of 0.5 mm sand.
 - c. If the simulation represents a channel having a bed with more than a single particle size, the other columns in the spreadsheet should be filled in with the remainder of the particle size distribution.
 - d. Click OK to exit the Global Bed Control dialog.
10. Select OK to exit the FESWMS Model Control dialog.

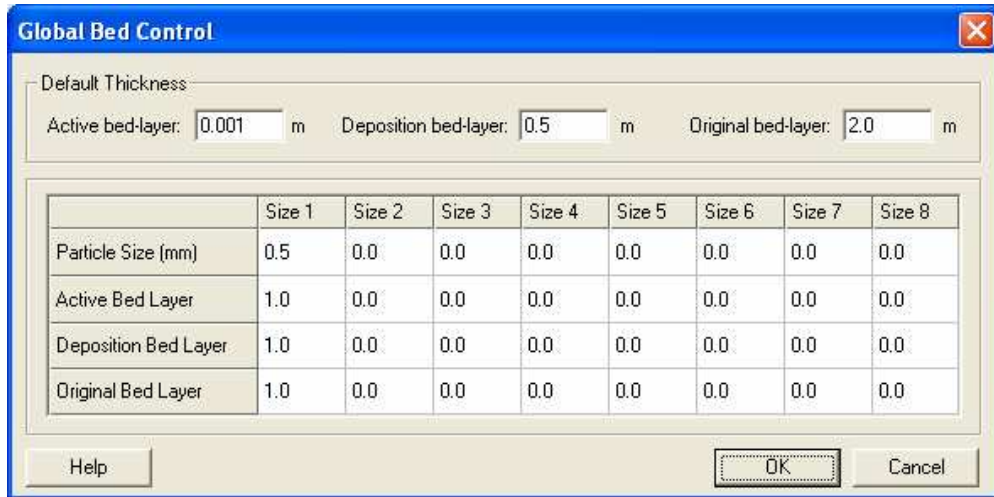


Figure A-3: FST2DH Global Bed Control Dialog

Specifying Equilibrium Transport Rate Inflow

FST2DH provides the user with several options for the specification of sediment entering the mesh through the inflow boundary. For this lesson, the equilibrium transport rate will be applied. For this boundary condition, FST2DH uses flow characteristics to determine the sediment inflow required to maintain channel equilibrium. To assign this condition to the inflow boundary:

1. Click the **Select Nodestring** tool  and select the inflow nodestring (at the lower right corner of the mesh).
2. Select **FESWMS | Assign BC...**
3. In the Sediment Options Tab, check the toggle for “Specify sediment volumetric flow rate” and select the “Equilibrium rates applied” radio button (Figure A-4).
4. Click OK to exit the FESWMS Nodestring Boundary Conditions dialog.

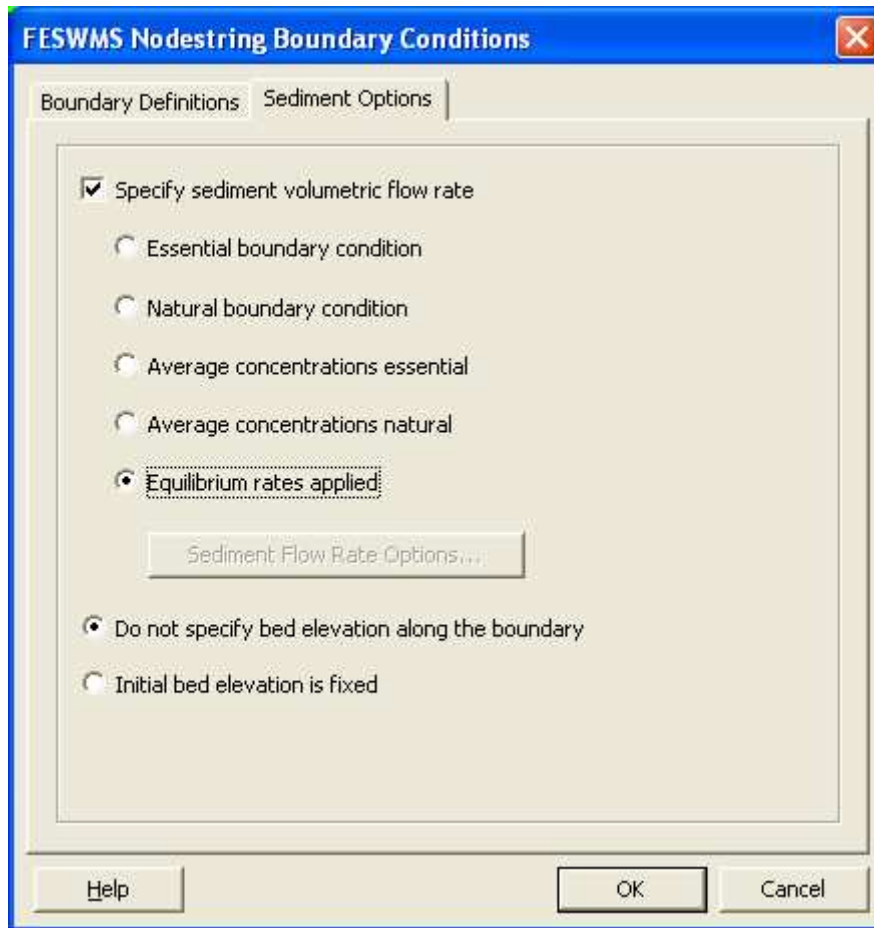


Figure A-4: FESWMS Nodestring Boundary Conditions Dialog

Running FST2DH for the 0.5 mm Grain Size Case

Now that the sediment parameters have been set, the data is ready to be saved and FST2DH can be run. To save the data, select **FileSave Project**. Once the data is saved, select **FESWMS | Run FST2DH** to start the simulation. Depending on the speed of your computer, this may take several minutes to run.

After the model finishes running, make sure that the “Load solution” toggle is checked and click the Exit button. This loads the hydrodynamic solution for each

timestep. To load the sediment solution, select **File|Open** and open the file called “hwy_cross_sed_out.sed” (located in the fst2dh_sediment\output folder). A message will appear, informing you that the depths given in the solution folder are incorrect. This is because when the hydrodynamic solution is read in, SMS calculates the depths by subtracting the *initial* bed elevation from the water surface elevation computed by FST2DH instead of the *new* bed elevations. Click OK to close the message box.

Viewing the Results for the 0.5 mm Grain Size Case

The sediment data file output by FST2DH (*.sed) contains the bed elevations, the time-derivatives of the bed elevations, the thickness of the active, deposition, and original bed layers, and additional data specific to each of the particle sizes modeled. To view the sediment results, select the **bed elevation** dataset in the project explorer. If the contours are not on, you may need to turn them on by selecting **Display|Contour Options...** and setting the desired contour scheme.

The two main solutions from the model run include the hydrodynamic data (hwy_cross_sed_out.flo) and the sediment data (hwy_cross_sed_out.sed). Feel free to explore the datasets contained in these folders in the project explorer. Specifically, you may want to step through the timesteps to see how the bed elevations change over time.

Creating a Second Sediment Simulation for a Grain Size of 2.0 mm

You will now run a second simulation, with a larger grain size (2.0 mm) for comparison to the first sediment solution (for 0.5 mm). Before running the simulation

with a different grain size, delete the hydrodynamic files (*.flo) from the project explorer
save the project with a new name:

1. Right click on “hwy_cross_out.flo” in the project explorer and select **Delete** from the menu that appears.
2. Repeat step 1 for “hwy_cross_sed_out.flo”.
3. Select **File | Save As...**
4. Change the File name to “hwy_cross_sed_out_2mm.sms” and click Save.

Setting the Sediment Parameters in Model Control

All the options from the previous model were preserved when you saved the project under a new name. You will now change the particle size that is to be modeled in the second run:

1. Select **FESWMS | Model Control...**
2. Select the Sediment Control Tab and then the **Bed Control...** button to open the Global Bed Control dialog. Change the particle size from 0.5 mm to 2.0 mm.
3. Exit the dialogs by selecting OK twice.

Running FST2DH for the 2.0 mm Grain Size Case

Save the data (**File|Save Project**) and run FST2DH (**FESWMS | Run FST2DH**). Again, depending on the speed of your computer, this may take several minutes to run. After the model finishes running, make sure that the “Load solution” toggle is checked and click the Exit button. The dynamic hydrodynamic solution loads automatically.

Select **File|Open** and open the file called “hwy_cross_sed_out_2mm.sed” (located in the fst2dh_sediment\output folder). Click OK when the message box appears.

Comparing the Results from the 0.5 mm and 2.0 mm Cases

Feel free to explore the solution for the 2.0 mm simulation. Once you are through, you can compare the resulting bed elevations from the 0.5 mm and 2.0 mm simulations. While this can be done in many ways, the following steps outline one method:

1. Open the data calculator (**Data|Data Calculator...**)
2. Select “v. bed elevation” from the list of datasets, check the **Use all time steps** toggle box, and click **Add to Expression**.
3. Click the minus “-“ button.
4. Repeat step 2 for the “i. bed elevation” dataset.
5. Change the **Result** to “diff_bed” and click **Compute** to create the new dataset.
6. Once the calculation is complete, click **Done** to exit the Data Calculator.
7. In the project explorer, select the “diff_bed” dataset.
8. Loop through the timesteps to see the difference in bed elevations predicted by the two simulations. You will notice that the largest differences occur in the areas of the most scour and deposition—through the contraction and just downstream from it.

After you have finished any additional analysis you desire to complete, select **File|Exit** to exit SMS.

Conclusion

In this lesson you have set up and run a steady-state hydrodynamic simulation in FST2DH and used that hydrodynamic solution as a hotstart file for two separate semi-coupled sediment simulations for different particle sizes.